Blue Stragglers

by

John Anders Ouellette
B.Sc. Victoria 1991

A Dissertation Submitted in Partial Fulfillment of the
Requirements for the Degree of

DOCTOR OF PHILOSOPHY

in the Department of Physics and Astronomy

© John Anders Ouellette, 1999,
University of Victoria.

Abstract

Blue stragglers are enigmatic stars which appear to have undergone some form of rejuvenation, bringing them near the zero-age main sequence of the cluster in which they reside. The most likely explanation for the existence of these stars is that they have formed recently, through the merger of two stars, either through a direct stellar collision, or through binary mass-transfer and coalescence. This thesis presents models of the remnants of these processes, and a comparison of the predictions of these models with observed blue stragglers in several clusters.

The predictions of smoothed particle hydrodynamic simulations of colliding stars have been used to create models appropriate for input into a stellar evolution code. Since these models develop only thin, short-lived, convective envelopes, angular momentum loss via a magnetically driven stellar wind is unlikely to be a viable mechanism for slowing the rapidly rotating blue stragglers predicted by the collisional scenario. Angular momentum transfer to either a circumstellar disk (possibly collisional ejecta) or a nearby companion remain plausible mechanisms for explaining the low rotation velocities observed for most blue stragglers.

In addition to these models of collisional mergers, simplistic models of the remnants of binary coalescence and mass-transfer were also developed. The predictions of both sets of models were compared with the observed blue straggler populations of six globular clusters (NGC 104, NGC 2419, NGC 5024, NGC 6809, NGC 7099). While most of the clusters' blue stragglers appear to be well matched by the predictions of the collisional mergers, the blue stragglers in the cluster with the highest central density, NGC 7099, appear to be a hybrid population of both collisional and binary mergers. The blue stragglers of NGC 2419 — the least dense of the clusters studied here —

are well matched solely by the predictions of the collisional mergers of equal mass stars. However, due to the low density of this cluster, it is likely that some fraction of these blue stragglers are being formed via binary mergers and that the simple models of binary mergers used here are inadequate.

Contents

List of Tables

List of Figures

Acknowledgements

What exactly does one put in the Acknowledgements section? Ideally, as far as I understand, it is the appropriate place to recognise those who have assisted, encouraged, and supported me during the writing of this dissertation (and during all of the time leading up to the contact of the proverbial pen with the equally proverbial paper). This dissertation is already about 200 pages long, acknowledging all those who have assisted me in some way in reaching this point would bring that up to about 400 pages. A quick read through the Acknowledgements in the dissertations of past Astro-grads gave me a clearer picture – and some time to reflect on the people that actually wrote those pages. Here goes.

It seems common practice to acknowledge one's spouse last, allowing the last words to give emphasis to the encouragement and emotional support given by this singularly important person. I can't do that. Andrea is the first thought in my mind at the beginning of the day, her love and warmth are more essential to me than the rising of the Sun. Her place is at the beginning. Her sparkling blue eyes have encouraged me (and captured me), her musical voice has consoled me (and charmed me), her presence has supported me (and sustained me). She has given me the strength to continue, and to finish, this dissertation.

It has taken me far too long to get to this point, but Chris Pritchet, my supervisor, has demonstrated an almost god-like patience while this dissertation was being written. I always left our talks regarding my work with a renewed sense of optimism. His support (both financial and scientific) has

To my wife, Andrea, and to our first child, whose arrival we await eagerly.

Chapter 1

Introduction

1.1 What are Blue Stragglers?

A simple definition of blue stragglers is that they are hot, bright, massive, main sequence stars existing among a population of evolved stars.[1] Figures 1.1 and 1.2 show colour-magnitude diagrams for the globular clusters NGC 6397 (Kaluzny, 1997) and NGC 7099 (M30; Guhathakurta *et al.*, 1998). According to canonical theory, the most massive, core hydrogen burning, main sequence stars in clusters such as these are located at the main sequence turnoff, while the other sequences (the sub-giant branch, the red giant branch, and the horizontal branch) are defined by the evolution of stars after they have left the main sequence. The blue straggler sequence extends beyond the turnoff to where, in much younger clusters, main-sequence stars more massive than the current turnoff stars would lie. Figure 1.3 shows the same colour-magnitude diagram as shown in Figure 1.1 with theoretical evolution-

---

[1]This definition is somewhat biased toward describing blue stragglers in clusters. Blue stragglers have been shown to exist in the field of the Galaxy (Hobbs & Mathieu 1991; Glaspey, Pritchet & Stetson 1994) where it is not unusual to find 'normal' stars matching the same description.

ary tracks for stars of various masses overplotted. The fact that blue stragglers appear to be more massive than the turnoff stars (an appearance which is supported by spectroscopic observations), is the essence of the enigma that blue stragglers represent: if they are massive stars, then they should have evolved away from the main sequence long ago.

But does the presence of blue stragglers *really* indicate a problem with standard stellar theory? After all, the agreement of current stellar calculations with observations of stars in our own Galaxy (e.g. Renzini & Fusi Pecci, 1988) demonstrates that the models are quite adequate. On the other hand, there are known omissions and simplifications in the standard theories, but none seem adequate to explain how blue stragglers can apparently remain on the main sequence while the the bulk of the stars in their parent cluster happily evolve in accordance with the theoretical predictions.

If blue stragglers were formed at the same time as the rest of the stars in the cluster, with the same – apparently high – masses as they now possess, then they must indicate a problem with our standard treatment of stellar formation and evolution. Canonical stellar theory attempts to model stars as gaseous spheres which are in hydrostatic and thermal equilibrium; the 'evolution' of a star is a result of the continuous adjustment of the (quasi-static) equilibrium structure of the star in response to the changing conditions in the interior. Deviations from this idealised structure, due to, for example, rotation or the presence of a close companion star, will result in the star's evolution departing from the predicted course. In general, however, departures significant enough to modify the lifetime of a star significantly will also result in the star having other, observable, peculiarities: for example, ex-
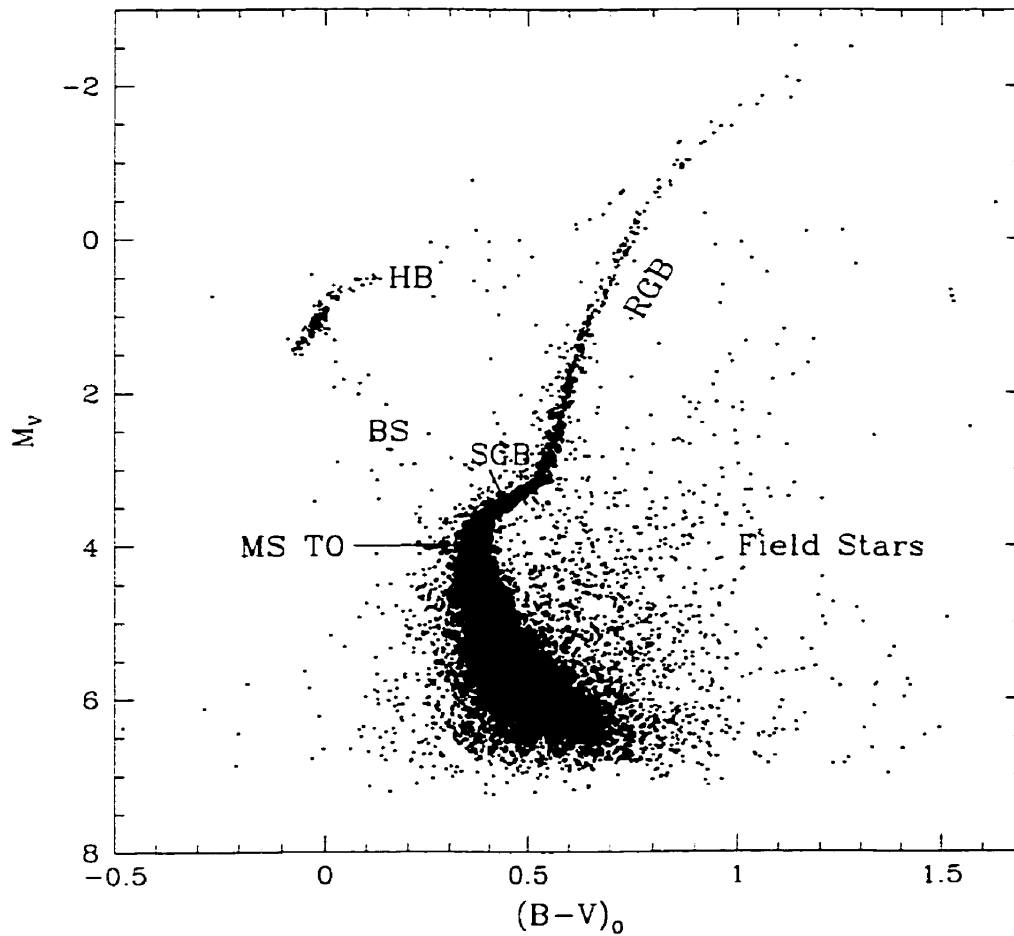
Figure 1.1: Colour-magnitude diagram for the globular cluster NGC 6397 (Kaluzny *et al.*, 1997). The various evolutionary sequences are labelled as follows: BS - blue stragglers, SGB - sub-giant branch, RGB - red giant branch, HB - horizontal branch, MS TO - main sequence turnoff.
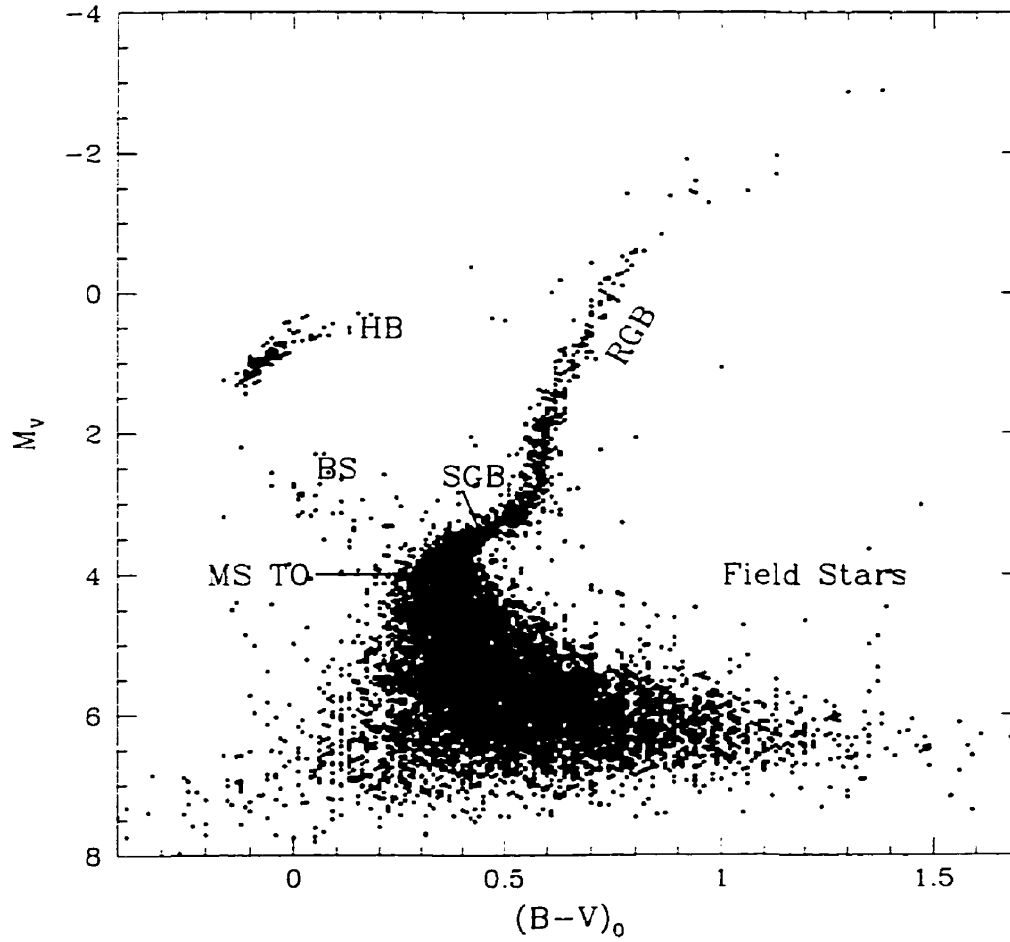
Figure 1.2: Colour-magnitude diagram for the globular cluster NGC 7099 (M30; Guhathakurta *et al.*, 1997). Sequences are labelled as in Figure 1.1.
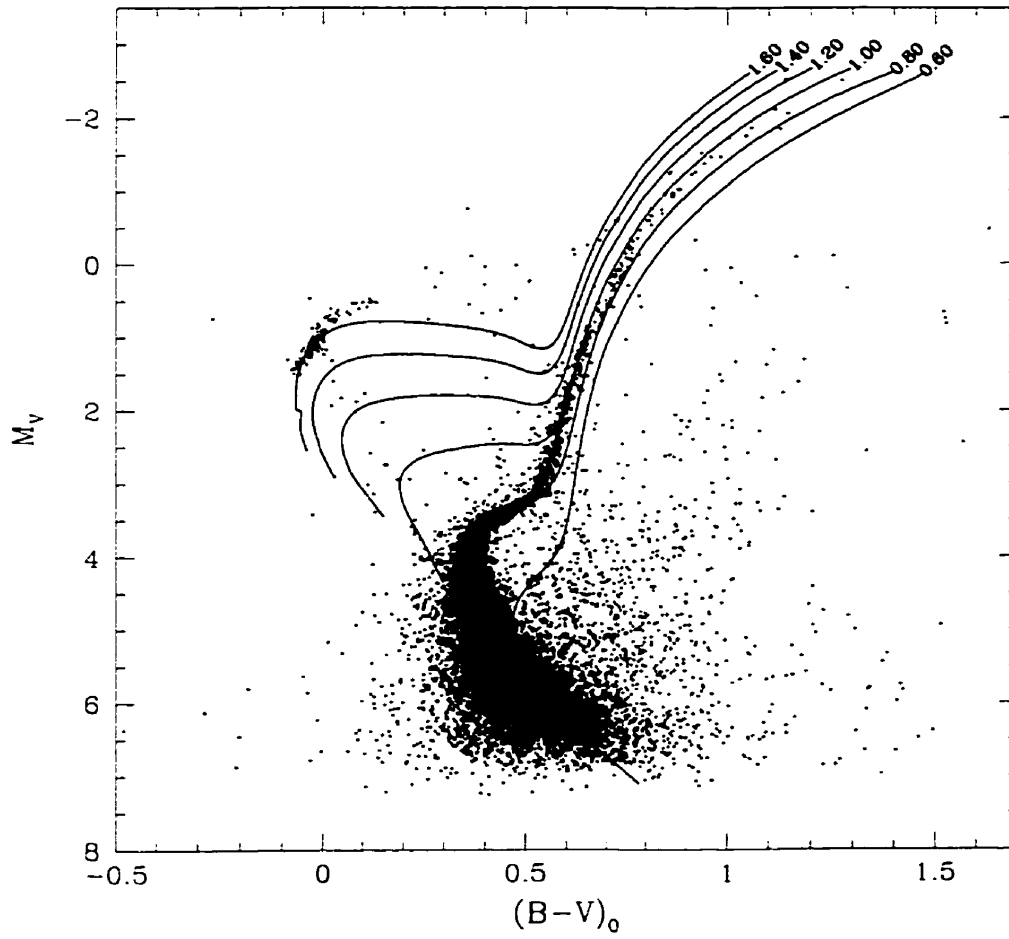
Figure 1.3: CMD of NGC 6397 with evolutionary tracks overlaid. The masses indicated are in solar masses.

treme rotation, which could extend the lifetime of a star by a factor of two or more (Clement, 1994) by providing a non-thermal form of pressure support, reducing the requirements for nuclear energy generation, would also result in the star having a much lower luminosity and temperature than a similar, non-rotating star.

Nature, perhaps being loath to follow theory, provides stars for which deviations at some level from the assumptions implicit in the standard theories are the norm rather than the exception. For instance: all stars rotate, many stars are members of binary systems, and composition variations are seen among stars even within clusters (where we usually assume all stars form with the same composition). And yet the standard models have proven to be quite successful in their prediction of stellar evolution: departures from theory, due to the aforementioned processes and others, are observed (e.g. VandenBerg, Larson, & De Propris 1998), but are generally small. The obvious interpretation of this is that, for the majority of stars, canonical stellar theory is an adequate approximation to reality.

Since the standard theories seem sufficient, it may be that the evolution of blue stragglers, assuming they have maintained the same mass over the course of their lives, differs dramatically from that of normal stars. On the other hand, if a process could be found to extend the life of a star by a large factor (such as internal mixing or some non-thermal pressure support; Wheeler 1979, Saio & Wheeler 1981), it is unlikely that a star, being affected by this process, would follow the normal course of evolution (that predicted by the standard models): since blue stragglers appear to have masses consistent with their location in the colour-magnitude diagram and appear to have

normal internal structures (Schoenberner & Napiwotzki, 1994) their evolution cannot deviate greatly from that of a normal star. Recalling the example of a rapidly rotating star: due to its lowered temperature and luminosity, it will appear to be a lower mass star than it actually is, possibly preventing it from being identified as a blue straggler.

If blue stragglers do not differ from normal stars solely in their evolution, then their formation must differ also. This provides a second answer to the question posed earlier: if blue stragglers do not form in the same fashion as normal stars, then they do not necessarily indicate a flaw in our theories of stellar evolution. If, for example, blue stragglers do evolve as normal stars, and perhaps form in the same manner as normal stars, but formed later than the other stars in the cluster, then they would naturally appear as main sequence stars extending above the turnoff (those stars forming with a mass less than that of a turnoff star would likely blend in with the less evolved, but normal, cluster main sequence). In other words, if one could, through some hypothetical mechanism, form an otherwise normal star long after stars of the same mass had evolved away, the star could then evolve in the 'correct' manner and still appear as a blue straggler.

Since canonical theory is apparently on sound footing, and processes by which the evolution of blue stragglers can be altered do not present themselves, it is likely that it is in their formation that blue stragglers differ from normal stars. This is not to say that the processes which can alter the evolution of a star (such as rotation or binarity) are not acting on blue stragglers — in fact, there is nothing to say that these processes are not more effective among blue stragglers than normal stars. Throughout this work, I will be

assuming the *status quo*: canonical theory holds for blue stragglers as it apparently does for normal stars, and that deviations from the theory have no more an effect on blue stragglers than they appear to have on normal stars.

1.2   Scope of this Work

The main goal of this work is to develop and evolve models of the remnants of stellar collisions. Stellar collisions have been proposed as a possible formation mechanism for blue stragglers (Hills & Day, 1976) and are very likely to occur in globular clusters, especially if interaction rates are enhanced by the presence of a population of binaries (Leonard & Fahlman, 1991). These models, once developed, will be compared to the observed populations of blue stragglers in several globular clusters with prominent blue straggler populations.

Chapter 2 contains a review of blue stragglers, the theories proposed for their formation and the observations which have been made of them. In Chapter 3 I will describe the models of stellar remnants, which will be used in Chapter 4 in a comparison with observed blue stragglers.

Executive summary: Blue stragglers are blue and twinkly and, much like the little star immortalised in song, we wonder what they are.

Chapter 2

Blue Stragglers

There have been many mechanisms proposed for the formation of blue strag-
glers and, like any other theory, their success is gauged by their agreement
with observations. However, the situation seems somewhat too complicated
to allow for a single theory to explain *all* blue stragglers: no single mechanism
is able to explain all of the observed properties of blue stragglers. Environ-
mental factors (e.g. stellar density, binary fraction and period distribution,
the presence of gas and dust) play a role in the efficiency of most of the
proposed formation mechanisms, so it is reasonable to require that a mech-
anism be able to explain the observations of blue stragglers in its preferred
environment.

In this Chapter, I will review the observed properties of blue stragglers
outside the context of any of the proposed mechanisms; only after the obser-
vations have been reviewed will I describe these mechanisms in any detail.

2.1 Observed Properties of Blue Stragglers

2.1.1 Observed Masses

Because of their location on the colour-magnitude diagram (**CMD**[1]) – generally brighter than the parent cluster's main-sequence turnoff (**MS TO**) (see Figures 1.1 and 1.2) – blue stragglers are usually assumed to be massive stars. However, the mass of a star is one of the most difficult properties to determine: the only way to measure the mass of a star without resorting to assumptions about its luminosity, or evolutionary state, is through its gravitational effect on nearby objects. For stars other than the Sun, this is possible only in binary systems. Although there are blue stragglers which are components of binary systems (e.g. Kaluzny 1997, Kaluzny *et al.* 1996, Yan & Reid 1996) none have been studied with the intention of obtaining mass estimates. Despite this, there are other, less direct methods, which can be used to estimate the mass of a blue straggler.

Shara *et al.* (1997) and Rodgers & Roberts (1995) attempted to determine the mass of blue stragglers in 47 Tuc and NGC 6397, respectively, by spectroscopically measuring their surface gravities and temperatures. The measurements of Shara *et al.*, which were more precise than those of Rodgers & Roberts, showed that BSS-19 in 47 Tuc (Guhathakurta *et al.* 1992) has a mass of $1.70 \pm 0.40 M_\odot$, roughly twice the main-sequence turnoff mass of the cluster as inferred from isochrone fits to the cluster CMD. The results of Rodgers & Roberts similarly showed that the blue stragglers in NGC 6397 are, on average, more massive than the cluster turnoff stars. Unfortunately,

---

[1]See the Glossary of Abbreviations for the definition of such acronyms

the method used in both studies required that the absolute luminosity of the stars be known, or assumed.

It is possible to use the surface gravities and temperatures measured by Rodgers & Roberts and Shara *et al.* to estimate the masses of blue stragglers in a different, distance independent, method. Figures 2.1 and 2.2 show $\log g - \log T_{eff}$ diagrams for NGC 6397 and 47 Tuc, with the measurements of Rodgers & Roberts and Shara *et al.* also plotted. Since the surface gravities and temperatures are derived from spectroscopic observations by comparison with model atmospheres, there is no distance dependence (although there is a reddening dependence on the results of Shara *et al.*, but it is a small effect). Rodgers & Roberts found masses for the blue stragglers in NGC 6397 ranging from $0.62 M_\odot$ to $1.15 M_\odot$, which are quite different than the fairly narrow range of masses inferred from the $\log g - \log T_{eff}$ diagram — this difference is probably due in part to the poor photometry they used for the luminosity information necessary for their analysis. The mass Shara *et al.* found for BSS-19 agrees quite well with the mass from the $\log g - \log T_{eff}$ diagram ($\sim 1.55 M_\odot$) — it is also rather encouraging to note that this mass agrees with the photometric mass derived from the CMD in Figure 2.2, although the apparent evolutionary state of the blue straggler is different in the two diagrams.

Strömgren 4-colour photometry has also been used (Strom & Strom 1970, Bond & McConnell 1971, Bond & Perry 1971) to show that blue stragglers have normal surface gravities for their locations on the CMD, suggesting that they must be more massive than the stars which are lower on the main-sequence — including the cluster turnoff stars.
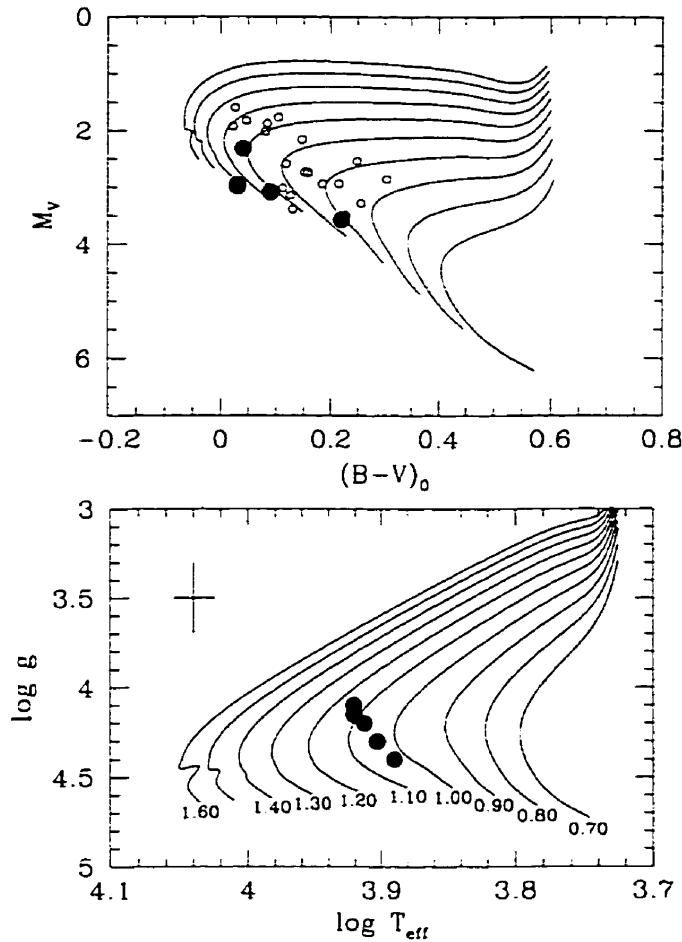
Figure 2.1: Top - CMD for the blue stragglers in NGC 6397 from Alcaino *et al.*(1987) (filled circles) which were studied by Rodgers & Roberts (1995). The photometry for the blue stragglers from Alcaino *et al.* is somewhat noisy, so the photometry shown from Lauzeral *et al.*(1992), which is of much better quality, is shown for reference. The evolutionary tracks are of a metallicity appropriate for NGC 6397 ([Fe/H]=-2.14, [α/Fe]=0.3) and have the same masses as those shown in the bottom diagram. Bottom - $\log g - \log T_{eff}$ diagram for the blue stragglers studied by Rodgers & Roberts. A typical 1-σ error bar is shown in the diagram for reference. The evolutionary tracks are labelled in units of solar masses.
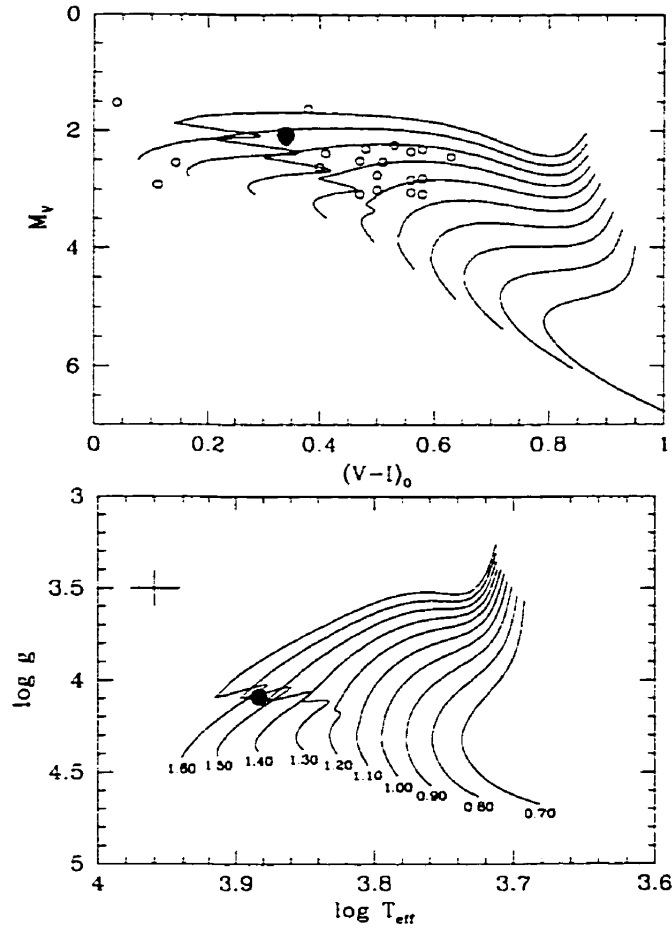
Figure 2.2: Top - CMD for the blue stragglers in 47 Tuc from Guhathakurta *et al.* (1992). BSS-19 (filled circle) was the blue straggler targeted by Shara et al. (1997). The evolutionary tracks are of a metallicity appropriate for 47 Tuc ([Fe/H]=-0.83, [α/Fe]=0.3) and have the same masses as those shown in the bottom diagram. Bottom - $\log g - \log T_{eff}$ diagram for the blue straggler studied by Shara *et al.*. A typical 1-σ error bar is shown in the diagram for reference. The evolutionary tracks are labelled in units of solar masses.

An indication of whether or not blue stragglers are more massive than other stars in the parent cluster can be found by comparing their radial distribution to that of other cluster stars. Due to mass segregation, the more massive stars, whether they are single stars or tightly bound binaries, will tend to settle to the core of a cluster on a timescale equal to the relaxation time of the cluster. Blue stragglers are found to be more centrally concentrated than the cluster giants and main-sequence stars (e.g. Sarajedini & Forrester 1995, Guhathakurta *et al.* 1994, Sarajedini 1994, Ferraro *et al.* 1992, Côté *et al.* 1991, Nemec & Harris 1987) and as centrally concentrated as cluster binaries (Mathieu & Latham 1986, Edmonds *et al.* 1996).

With several 10 meter class telescopes available, or becoming available soon, it should be possible to make direct measurements of the masses of those blue stragglers that are in binary systems. Since obtaining spectroscopic measurements of a binary blue straggler over its entire orbit – necessary to determine orbital parameters and, hence, its mass – would be time consuming (on telescopes which are in extremely high demand), mass estimates for single blue stragglers, such as those obtained by Shara *et al.* (1997), would make more efficient use of telescope time. Also, determination of the surface gravity and effective temperature of a large number of blue stragglers in a cluster would be invaluable for studies of their evolution since these measurements could be compared directly with stellar evolution calculations, without having to resort to uncertain colour-temperature and bolometric corrections (e.g. Figures 2.1 and 2.2).

2.1.2 Binary Blue Stragglers

Between ~ 15% (Duquennoy & Mayor 1990, Padget *et al.* 1997) and 50% (Abt 1979) of the stars we see in the sky are actually binaries. Whether a similar frequency of binarity exists among the stars in clusters, particularly globular clusters (**GC**), is still a matter of some debate (e.g. Côté *et al.* 1994, Yan & Mateo 1994, Yan & Reid 1996, Côté *et al.* 1996). Although the *exact* nature of the connection between blue stragglers and binaries is unclear, the more successful mechanisms for the production of blue stragglers are dependent in at least some way on binaries, and should make predictions about the binary properties of the blue stragglers themselves.

Surveys for binaries in clusters have been done either photometrically or spectroscopically. Photometric surveys for binaries rely on the chance alignment of the plane of the orbit of a cluster binary and the line of sight (i.e. inclination $i \sim 90°$) for detection. If such an alignment occurs, then one component of the binary will periodically eclipse the other, causing a change in the combined apparent brightness of the object. This method relies largely on serendipity: the inclination of the binary to the line of sight must be such that eclipses will occur, and observations of the star must be done both in and out of eclipse in order to detect its binary nature. Spectroscopic surveys rely on radial velocity variations. As the two components of the binary orbit their common centre of gravity, the stars will undergo velocity shifts which will be visible to an observer as shifts of the components' spectral lines. Although this method also requires that the inclination be large, eclipses do not have to occur.

Table 2.1 presents the results of various surveys for variability of blue

stragglers. This table constitutes a rather mixed bag of observations: all but two (Latham & Milone 1996, Stryker & Hrivnak 1984) are photometric surveys, most are of rather short (3-5 nights of observations) duration, and all have different photometric accuracy at the magnitude of the blue stragglers and, hence, differing degrees of sensitivity to photometric variations. The columns in the table show the number of blue stragglers monitored N_{BS} (according to the authors, or the number appearing in the survey's CMD), the number of binary blue stragglers[2] N_{bb}, detected by the survey, and the number of pulsating blue stragglers N_{pb}, observed. The number of monitored blue stragglers is somewhat arbitrary for some clusters (those marked with a '*') due to contamination from foreground stars. The numbers presented in this table are by no means complete: only a couple of the clusters have been surveyed over close to their entire area (e.g. ω Cen, M67) and none of the surveys are necessarily complete in their detections of variable blue stragglers, due to the duration of the observations and/or photometric accuracy.

According to the numbers in Table 2.1, the observed fraction of blue stragglers in globular clusters which are binary systems is $f_{bin} \sim 0.03$. This, however, is not the *true* fraction of binary blue stragglers: as mentioned above, a photometric search for binaries is completely dependent upon the chance alignment of the binary orbital plane near to the line of sight; this means that these surveys are sensitive only to a small fraction of all binaries. Also, because the chance of observing an eclipse decreases as the period of the binary increases, these same surveys are sensitive only to short period binaries. Because of these biases, the correction needed to estimate the true

---

[2]By 'binary blue stragglers' I mean 'blue stragglers which are one component of a binary system'.

Table 2.1: Blue Straggler Variability

Cluster	N_{BS}	N_{bbs}	N_{pbs}	Reference
Globular Clusters				
NGC 104(47 Tuc)	25	3	3	Edmonds *et al.* 1996
NGC 288	43	0	6	Kaluzny 1996
				Kaluzny*et al.* 1998
NGC 5053	27	0	5	Nemec *et al.* 1995
NGC 5139(ω Cen)	200	11	24	Kaluzny *et al.* 1996
				Kaluzny *et al.* 1997
NGC 5272(M3)	30	1	3	Nemec & Park 1996
	30	0	2	Guhathakurta *et al.* 1994
NGC 5466	47	3	6	Mateo *et al.* 1990
NGC 5904(M5)	24	0	1	Drissen & Shara 1998
NGC 6121(M4)	50	2	0	Kaluzny *et al.* 1997c
NGC 6366	27	0	0	Harris 1993
NGC 6397	49	0	2	Kaluzny 1997
	18	0	5	Rubenstein & Bailyn 1996
NGC6838(M71)*	10	0	0	Yan & Mateo 1994
Ruprecht 106	35	0	3	Kaluzny *et al.* 1995
Open Clusters				
NGC 188	14	0		Kaluzny & Shara 1987
NGC 2420*	3	0		Kaluzny & Shara 1988
NGC 2682	10	6	0	Latham & Milone 1996
	6	1	2	Gilliland *et al.* 1991
NGC 6802*	6	0		Kaluzny & Shara 1988
NGC 6819*	20	1		Kaluzny & Shara 1988
		1	1	Robb, Cardinal & Ouellette 1997
Melotte 66	6	0		Kaluzny & Shara 1988
Berkeley 39*	25	4	0	Kaluzny *et al.* 1993
Collinder 261*	40	10	0	Mazur *et al.* 1995
NGC 6791*	25	3	0	Rucinski *et al.* 1996
NGC 7789	8	0		Stryker & Hrivnak 1984

fraction of binary blue stragglers from the results of photometric surveys is large. Perhaps a better indication of the true binary fraction comes from spectroscopic surveys, such as that of Latham & Milone (1996): of the 10 blue stragglers they have monitored, 6 have turned out to be binaries with periods in the range of a few days to several years. Since spectroscopic surveys do not require as close an alignment of the orbital plane with the line of sight, and since velocity variations occur over the entire orbit, not just during eclipses, the size of the correction needed to estimate the true fraction of binary blue stragglers is smaller.

The fraction of blue stragglers in open clusters (OCs) which are apparently in binary systems is $f_{bin} \sim 0.16$ from all of the open cluster surveys noted in Table 2.1, or $f_{bin} \sim 0.13$ from only the photometric surveys. Comparison of the results from globular cluster surveys and open cluster surveys is more correctly done using only the results of the photometric surveys in open clusters, since no spectroscopic surveys for binary blue stragglers in globular clusters have been done, and the biases in the resulting photometric values for f_{bin} should be roughly the same. From the results of the photometric surveys, f_{bin} in open clusters is roughly four times that in globular clusters. Although part of this difference could be due to incompleteness in the surveys themselves, the change in f_{bin} from low density open clusters to high density globular clusters implies that the formation mechanism(s) for blue stragglers differs with the local stellar environment and/or cluster age.

For comparison, the fraction of stars that are eclipsing binaries in the solar neighbourhood is ~ 0.003 (Hut *et al.* 1992). The fact that the binary fraction in globular clusters is roughly ten times that observed locally points

to binaries and blue stragglers having some close connection.

Of those blue stragglers which are observed to be eclipsing binaries, roughly 50% are actually W Ursae Majoris (**WUMa**) stars which are *contact* binaries – binary stars in which the two components are orbiting within a common envelope made of material contributed from each star.

Spectroscopic surveys for blue stragglers in clusters are necessary to obtain a better understanding of the binary nature of blue stragglers. Milone & Latham (1994) have undertaken such a survey in several open clusters. To date, results for only one cluster, M67, have been presented, but they find that of the ten blue stragglers they have been monitoring, six are in binary systems – none of which are eclipsing binaries. Of these six binary systems that Milone & Latham have found, four are in eccentric orbits.

Stryker & Hrivnak (1984) obtained spectra for 7 blue stragglers in NGC 7789 and detected no radial velocity variations, on the basis of a comparison between observed and expected scatter in the derived velocities. Their observations were spread out over $\sim$ 300 days, but only roughly a dozen spectra were obtained per star. While their results are not as sensitive to long period binaries as those of Milone & Latham (1994), Stryker & Hrivnak should have easily detected shorter period binaries due to their much larger velocity amplitudes.

As will be discussed later, binarity among blue stragglers, and the properties of such binaries (e.g. period, eccentricity), are observations which can possibly be used to discern between different blue straggler formation mechanisms. Additionally, since it is possible that the binary properties of blue stragglers will change with environment, knowledge of the binary charac-

teristics in, say, globular cluster cores would also be useful (e.g. Edmonds *et al.*,1999).

2.1.3 Pulsating Blue Stragglers

An additional phenomenon which appears to have some connection to blue stragglers is pulsation. Within a fairly narrow, nearly vertical band in the CMD, called the *instability strip*, stars are potentially unstable to pulsations. Among the luminous giants, the classical Cepheids and W Virginis stars pulsate with periods ranging from $\sim 10 - 100$ days; on the horizontal branch (the location of the low mass, core helium burning stars), the RR Lyræ stars pulsate with periods of ~ 0.5 days; near the main-sequence, δ Scuti and SX Phœnicis stars pulsate with periods of $\sim 0.03 - 0.3$ days. The pulsating blue stragglers belong to either the δ Scuti or SX Phœnicis class of pulsating stars (collectively, these will be referred to as Dwarf Cepheids or **DCs**).

From Table 2.1, the fraction of blue stragglers that are observed to be pulsating is $f_{pb\delta} \sim 0.10$ in globular clusters and $f_{pb\delta} \sim 0.02$ in open clusters. Of those blue stragglers which are actually located in the instability strip, $\lesssim 30\%$ are actually observed to pulsate. Among stars in the solar neighbourhood with the same spectral type as the DCs, $\sim 30 - 50\%$ are observed to pulsate (Breger 1979), while virtually all of the giant stars located in the instability strip pulsate. The fact that all of the main-sequence stars located in the instability strip do not pulsate could be related to some physical process which stabilises those stars against pulsation. Alternatively, the pulsational amplitude of these stars might be too low to have been detected in the variability surveys.

Solano & Fernley (1997) have shown that the pulsation amplitude and rotation velocity of DCs are related in that those with low rotation velocities show a much broader distribution of pulsation amplitudes than those with high rotation velocities: fast rotators show very small pulsation amplitudes (< 0.10mag). It is possible that those stars in the instability strip which do not appear to pulsate are, in fact, fast rotators, and so have a small pulsation amplitude. However, Breger (1979) points out that many of the non-pulsators in the instability strip are spectroscopically anomalous Am stars, which are usually slow rotators. Kaluzny *et al.* (1997a) note that roughly 2/3 of the pulsating blue stragglers in their sample for ω Cen have pulsational amplitudes below 0.10 mag.

2.1.4 Rotation Rates

The rotation rates of normal main-sequence stars, like our Sun, are observed to be roughly correlated with spectral type: the average rotation velocity of early type stars (O and B) in the solar neighbourhood is $\overline{V}_{rot} \sim 200$ km/s; for mid-spectral types (A to early F) the average rotation velocity drops steadily with spectral type down to $\overline{V}_{rot} \sim 70$ km/s at spectral type F2; below spectral type F, the average rotation velocity drops rapidly below $\overline{V}_{rot} \sim 10$ km/s. Since blue stragglers have spectral types in the range of A to early F, we would expect them to be fairly rapidly rotating, with the average rotation velocity in the range of $\sim 100 - 180$ km/s. However, measured rotation velocities for blue stragglers typically fall below this.

Peterson *et al.* (1984) find that the rotation velocities of blue stragglers in M67 (NGC 2682) vary from 10 km/s to 120 km/s, with spectral types

from B8 to A8. Also, for a sample of field blue stragglers, Glaspey *et al.* (1994) found rotation velocities consistently below 100 km/s. Of course, when a rotation velocity is determined for a star, what is actually measured is $V_{rot} \sin i$ – the projection of the true rotation velocity. For the field stars, rotation velocities have been obtained for a large enough sample for each spectral type that a statistical correction can be applied to estimate the true rotation velocity ($i = 90°$). Applying a similar sort of correction to the *average* rotation velocity of blue stragglers shows that they are slightly slower than normal rotators (Mathys 1991). Of course, a complete survey — measuring rotation velocities of a large sample of blue stragglers in different environments — would be useful in this instance, especially since rotation may be one way to discriminate between possible formation mechanisms for blue stragglers.

The only reported observation of the rotation velocity of a blue straggler in a globular cluster (Shara *et al.* 1997) is $V \sin i = 155 \pm 55$ km/s for BSS-19 in 47 Tuc (Guhathakurta *et al.* 1992). This is high, but not necessarily unusual for its spectral type (A7V), nor is it rotating near to its estimated break-up velocity of ~ 410 km/s.

2.1.5 Chemical Abundances

Mathys (1991) analysed two of the M67 blue stragglers, F153 and F185, in detail. One of the two stars studied, F153, was classified as an Am star[3] while the other star, F185, was not strictly classified as an Am star, but

---

[3]The Am phenomenon is a chemical peculiarity among some A stars causing them to be underabundant in some elements (e.g. Ca, Sc, Si), relative to iron, while normal (or 'solar') in others. The driving mechanism is thought to be diffusion.

had some of the same peculiarities as F153. Mathys found that the two stars had nearly identical, roughly solar, abundances in most elements, except that F153 was extremely underabundant in calcium and scandium while F185 was underabundant in calcium, but not in scandium. An additional peculiarity of these stars is that, while the abundance of nitrogen is roughly solar, the total abundance of carbon, nitrogen and oxygen is lower than solar. Adding to the growing list of chemical peculiarities of these stars, they have O/N and C/N ratios similar to M67 giants which have brought nuclear processed material to their surface (the 'first dredge-up').

In addition to those peculiarities observed by Mathys (1991), Pritchet & Glaspey (1991) and Hobbs & Mathieu (1991) found that blue stragglers are underabundant in lithium, suggesting that some form of mixing of the surface layers of these stars has occurred. The depletion of lithium can be used as an indicator of mixing for these stars because, for normal, quiescently evolving stars in the same temperature range as the blue stragglers studied, the lithium abundance is expected to be enhanced, or depleted only slightly, by the effects of diffusion (Boesgaard, 1987) — the same holds for Am stars. However, lithium is destroyed at temperatures greater than $\sim 2.5 \times 10^6$K, so an observed depletion of lithium can be explained by the mixing of material from the interior to the surface of the star. Since the dredge-up of nuclear processed material during the ascent of the giant branch results in O/N and C/N ratios which are lower than those of main-sequence stars, the giant-like composition ratios observed by Mathys and the observed lithium depletion are strong indicators of some very deep mixing occurring during the blue straggler formation process. As concluded by Pritchet & Glaspey, all for-

mation mechanisms which do not involve some sort of mixing of material to the surface of the blue stragglers can be ruled out by these observations – at least for the M67 blue stragglers.

Very little is known about the surface abundances of any of blue stragglers other than those in M67 and a few field blue stragglers (e.g. Hobbs & Mathieu 1991, Glaspey *et al.* 1994). Similar studies of blue stragglers in globular clusters have yet to be done, although a low resolution spectroscopic study of six blue stragglers in ω Cen by Da Costa, Norris & Villumsen (1986) found no evidence for chemical peculiarities.

2.2 Formation Mechanisms

Several possible formation mechanisms for blue stragglers have been proposed since they were noted by Sandage (1953) in the globular cluster M3 and by Johnson & Sandage (1955) in the open cluster M67. This section will outline the proposed mechanisms and the evidence for and against each of them.

2.2.1 Foreground Contamination

Perhaps the simplest explanation for blue stragglers, at least those in clusters, is that they are not physically associated with the cluster at all, but are merely objects in the foreground; such objects could easily fall into the region on the CMD where blue stragglers are observed if they have the correct colour. Although such contamination of the blue straggler region does occur, especially for those clusters which lie near the galactic plane, many blue stragglers can be shown to be likely cluster members on the basis of proper motion or radial velocity studies (e.g. Girard *et al.* 1989, Milone &
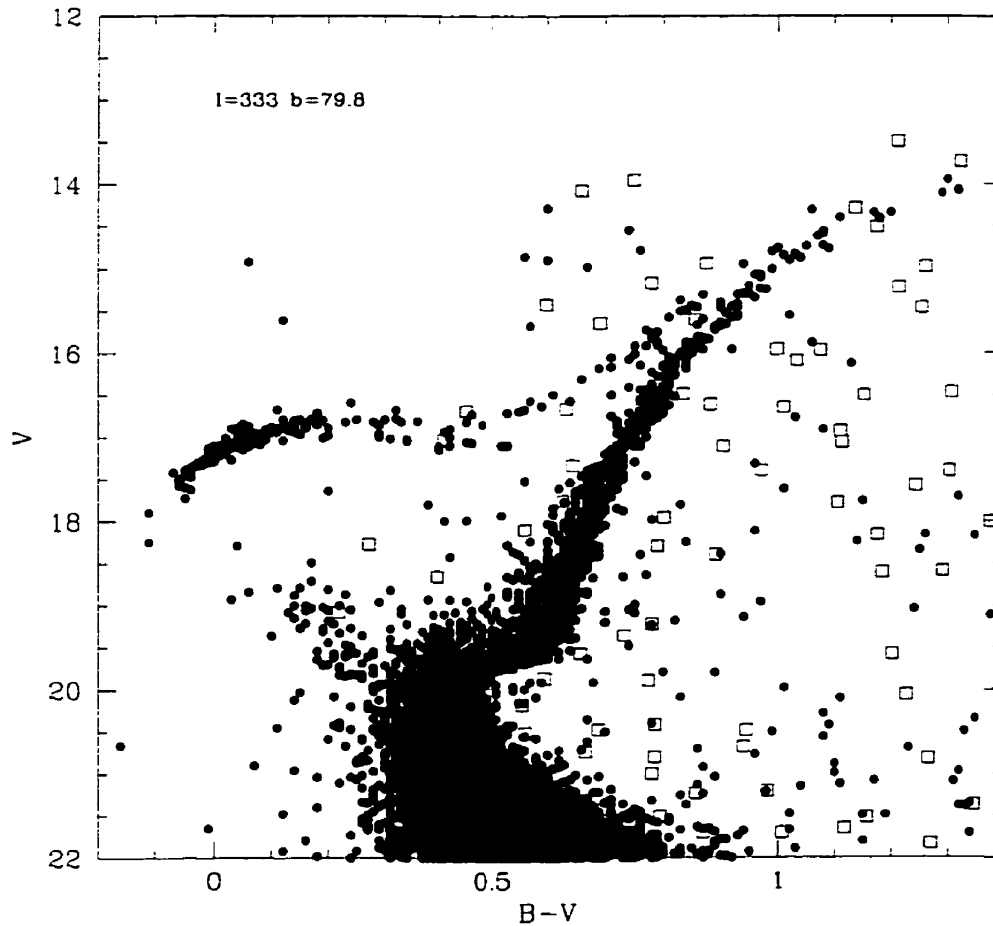
Figure 2.3: Example of foreground contamination for NGC 5024 (l=333, b=79.8) using the Bahcall & Soneira (1984) model. The distribution of model 'foreground stars' (*open squares*) were found by finding the predicted number of stars, using Bahcall & Soneira model, within small (0.1 × 0.5) colour-magnitude bins and then randomly distributing the appropriate number of points within each bin. The field size which was observed is 12' × 13'; the observed CMD for NGC 5024 is plotted with *filled circles* (Rey *et al.*, 1998).
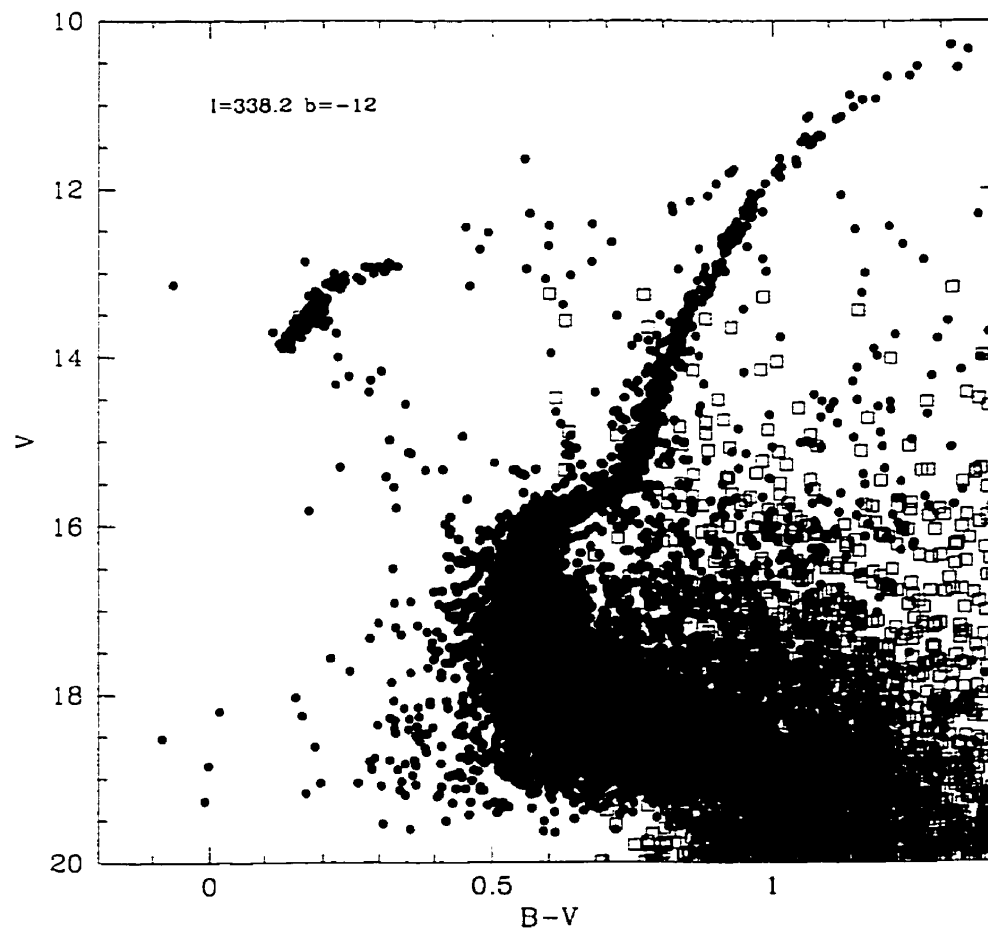
Figure 2.4: Same as Figure 2.3, except for NGC 6397 (l=338.2,b=-12). The field size is 13′ × 13′ (Kaluzny, 1997).
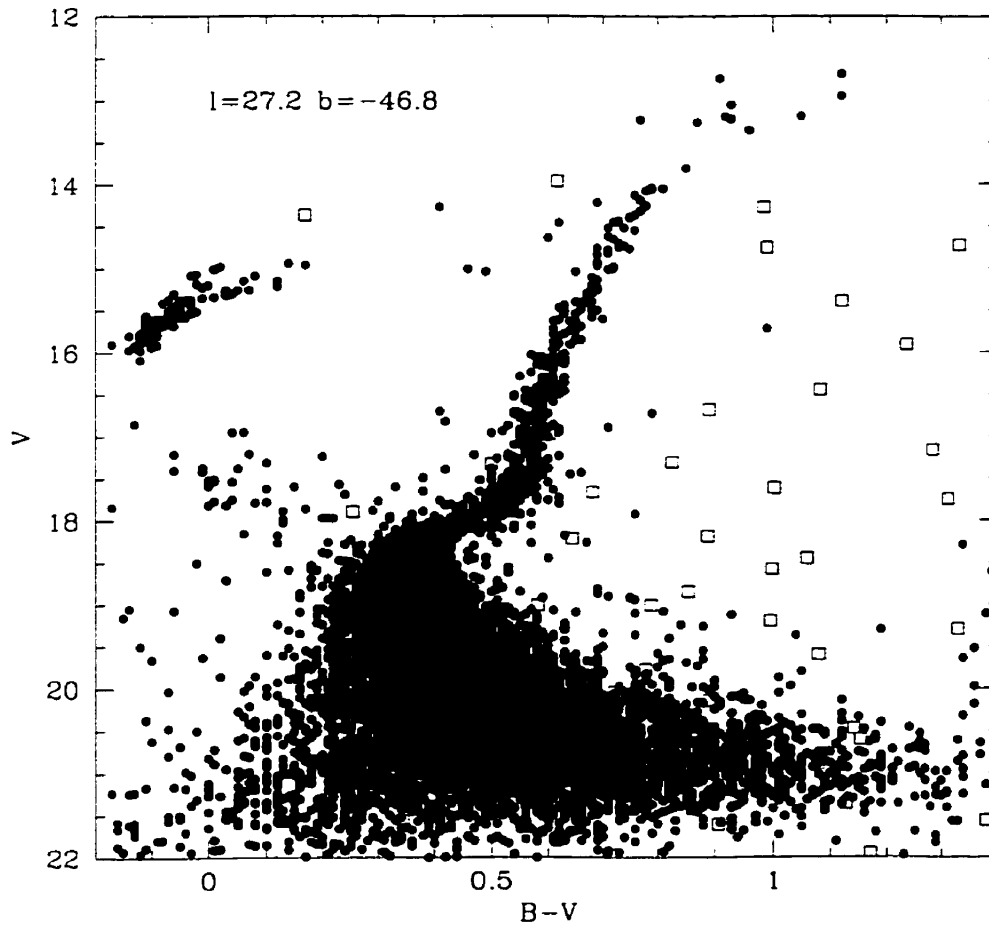
Figure 2.5: Same as Figure 2.3, except for NGC 7099 (l=27.2, b=-46.8). Field size is 5.1 square arc-minutes (Guhathkurta *et al.*, 1998).

Latham 1994). For clusters at high galactic latitudes, the probability of con-
tamination by bright, blue, foreground objects can account for only a small
fraction of observed blue stragglers.

The Bahcall & Soneira model of the Galaxy can be used to predict the
number of stars per square arc-minute as a function of Galactic latitude and
longitude. In essence, the model assumes scale lengths and stellar densities
for the Galactic disk, bulge, and halo, and assigns appropriate luminosity and
colour functions to each component: integrating along the line of sight gives
the numbers and apparent magnitudes of stars. Figures 2.3,2.4, and 2.5 show
the CMDs for NGC 5024 (Rey *et al.*, 1998), NGC 6397 (Kaluzny, 1997), and
NGC 7099 (Guhathkurta *et al.*, 1998), respectively, with the predicted distri-
bution of foreground stars also plotted. While the Bahcall & Soneira model
over-predicts the number of stars at small ($|b| < 20°$) Galactic latitudes, the
predictions are reasonable for higher latitudes. For the three clusters shown
here, the number of foreground stars predicted in the blue straggler region
is obviously smaller than the observed number of stars, suggesting that the
blue stragglers observed in these clusters are not foreground stars.

2.2.2 Delayed Star Formation

Since blue stragglers are apparently younger than the rest of the stars in their
parent clusters, one obvious explanation is that they formed more recently
than the rest of the stars in the cluster. If this mechanism is acting in a
cluster, then the blue stragglers should be, except for their anomalous age,
presumably normal stars: they should possess normal abundances, binary
properties, rotation rates, *etc.*.

For very young clusters, those younger than a few times 10^8 years, the gas and dust necessary to form blue stragglers is observed between the existing cluster stars. However, in globular clusters, little or no gas or dust is observed (e.g. Smith *et al.* 1995, Borkowski et al. 1991, Lynch & Rossano 1990, Bowers *et al.* 1979, Troland *et al.* 1978) from which to form future generations of blue stragglers.

Also, at least in M67, blue stragglers do not have 'normal' surface abundances or rotation properties, as noted in the previous section. The binary fraction of blue stragglers, in both globular clusters and open clusters, is also anomalously high when compared to that of normal stars.

2.2.3 Chemical Mixing and Non-thermal Pressure Support

Sandage (1953) noted that the blue stragglers in the globular cluster M3 were located in the CMD where one would expect to see stars which were evolving toward the helium burning main-sequence. Later, Wheeler (1979) and Saio & Wheeler (1981), found that stars which were undergoing some form of internal mixing, or were being acted upon by some form of non-thermal pressure support, would evolve through the blue straggler region of a cluster's CMD. There is some observational support for internal mixing: the anomalous chemical abundances observed in the M67 blue stragglers *might* be explained by large scale mixing. Non-thermal pressure support might be caused by rotation, or perhaps by magnetic fields.

It is fairly difficult to disprove the claim that there is some arbitrary mechanism acting to mix a blue straggler's interior, or providing some ad-

ditional support for the star. It is, however, difficult to explain the source of the mechanism itself. One possible source of either large scale mixing or pressure support is large magnetic fields – blue stragglers are not observed to have large magnetic fields. Rapid rotation could provide pressure support and perhaps mix the star through meridional currents – blue stragglers are observed to be slower than average rotators.

Additionally, Schoenberner & Napiwotzki (1994) have shown, based on surface gravity and temperature measurements, that blue stragglers should have fairly normal internal structures: a result which would not be expected if the stars were evolving homogeneously or were receiving some form of non-thermal pressure support. Ouellette & Pritchet (1996, 1998) have shown that the distribution of the majority of blue stragglers in the CMD is readily explained by stars which are not highly mixed during their formation, and that it is unlikely that rotation can be greatly prolonging their observable lifetimes.

2.2.4 Binary Mass Transfer

If the separation of two stars in a binary system is small enough, it is possible that one star may eventually transfer some of its mass to its companion. Mass transfer is observed to occur in many close binaries and it is possible that the mass gainer in such a system would eventually appear as a blue straggler (McCrea 1964, Giannuzzi 1984). In fact, many binary blue stragglers are observed to be in contact systems and semi-detached systems (discussed earlier) which are undergoing mass transfer. Additional direct evidence for mass transfer as a source of blue stragglers comes from the evolved blue

straggler S1040 in M67 (Landsman *et al.* 1997): this star has a hot, helium white dwarf companion in an orbit which is close enough that the stars must have exchanged mass as the primary (now the white dwarf) evolved from the main sequence.

Binary mass transfer occurs in three flavours which depend on the evolutionary state of the primary: Case A mass transfer occurs when the primary is still burning hydrogen in its core; Case B mass transfer occurs when the primary's main energy source is a hydrogen burning shell surrounding an inert helium core; Case C transfer occurs when the primary is undergoing helium burning or a later burning stage. Case A transfer will, except under a few circumstances, result in the coalescence of the two stars; this is different enough from the other two cases that it will be discussed in a later section on binary coalescence (Webbink, 1976, 1977).

After a mass transfer episode, the resultant blue straggler should be left with a distant, low mass companion which should be detectable through the radial velocity variations of the blue straggler. The type of remnant left by the mass donor depends on its evolutionary state when the mass transfer commences: a helium white dwarf should remain after Case B mass transfer, and a CO white dwarf should be left after Case C mass transfer – if the mass transfer is incomplete, (i.e. the former primary is not stripped to the inert core) a hydrogen/helium atmosphere will be retained by the remnant.

In addition to a stellar remnant as a companion, the newly formed blue straggler will possess anomalous surface abundances: as mass is stripped from the donor, nuclear processed material is exposed and transferred. This should result in a depleted lithium abundance, CNO abundance ratios typical

of evolved stars, and perhaps a slightly increased surface helium abundance – all of which (except, perhaps, an increased helium abundance) have been observed in blue stragglers. On the other hand, it is possible that circulation currents, initiated by the accretion itself, may act to mix the envelope of the accreting star (Sarna 1992) which might lessen the chemical peculiarities.

One limitation of the binary mass transfer mechanism is that the maximum mass for a blue straggler formed in this way is twice the cluster's turnoff mass. Most blue stragglers are observed (or inferred) to have masses less than this; however, there are possible exceptions (notably F81 in M67 which appears to have a mass roughly 2.5 times the cluster turnoff mass).

Except for Case A mass transfer, binary mass transfer will not necessarily result in a remnant which is rapidly rotating.

The process of mass transfer (and, hence, angular momentum transfer) will tend to circularise the orbit of a binary; hence, we should expect that any binary blue stragglers created by mass transfer should have very nearly circular orbits. Of the six M67 binary blue stragglers studied by Latham & Milone (1996), two have eccentricities consistent with being circular, while the other four are in highly eccentric orbits. One possibility for explaining these highly eccentric binaries in the mass transfer scenario is that their orbits have been perturbed by other stars in the cluster. Leonard (1996) examined this possibility, using the results of Rasio & Heggie (1995), and found that the induced eccentricity would be on the order of 10^{-3} for a typical binary blue straggler in M67. However, Leonard misinterpreted the results of Rasio & Heggie: the eccentricities produced by their results are *per* encounter with a perturbing star. Since a binary in the core of a cluster, even an open cluster

such as M67, could undergo many such encounters during the lifetime of a blue straggler, and since the incremental increase in the eccentricity is proportional to the eccentricity itself, the eccentricity of an initially circular, albeit wide, binary could become quite significant.

Webbink (1976, 1977) has made an extensive study of the effects of mass loss and accretion on the components in a binary system. In summary, stars with radiative envelopes (or very thin, $\lesssim 5\% M_*$ by mass, convective envelopes) tend to expand in response to mass accretion and contract in response to mass loss; stars with very deep convective envelopes tend to contract in response to mass accretion (the convective envelope also deepens) and expand in response to mass loss. During Case B and Case C mass transfer, the primary will have a deep convective envelope, resulting in rapid mass loss. If the secondary overflows its Roche lobe, the system will enter a common envelope stage which may result in a large fraction of the material lost from the primary being ejected from the system ($\sim 50\%$; Sandquist et $al.$ 1998, Terman & Taam 1996). If the secondary remains within its Roche lobe, a large fraction of the material lost from the primary will be accreted and the secondary will become a blue straggler with a white dwarf companion. The new blue straggler will appear highly mixed, due to the high helium abundance of the material accreted from the evolved primary. Whether a significant fraction of the mass lost from the primary is ejected from the system or accreted by the secondary is determined by the rate at which mass is lost from the primary and by the ability of the secondary to accommodate the rate of accretion. Regardless of the outcome, if the secondary begins a new life as a blue straggler, it will be as one with a degenerate companion

(the core of the former primary) and with unusual surface abundances (most notably a high helium abundance).

2.2.5 Binary Coalescence

Case A mass transfer in binary stars is somewhat of a special case since it leads to a different class of remnant than either Case B or C mass transfer – a single star, rather than a binary. As the primary slowly expands to fill its Roche lobe (or the Roche lobe decreases in volume due to angular momentum losses from the binary system) mass is transferred to the secondary star. Eventually, the secondary overflows its Roche lobe, either due to its Roche lobe shrinking as the orbit shrinks or by a rapid expansion in response to the mass accretion (Webbink 1976,1977), and the net mass transfer reverses direction. The size of the orbit will then increase as mass is transferred from the secondary to the primary. However, the orbit at this point will be too small to accommodate the primary as it evolves off the main-sequence – eventually, the two stars must coalesce. Also, when the mass ratio $(M_{secondary}/M_{primary})$ becomes less than ~ 0.10, an orbital instability develops and the two stars merge on a very short timescale (Rasio, 1995).

Assuming that there is little mass loss, the total angular momentum of the original binary will be contained in the single remnant after coalescence – hence, it should be a very rapidly rotating object. However, the assumption of no mass loss is probably not correct – as the two stars merge, mass loss through the outer Lagrangian points will likely occur, removing angular momentum from the system. Also, because the direction of mass transfer is eventually from the unevolved component to the evolved one, the chemical

peculiarities should be less pronounced than those after Case B or Case C mass transfer.

There is some evolutionary evidence which supports the hypothesis that coalesced stars are related to blue stragglers: Mateo *et al.* (1990) compared the observed fraction of blue stragglers in NGC 5466 which are in contact systems with that expected from the theoretical lifetime of a contact system and the lifetime of a blue straggler. Mateo *et al.* assumed a contact lifetime of $\sim 5 \times 10^8$ years (as a rough median value between theoretical extremes of 5×10^7 and 5×10^9 years required for contact systems to coalesce) and a blue straggler lifetime of $\sim 7 \times 10^9$ years (from the isochrones of VandenBerg & Bell, 1985) and found that the ratio of these ($\simeq 0.07$) agreed remarkably well with the observed ratio of $3/47 (\simeq 0.064)$ for the number of contact binaries/total number of blue stragglers. If correct, this suggests that the observed number of blue stragglers is not inconsistent with all of the blue stragglers in NGC 5466 having been formed by binary coalescence. However, as the models of Ouellette & Pritchet (1998) show, the average blue straggler lifetime used in the above calculation is an overestimate by a factor of as much as two to five. So, either the lifetime of a contact system is much shorter than that assumed by Mateo *et al.*, or only $10\% - 50\%$ of blue stragglers in globular clusters are formed by contact systems.

A similar argument to that above can be made for Case B and Case C mass transfer, during which the binary would appear as a semi-detached system. Of the 11 binary blue stragglers in ω Cen[4], two are in a semi-detached phase (the other nine are contact systems). The ratio of semi-

---

[4] ω Cen is used here purely because of the large number of observed binary blue stragglers.

detached systems to the total number of blue stragglers ($\sim$ 200, see Table 2.1) is $\sim$ 1%, compared to the ratio of the lifetime of a system undergoing Case C or Case B mass transfer, $\lesssim$ 1Gyr, to the average lifetime of a blue straggler, $\sim$ 1Gyr. Hence, roughly 1% of the blue stragglers in ω Cen can be explained by Case B or Case C mass transfer.

2.2.6 Stellar Collisions

The stellar density in the cores of some globular clusters is high enough that a significant number of collisions between single stars should have occurred over the lifetime of the clusters (Hills & Day 1976). The fact that we see many blue stragglers in the centres of the densest clusters lends support to this (e.g. Guhathakurta *et al.* 1992, Lauzeral *et al.* 1992). In addition, Hoffer (1983) and Leonard (1989) have shown that, if even a small fraction of the stars in a cluster are binaries, the rate at which collisions occur is greatly enhanced by the increased physical cross-section (essentially the semi-major axis of the binary) and the additional gravitational focusing due to the larger mass of the bound pair.

Leonard (1996) noted that the high frequency of binaries observed among blue stragglers (e.g. Kaluzny et al. 1997, Kaluzny 1997, Edmonds et al. 1996) could be accounted for by binary-binary interactions. A dynamical encounter that is strong enough to result in a direct collision between two of the component stars is also likely to result in a third star being captured into an eccentric orbit around the newly formed blue straggler. As noted earlier, very little is known about the orbital parameters of binary blue stragglers in globular clusters, but four out of the six binary blue stragglers in M67 which

have been studied by Latham & Milone (1996) are in highly eccentric orbits.

Whether a stellar collision is the result of an encounter between two single stars or two binaries, the actual impact parameter of the collision is essentially random: the collision will occur, on average, off the axis connecting the centres of the two stars. Angular momentum conservation then requires that the resultant merger remnant be rapidly rotating.

Early attempts to model the hydrodynamics of the collision itself (Benz & Hills 1987,1992) found that the material from the two parent stars could be highly mixed throughout the merger remnant. In a collision between two equal mass stars, Benz & Hills found that the remnant was a homogeneous mixture of the material from the parent stars: this results in a chemically homogeneous merger remnant, producing what is essentially a zero-age main-sequence (**ZAMS**) star. After a collision involving two unequal mass stars, the material from the less evolved, low mass parent star will have settled to the core of the merger remnant; the material from the high mass star will have been mixed throughout. Again, the result of such a merger results in a remnant which resembles a ZAMS star, due to the increased hydrogen content in the core.

Lombardi, Rasio & Shapiro (1996, hereafter **LRS**) found that the high degree of mixing which Benz & Hills had observed in their merger remnants was largely an artifact of their choice of $n = 3/2$ polytropes as approximations to GC stars. LRS noted that evolved globular cluster stars would be more centrally condensed than $n = 3/2$ polytropes and so chose to use $n = 3$ polytropes to approximate the structure of turnoff stars, and $n = 3/2$ polytropes for lower mass stars. Smoothed particle hydrodynamic (**SPH**)

simulations using these approximations demonstrated that there should be little or no hydrodynamical mixing during a stellar collision. So, in fact, the remnant should start its new existence as a blue straggler as a slightly evolved star.

Both Benz & Hills and LRS found that the remnant of a stellar collision would be swollen to pre-main sequence sizes after the collision. Leonard & Livio (1995) noted that this provided a possible solution to the discrepancy between the observed blue straggler rotation velocities and those predicted by the collisional merger scenario: if the swollen merger remnant truly does resemble a pre-main sequence star, it should possess a thick convective envelope, providing a possible mechanism for angular momentum loss and slowing the star's rotation.

The highly convective, pre-main sequence phase hypothesised by Leonard & Livio would have the additional consequence that the star should become highly mixed: fresh, hydrogen-rich material should be brought to the core, while nuclear processed material should be dredged-up to the surface. Bailyn & Pinsonneault (1995) and Sills, Bailyn & Demarque (1995) found that such a high degree of mixing is needed to explain the colours and luminosities of blue stragglers seen in some globular clusters. On the other hand, Ouellette & Pritchet (1996,1998) found that blue stragglers tend to avoid the ZAMS and that a high degree of mixing during a pre-main sequence phase is essentially ruled out for most blue stragglers by their distribution on the CMD.

In a similar fashion to that of Mateo et al. (1990), Leonard & Fahlman (1991) found that the rate of production of blue stragglers in the globular cluster NGC 5053 needed to be at least one blue straggler every 2.5×10^8

years, assuming that the average lifetime of a blue straggler is $\sim 6 \times 10^9$ years. From their scattering experiments, a strong binary-binary interaction should occur every $\sim 2.2 \times 10^7$ years, with only 1 in 20-40 such interactions actually resulting in a stellar collision. As noted earlier, the blue straggler lifetime assumed here is a overestimate, if the calculations of Ouellette & Pritchet (1998) are correct. Using a more accurate estimate for the average blue straggler lifetime ($\sim 1 \times 10^9$ years), the production rate becomes one blue straggler every $\sim 4.1 \times 10^7$ years. This implies, using Leonard & Fahlman's rate for binary-binary interactions, that roughly 1 in 2 encounters eventually leads to the production of a blue straggler.

Even though not every strong dynamical encounter will result in a stellar collision, any strong interaction may result in the production of a blue straggler. Sigurdsson & Phinney (1993) found that 'near misses' would produce a gradual hardening of a binary by transferring angular momentum from the binary to the passing star. Potentially, a binary could be hardened to the point where mass transfer, or binary coalescence, becomes a possibility. Also, Sigurdsson & Phinney found that the probability that the two most massive stars involved in a strong interaction would be exchanged into a binary — a binary with less net angular momentum than the original one — is higher than the probability of a significant angular momentum transfer to a passing star.

Chapter 3

Development of Models

The main goal of this work is to develop and evolve models of the remnants of stellar collisions. This chapter focusses on the development of these models, and discusses them in relation to what we know about the physical characteristics of blue stragglers — much of the work in this chapter has already been discussed in Ouellette & Pritchet (1998). In addition to these models, simple models of the remnants of binary mass exchange and binary coalesence are also developed.

It should be noted that all calculations of stellar evolutionary tracks in this work were done using a modified version of D. A. VandenBerg's stellar evolution code (VandenBerg *et al.*, 1999).

3.1   Remnants of Stellar Collisions

As mentioned earlier (Section 2.2.6), Lombardi, Rasio & Shapiro (1996) (**LRS** hereafter) have studied stellar collisions by performing smoothed particle hydronamic (**SPH**) simulations of colliding polytropes. Their results showed that little, if any, hydrodynamical mixing occurred during the col-

lision. The composition profiles of their merger remnants can be described as a stratification of the stellar material during the collision: the gas from the parent stars settles in the merger remnant such that the profile of the entropy-like quantity $A = P/\rho^{5/3}$ (hereafter referred to as "hydrodynamic entropy") increases from the core of the remnant outward. This hydrodynamic entropy stratification ("hydrodynamic stratification") can result in some unusual chemical profiles (as shown by LRS), but also allows some prediction of the chemical profile of a collisional remnant — which will be used in the creation of our models.

The collisions studied by LRS were between equal mass polytropes and unequal mass polytropes, for a variety of different masses. We have chosen here to model only mergers between equal mass stars and mergers between a turnoff star and a lower mass star. Throughout the rest of this work, we will refer to these merger events as "equal-mass mergers" and "turnoff mergers", respectively. Although there are any number of possible combinations of parent star masses which would result in a particular merger mass between $1M_{TO}$ and $2M_{TO}$, the mergers considered here represent the extremes of hydrogen content: equal mass mergers will result in the highest possible hydrogen content for a particular merger mass, whereas turnoff mergers will result in the lowest possible hydrogen content. For example, to model a $1.20M_\odot$ collisional merger, two models will be created and evolved: an equal-mass merger using two $0.60M_\odot$ stars, and a turnoff merger involving a turnoff mass star ($0.874M_\odot$ for a 12 Gyr old cluster with an [Fe/H] of -0.83) and a lower mass star ($0.326M_\odot$). The total hydrogen content in the equal-mass merger is higher (mass-averaged hydrogen mass fraction, $\bar{X} = 0.729$) than

that in the turnoff merger ($\bar{X} = 0.655$).

3.1.1 Predictions from Hydrodynamic Stratification

In their simulations, LRS approximated main-sequence turnoff stars by $n = 3$ polytropes while lower mass stars were approximated by $n = 3/2$ polytropes or composite polytropes. Their initial polytropic models had hydrodynamic entropy and density profiles similar to those shown in Figure 3.1. During a collision involving an $n = 3$ polytrope (approximating a $\sim 0.80 M_\odot$, main-sequence turnoff star) and a $n = 3/2$ polytrope (approximating a $M \leqslant 0.40 M_\odot$, lower main-sequence star), hydrodynamic stratification predicts (LRS) that the material of the lower mass, and presumably less evolved, $n = 3/2$ polytrope will settle into the core of the merger remnant, bringing with it a fresh supply of hydrogen (Figure 3.2). The subsequent evolution of the merger remnant will be strongly affected by the amount of hydrogen brought into the core by the hydrodynamic stratification. This stratification of the material also provides a simple explanation of why no nuclear processed material is brought to the surface of the merger remnant during a collision.

If the hydrodynamic entropy of the stellar gas is not modified during a collision, the distribution of the parent stars' material throughout the merger remnant can be found using the hydrodynamic entropy profiles in Figure 3.1 — this leads directly to the merger remnant's chemical profile if those of the parent stars are also known. However, shock heating during the collision can modify the hydrodynamic entropy of the gas depending on the dynamics of the collision and the form of viscous dissipation chosen for the hydrodynamic
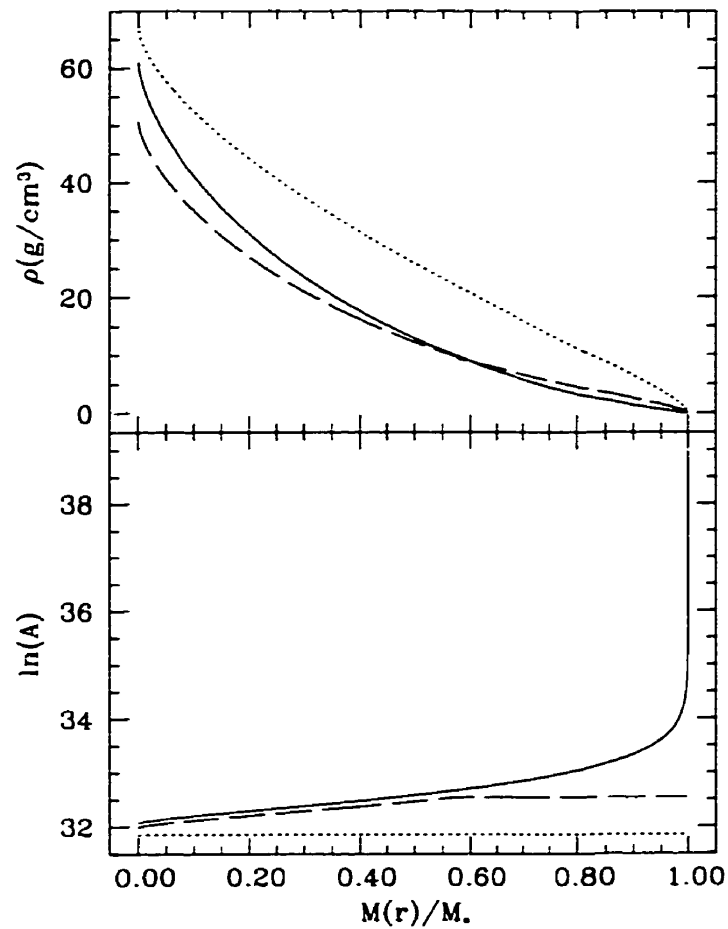
Figure 3.1: Density (ρ) and entropy (A) profiles for representative polytropes. Shown are profiles for $0.80M_\odot$ (solid line, $n = 3$, $R = 1.0R_\odot$), $0.60M_\odot$ (dashed line, $n = 3$, $R = 0.56R_\odot$), and $0.40M_\odot$ (dotted line, $n = 3/2$, $R = 0.37R_\odot$) polytropes, calculated using the radii and polytropic indices given. The $0.6M_\odot$ composite polytrope has an $n = 3$ core and an $n = 1.5$ envelope with the boundary between the two located at $R_{bnd} = 0.29R_\odot$.
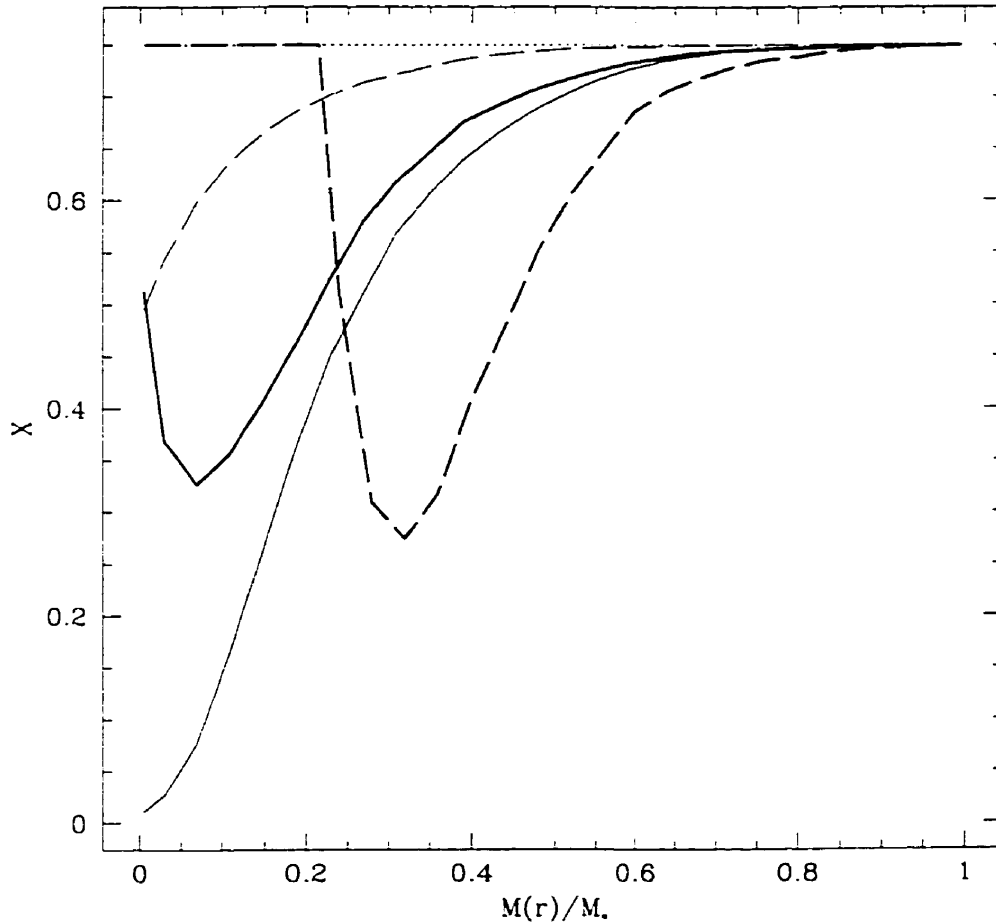
Figure 3.2: Hydrogen mass fraction (X) profiles for mergers between polytropes shown in Figure 3.1 (from LRS). Thick solid line: profile for a merger between a $0.80M_\odot$ polytrope and a $0.60M_\odot$ polytrope; thick dashed line: profile for a merger between a $0.80M_\odot$ polytrope and a 0.40 $M_\odot$ polytrope; thin solid line: profile for the $0.80M_\odot$ polytrope ; thin dashed line: profile for the $0.60M_\odot$ polytrope; thin dotted line: profile for the $0.40M_\odot$ polytrope.

simulations (LRS). During relatively gentle collisions, such as the head-on, parabolic collisions studied by LRS, little shock heating will occur and so the hydrodynamic entropy of the gas at the time of the collision can be used to determine the final merger profile.

3.1.1.1   Stellar Collisions versus Polytropic Collisions.

During the previous discussion we have tried to stress that the simulations of LRS and Benz & Hills (1987, 1992) describe *polytropic* collisions. The reason for this pointed emphasis is that stars, especially evolved ones in globular clusters, are not polytropes.

The structure of a polytrope is given by

$$P(r) = K\rho(r)^{(1+1/n)} \tag{3.1}$$

where P is the pressure, ρ is the gas density, n is the polytropic index and K is a constant. Using this relationship as a constraint, $\rho(r)$ and K can be found using only two of the equations of stellar structure: the equations of hydrostatic equilibrium and mass continuity. For a simple polytrope, the molecular weight μ is uniform throughout the star, in which case both K and n are also constants. This allows the structure of the polytrope to be determined with no information about sources of opacity or nuclear processes. Polytropes are, by definition, in hydrostatic equilibrium, but are not necessarily in thermal equilibrium.

The hydrodynamic entropy profile of a polytrope can be found by assuming a pressure equation of state of the form

$$P = A\rho^{\Gamma_1}, \tag{3.2}$$

where Γ_1 is one of the adiabatic exponents and is defined by

$$\left(\frac{d\ln P}{d\ln\rho}\right)_{ad} = \Gamma_1, \tag{3.3}$$

where the subscript *ad* refers to purely adiabatic changes. If radiation pressure within the gas can be ignored then, for an ideal, monatomic gas, $\Gamma_1 = \gamma = c_P/c_V = 5/3$. Equating the pressure from the polytropic structure to the pressure from the equation of state yields A throughout the gas. The relationship between the thermodynamic entropy S and A can be found by integrating the first law of thermodynamics, $TdS = dU + PdV$, using the definition of γ and Equation 3.2. This yields (Appendix B)

$$S = \frac{N_0 k}{\mu\gamma}\ln A + const \tag{3.4}$$

where N_0 is Avogadro's number and k is Boltzmann's constant. From the form of the polytropic structure equation (Eq. 3.1) and the equation of state (Eq. 3.2), if $1 + 1/n$ is not equal to γ, then A, and hence the entropy S, will not be uniform throughout the star. Polytropes with $n = 3/2$ will have $1 + 1/n = \gamma$ and so will have constant entropy, S.

Polytropes are reasonable approximations to zero-age main sequence (ZAMS) stars since they, like polytropes (as defined above), are chemically homogeneous, or at least nearly so. As pointed out by LRS, $n = 3$ polytropes approximate the structure of radiative stars while $n = 3/2$ polytropes have a structure similar to that of fully convective stars. However, although globular cluster turnoff stars are radiative, they are far from being chemically homogeneous. Figure 3.3 shows the hydrodynamic entropy and density profiles for a globular cluster turnoff star and two lower main-sequence stars for a cluster like 47 Tuc. The differences between the hydrodynamic entropy and density

profiles of globular cluster stars and the polytropes shown in Figure 3.1 are largely due to the chemical inhomogeneity of the globular cluster stars. The increased molecular weight toward the centre of an evolved star results in a lower pressure at a fixed density and temperature, requiring the star to adjust its internal structure to maintain hydrostatic equilibrium. A lower pressure at a constant density results in a decrease in the hydrodynamic entropy, A.

The decrease of the hydrodynamic entropy in the core of an evolved star will directly affect the final chemical profile of a merger found through hydrodynamic stratification. From Figure 3.3, it is obvious that no material from a low mass star will be able to penetrate to the core of a main-sequence turnoff star, leaving the merger remnant with a helium-rich core, unlike the collision between two equivalent polytropes (Figure 3.4). The evolution of two such merger remnants would be completely different if no mixing takes place in a subsequent convective phase of evolution.

Comparison of Figures 3.1 and 3.3 shows that an $n = 3$ polytrope underestimates the central density of a turnoff star by more than a factor of ten. This in itself is enough to argue that no hydrogen-rich material from a lower mass star will penetrate to the core of a merger involving a turnoff star and a lower main-sequence star (an turnoff merger in our terminology). Hydrodynamic stratification of the material during such a collision will produce a merger remnant with a dense, helium-rich core.

A collision involving equal mass stars or one involving equal mass polytropes should produce a merger remnant with a composition profile nearly identical to those of the parent stars.
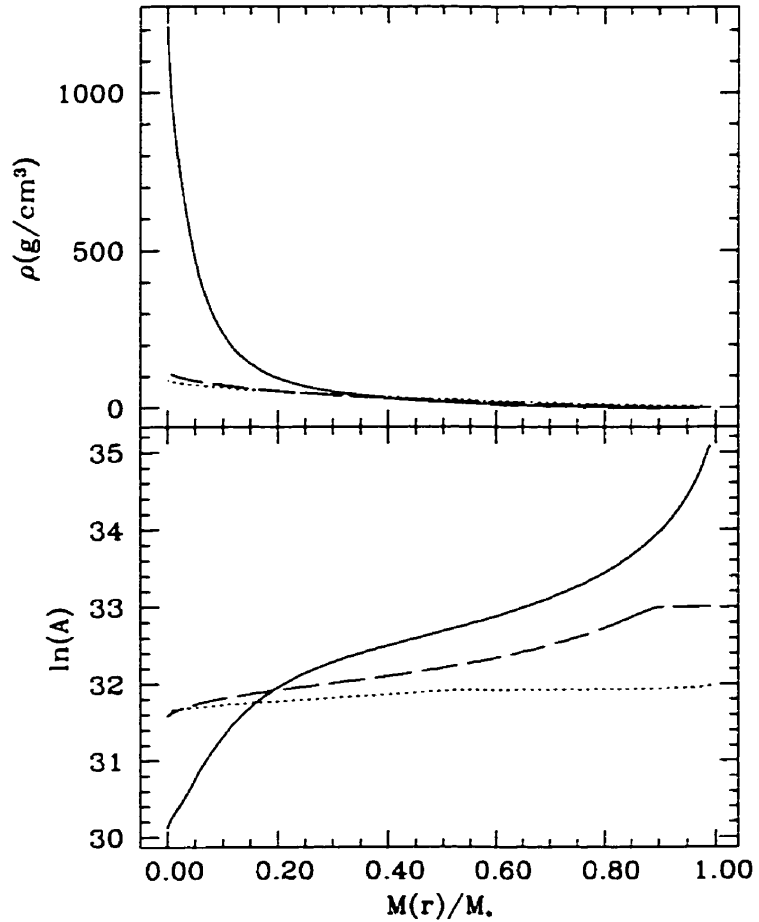
Figure 3.3: Density (ρ) and hydrodynamic entropy (A) profiles for real globular cluster stars. Shown are profiles for $0.874M_\odot$ (solid line), $0.60M_\odot$ (dashed line), and $0.40M_\odot$ (dotted line) stellar models at an age (12 Gyr) and metallicity ([Fe/H]=-0.83) appropriate for 47 Tuc.
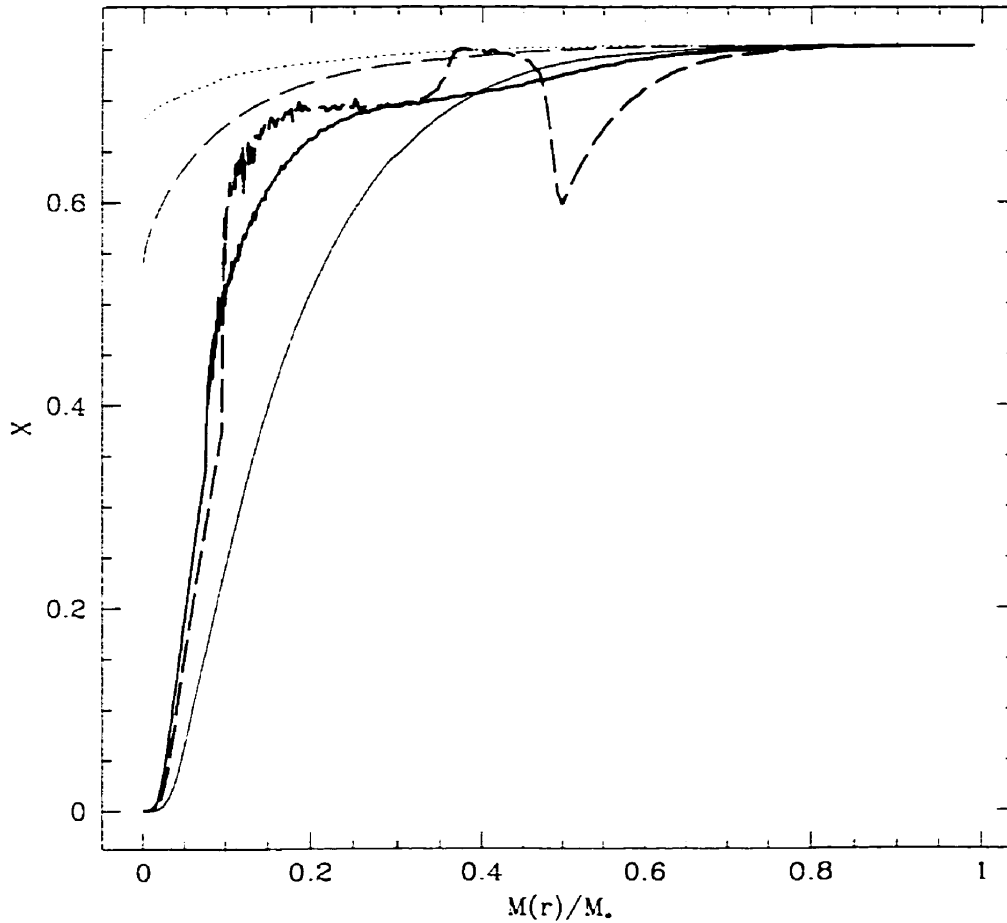
Figure 3.4: Hydrogen mass fraction (X) profiles for mergers between the stars shown in Figure 3.3. The thin lines refer to the same stars as shown in Figure 3.3. The thick solid line shows the hydrogen mass profile for the remnant of a collision between the $0.874M_\odot$ and $0.60M_\odot$ stars; the thick dashed line shows the profile for the remnant of a collision between the $0.874M_\odot$ and $0.40M_\odot$ stars.

3.1.2 Physical Structure of Merger Remnants.

Leonard & Livio (1995) have suggested that a blue straggler formed through a stellar collision would resemble a pre-main sequence star immediately after the collision. The SPH simulations of LRS show that the remnant of a collision involving two polytropes can be several times larger than either of the parent stars; however, unlike a pre-main sequence star, the central density of the remnant will be much higher than that found on the Hayashi track. The decrease in central density of polytropic mergers relative to the parent stars is generally less than 50%, and is as little as ~10% in head-on mergers (from the simulations of LRS). Because of the size and dense core of a merger remnant, it will more closely resemble a red giant branch star than a star on the Hayashi track.

3.2 Construction of Initial Models.

Despite the facts that the hydrodynamic simulations of LRS use polytropes rather than evolved stars, and that the differences between the two species of objects can be extreme, their results can be used as the basis for producing models for input into a stellar evolution code. Hydrodynamic entropy stratification of the material, which is a direct consequence of the dynamics of the fluid interaction and a requirement for the SPH fluid stability (see LRS for a discussion), can be used to predict the chemical profile of the merger remnant. Although there is no equivalent procedure for predicting the density profile of the remnant, the simulations of LRS show that the central density will not, in general, be much lower than that of the parent stars — this can

be used as an additional constraint when constructing models.

Since head-on collisions of stars on parabolic orbits are relatively gentle, they are also the easiest to approximate. We have chosen to ignore mass loss during the collision, the effects of rotation and the departure from spherical symmetry it produces. Because head-on collisions produce the least amount of mass loss and lowest rotation rates, these approximations are reasonably valid. We have also chosen to ignore shock heating during the collision and use the pre-collision hydrodynamic entropy profiles of the parent stars to define the chemical profile of the merger product using hydrodynamic stratification. The amount of shock heating during a head-on collision is small (LRS) and so should not strongly affect the end result.

The initial models to be used to investigate blue straggler evolution were formed in three steps from a series of standard stellar models of the appropriate age and metallicity. First, for collisions between a turnoff star and a lower main-sequence star, an appropriate turnoff model was scaled in mass so that its mass agreed with the total mass of the two parent stars; for equal-mass mergers, the mass of one of the parent stars was scaled. Next, the scaled model's composition profile was replaced with the chemical profile found by hydrodynamic stratification of the parent stars. This model was then expanded to simulate the expansion of the star during the collision.

The first step was accomplished by increasing the mass of each shell in the grid of mass shells which make up the stellar model by some small amount (usually $\sim 0.1\%$), allowing the model to relax for a few very short timesteps (without allowing the composition profile to change), and then repeating the procedure until the desired mass was reached. As it turns out

(discussed later) this step is actually quite unimportant: the very simple approximation of starting with a model of the desired mass and imposing the correct chemical composition profile produces identical blue stragglers (Sandquist et al. 1997).

The second step, replacing the initial model's composition profile with that found by hydrodynamic stratification of the parent stars' profiles, is the most crucial of the steps taken — not in its actual execution, but in the effect the composition profile has on the resulting blue straggler. The reason for this is explained by the Vogt-Russell Theorem, which states that the structure of a star in hydrostatic and thermal equilibrium is uniquely determined by the total mass and the run of chemical composition throughout the star (Vogt 1926, Russell 1927; see e.g. Cox & Giuli, 1968). Thus, regardless of the method used to produce the initial model, as long as the star is allowed to come into equilibrium before being allowed to evolve as a blue straggler, the composition profile and total mass will determine the subsequent evolution.

The third and final step was done by adding an additional term ϵ_x to the energy balance equation of stellar structure:

$$\frac{\partial L}{\partial M} = \epsilon_{nuc} - \epsilon_\nu + \epsilon_{grav} + \epsilon_x,$$

where ϵ_{nuc} is the nuclear energy generation rate, ϵ_ν is the energy loss due to neutrinos, and ϵ_{grav} is the energy generation due to contraction of the star $(= -T\frac{\partial S}{\partial t})$. This step is necessary to simulate injection of orbital kinetic energy, which can amount to a large fraction of the binding energy of the two stars, into the remnant. This energy injection is naturally accounted for in the SPH simulations by the acceleration of the individual SPH particles, but needs to be approximated here. If ϵ_x were held constant throughout the star,

the central density would decrease rapidly as the star expanded and the star would end up on, or near, the Hayashi track (this is similar to the procedure which Sandquist *et al.* (1997) used to produce their Hayashi models). As mentioned earlier, the density of the core does not decrease by a large factor during the collision; to ensure this, we assumed that ϵ_x falls off as $1/\rho$ (see below). During the expansion of our models, the central density does not decrease by more than 20% which, as explained below, results in the final models being virtually independent of the form of ϵ_x after they have relaxed to the main-sequence.

One additional consideration is how much energy to inject into the star before allowing it to contract to the main-sequence and evolve normally. We have chosen to use a criterion which takes into account the binding energy of the parent stars and the kinetic energy of the collision. The binding energy of a star can be expressed as

$$E_{bind} = -q\frac{GM^2}{R},$$

where M and R are the mass and radius of the star, and q is related to the degree of central concentration (Cox & Giuli, 1968):

$$q = \int_0^1 \frac{M(r/R)/M}{r/R} \cdot \frac{dM(r/R)}{M}.$$

In the centre of mass frame of the two stars the orbital energy is

$$E_{orb} = \frac{1}{2}\mu v^2 - \frac{GM\mu}{r},$$

which, for a parabolic orbit, is conveniently equal to zero. (Here, M is the total mass of the two stars, $M_1 + M_2$, and μ is the reduced mass of the system,

$\mu = \frac{M_1 M_2}{M_1 + M_2}$.) Hence, the kinetic energy of the orbit is

$$K = \frac{GM\mu}{r}.$$

Assuming that one half of the orbital kinetic energy goes into expanding the merger remnant, the final binding energy of the merger remnant is $E'_{bind} = E_{bind_1} + E_{bind_2} + \frac{1}{2}K$. For the purposes of determining the kinetic energy at the time of the collision, we have set the separation of the centres of the two stars r equal to the average of their radii, $r = \frac{R_1 + R_2}{2}$. The expansion of the model is halted when its binding energy equals E'_{bind}. For the same reasons that the form of ϵ_x is not critical, as long as the density constraint is obeyed (discussed below), the structure of the blue straggler after it has contracted to its main-sequence is not highly dependent on the exact value of E'_{bind}, although the duration of any convective zones during the pre-main sequence evolution is affected.

Figure 3.5 shows a series of tracks from a merger between a $0.864 M_\odot$ and a $0.836 M_\odot$ star. The total binding energy of the stars at the start of the tracks varies, in terms of the total binding energy of the parent stars, from 0.94 to 0.11. As expected from the Vogt-Russell Theorem, when the stars have relaxed to their main-sequence positions, they are almost identical: the one track which deviates slightly became so distended during its expansion that the convective envelope penetrated deeply enough into the star to mix a small amount of helium to the surface. Obviously, the amount of energy which is injected into a merger model is not critical in determining the evolution of the resultant blue straggler, as long as no convective mixing takes place. The tracks labelled 0.70A, 0.46B, and 0.11A all developed convective envelopes which penetrated to $0.96 M_*$, $0.81 M_*$, and $0.49 M_*$, respectively, and lasted

for 4×10^5yr, 1×10^5yr, and 4×10^6yr, respectively.

One might be concerned about the ramifications for the models of assuming an energy injection term proportional to $1/\rho$. We have investigated this by adopting different energy injection schemes and comparing the resultant models (Figure 3.5). We find that, although the tracks that the models follow on the colour-magnitude diagram (**CMD**) as they expand and contract can differ considerably, the final models that satisfy the above criteria for energy and central density are very similar and evolve identically after they have contracted to the main-sequence — this is again due to the Vogt-Russell Theorem. Thus, if the amount of mixing which takes place is not significantly affected by the form of the energy injection term, the evolution of the merger remnant, at least after it has contracted to the main-sequence, should also be unaffected by the choice. Our tests using different forms of ϵ_z show that this is the case as long as the central density does not decrease beyond what is indicated by the SPH simulations.

The energy injection scheme used here is similar to that used by Podsiadlowski (1996) in his investigation of the response of stars to heating by tidal effects. In his exploratory paper, Podsiadlowski investigated the effect of various forms of energy injection (e.g. centrally concentrated, uniform, surface) on a $0.8M_\odot$ globular cluster ZAMS star — the different forms of energy injection were intended to approximate the zones in which tidally excited oscillations might dissipate their energy. Podsiadlowski found that the response of the star and its structure after a fixed amount of energy had been injected were strongly dependent upon the way in which energy was injected. Our initial experiments into the various forms of ϵ_z were quite sim-
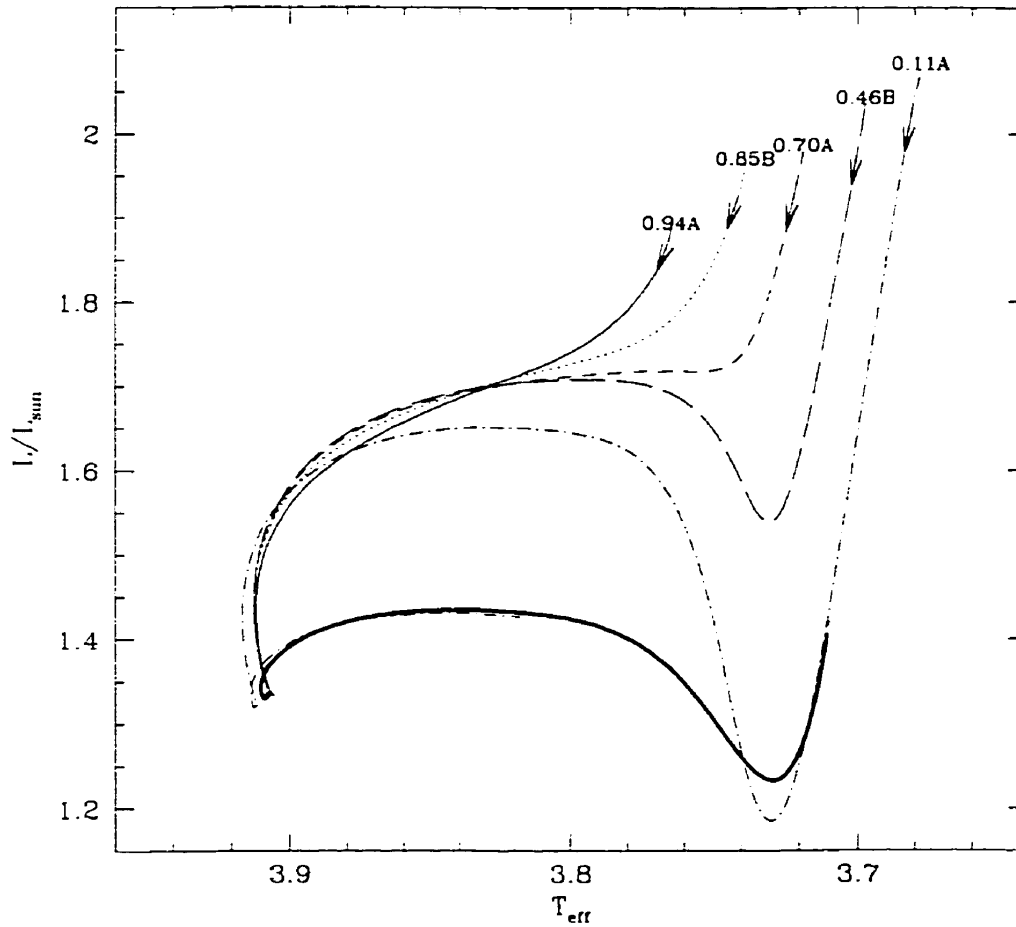
Figure 3.5: Evolutionary tracks for which the amount of energy injected, and the distribution with which it is injected, is varied. The tracks are labelled with the ratio of the star's initial binding energy to the sum of the parent stars' (a $0.864M_{\odot}$ and a $0.836M_{\odot}$ star) binding energy. For those stars labelled 'A', the energy injection term, ϵ_x, was proportional to $1/\rho$; for those stars labelled 'B', it was proportional to $1/\rho^{1/2}$. The density criterion, discussed in the text, was obeyed in all cases. The arrows indicate the initial direction of evolution, along the 'pre-blue straggler' portion of the tracks. The thick solid line indicates the 'blue straggler phase' for the models labelled 0.94A, 0.85B, 0.70A, and 0.46B.

ilar to Podsiadlowski's and lend support to his findings; the differences in the final structures from our early experiments and those of Podsiadlowski's were simply due to the fact that our initial models were evolved, whereas his were chemically homogeneous. Unlike Podsiadlowski's investigation, however, the form of ϵ_x for our models is constrained by the results of SPH: the central density of head-on mergers does not decrease dramatically relative to the central densities of the parent stars. From our experience, which is similar to what is reported by Podsiadlowski, forms of ϵ_x which are uniform throughout the star or are centrally concentrated result in a rapid decrease in the central density — by the time enough energy is injected to meet the energy constraint (E'_{bind} – discussed earlier), the star's structure would resemble that of a star on the Hayashi track.

3.3 Evolutionary Tracks

Using the above methods for creating models of collisional merger remnants, we have evolved sets of models for two different metallicities and ages, one set appropriate for very metal-poor clusters and another set appropriate for metal-rich clusters (Table 3.1), for both equal-mass and turnoff mergers, and for masses up to twice the turnoff mass for the assumed age. Figures 3.6 and 3.7 show the evolution of these models on the CMD. As would be expected, because of the chemical inhomogeneity of the merger remnant due to hydrodynamic stratification, the stars tend to avoid the ZAMS; only the low mass, relatively unevolved, equal-mass mergers approach what would appear to be normal ZAMS stars. The differences between the tracks for the metal-rich and metal-poor mergers are largely due to the difference in assumed cluster

metallicity.

Table 3.1: Assumed Cluster Parameters

	Metal-Poor	Metal-Rich
[Fe/H]	-2.14	-0.83
[α/Fe]	0.30	0.30
Age(Gyr)	14.0	12.0
$M_{TO}(M_\odot)$	0.77	0.874

3.3.1 Surface Convection

Leonard & Livio (1995) and Sills, Bailyn & Demarque (1995) have suggested that blue stragglers must become largely convective during their post-collision, pre-main sequence phase of evolution to explain both the observed rotation velocities and colours. While the blue straggler models of Sandquist *et al.* (1997) lend some support to this, our models do not, nor do the similar models of Sills *et al.* (1997).

Sandquist *et al.* (1997) performed SPH simulations of mergers of equal mass polytropes and evolved the products of these mergers by imposing the resultant composition profile on to standard stellar models of the same mass as the mergers, and then forcing the stars to expand until they had reached the Hayashi track. Their models developed deep surface convection, enough to bring at least some helium to the surface of the stars. However, forcing the stars onto the Hayashi track would decrease the central density beyond what is observed to occur in SPH simulations (LRS) — thus requiring an additional energy source which would not be present in the actual collision.
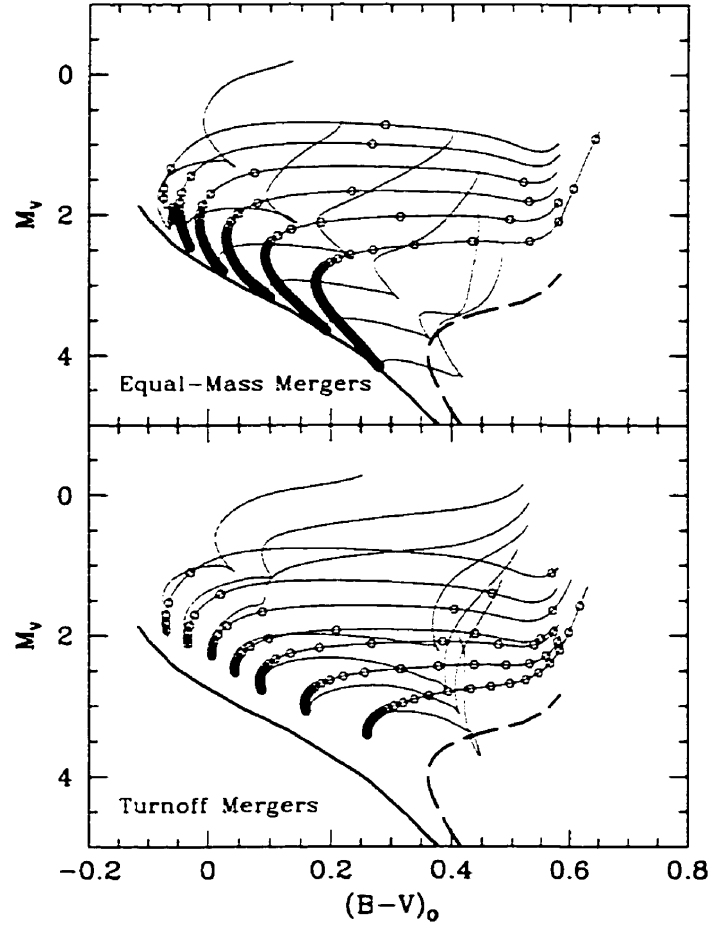
Figure 3.6: Evolutionary tracks (thin solid lines) for equal-mass (top) and turnoff (bottom) mergers models for metal-poor clusters. Masses of the models range from $1.00M_\odot$ to $1.5M_\odot$ in steps of $0.10M_\odot$. The open circles are placed along the tracks at equal intervals of 0.05Gyr. Also shown are the theoretical cluster ZAMS (thick solid line) and a 14Gyr isochrone (thick dashed line). Note the lack of a convective hook in all of the models, except for the most massive equal-mass merger model.
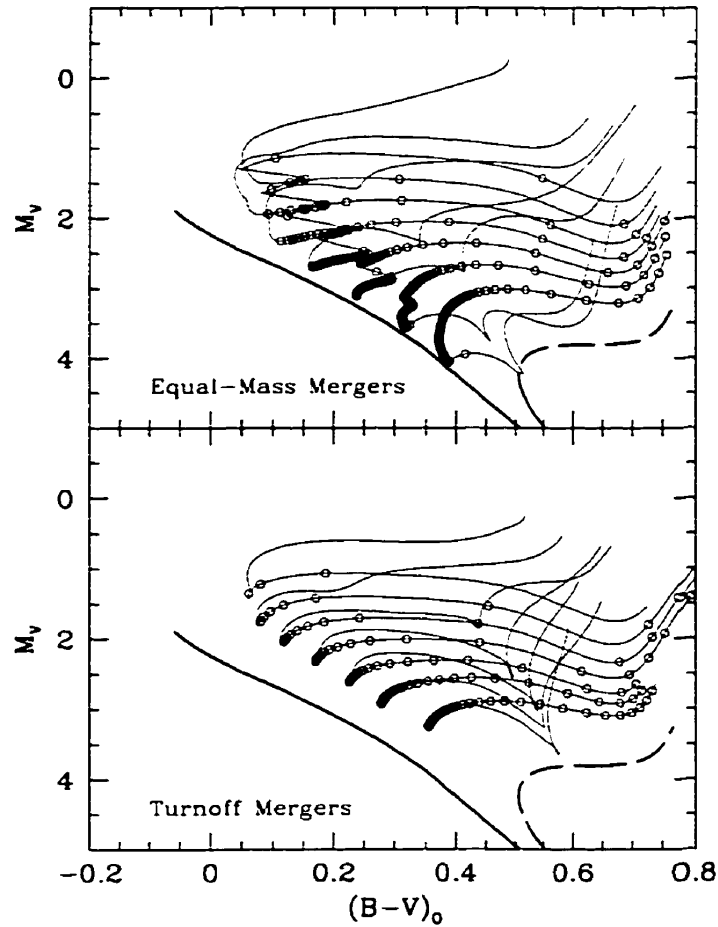
Figure 3.7: Similar to Figure 3.6, except for metal-rich merger remnants. The masses of the models range from $1.10M_\odot$ to $1.7M_\odot$ in steps of $0.10M_\odot$. The open circles are placed along the tracks at equal intervals of 0.05Gyr. Also shown are the theoretical cluster ZAMS (thick solid line) and a 14Gyr isochrone (thick dashed line). Note the lack of a convective hook in all of the models, except for the most massive equal-mass merger model.

In addition, the deep convective envelopes seen by Sandquist *et al.* are a consequence of the fact that their models are forced on to the Hayashi track, at which point the low surface temperatures will require surface convection. Surface convection will persist until the opacity in the outer regions of the star decreases to the point where radiative transfer becomes efficient — either when the star has evolved to higher surface temperatures, or convection has brought a significant amount of helium to the surface.

Sills *et al.* (1997) created initial blue straggler models directly from the hydrodynamic entropy and density profiles produced in the hydrodynamical simulations of LRS. None of their models developed any surface convection until they had evolved onto the red giant branch. The total lack of surface convection during the pre-main sequence phase prevents any helium-rich material from being dredged up to the surface layers of the star, and makes spin-down of a rapidly rotating blue straggler by a magnetic wind mechanism (Leonard & Livio, 1995) implausible. However, because the outer portions of SPH merger remnants are not necessarily in dynamical equilibrium, Sills *et al.* found it necessary to extrapolate the outer structure of their merger models from the purely radiative interior, forcing the envelope to be radiative, at least initially.

Surface convection does occur in some of our models during the pre-main sequence phase, unlike the models of Sills et al., but not to the extent found by Sandquist et al.. For the metal-poor tracks, only the lowest mass models ($M < 1.20M_\odot$) develop any surface convection; surface convection is somewhat more common in the metal-rich models – only the most massive stars ($M > 1.50M_\odot$) never develop any surface convection during the pre-main

sequence phase. The surface convection which does develop never contains more than $\sim 10\%$ of the star's mass and never lasts for more than a few times 10^6 years.

3.3.1.1 Consequences of Surface Convection and Angular Momentum Loss.

The thin, short-lived surface convection seen in our models, and the absence of surface convection in the models of Sills *et al.* (1997), precludes any wind-driven angular momentum loss (**AML**) mechanism for slowing down the rapidly rotating blue stragglers predicted by the collision scenario. However, blue stragglers are not observed to be rapidly rotating in open clusters where, despite the comparatively low stellar density, it is possible for a fraction of blue stragglers in open clusters to be formed by collisions (Leonard 1996, Leonard & Linnell 1992). To account for the low rotation velocities, there must be either an additional angular momentum loss mechanism acting which is not dependent upon surface convection, or the blue stragglers in open clusters are being formed by a mechanism other than collisions which might produce more slowly rotating blue stragglers (e.g. binary coalescence, binary mass transfer), in which case the estimated numbers of collisionally generated blue stragglers in open clusters is incorrect. Even if the production of blue stragglers by collisions is ruled out in open clusters other formation mechanisms can be assisted, or accelerated, by strong dynamical interactions (Sigurdsson & Phinney, 1993).

Little is known about the rotation of blue stragglers in globular clusters, although the stage has been set to rectify this problem by the observations of Shara *et al.* (1997). BSS-19 (Paresce *et al.*, 1991) in 47 Tuc is estimated

to have a mass of $1.70 \pm 0.40 M_\odot$,[1] compared to the cluster turnoff mass of $\sim 0.86 M_\odot$, and a high rotation velocity ($V \sin i = 155 \pm 55$km/s). From our models, this star should not have had a convective envelope at any time during its "pre-blue straggler" phase, assuming it was created by a collisional merger, and so should contain the same angular momentum with which it was created, unless an angular momentum loss mechanism other than a magnetically driven wind has acted upon it. During its contraction to the main-sequence, its rotational velocity should have increased from its initial value by a factor of $\sim 5 - 6$, due to angular momentum conservation, implying an initial rotation velocity of ~ 30km/s. From the results of LRS, this would have required a nearly head-on collision which, although not unlikely, is less probable than an off-axis collision. Hence, it is more probable that BSS-19, if created by a collision, is either inclined close to the line of sight ($\sin i \lesssim \frac{\pi}{4}$), has experienced some angular momentum loss, or was instead formed through some mechanism other than a collision, as suggested by Shara et al..

It is possible that angular momentum loss from an initially rapidly rotating blue straggler could be achieved by angular momentum transfer to a circumstellar disk, possibly ejecta from the collision, or to a nearby companion, possibly captured during a binary interaction. Cameron et al. (1995) found that angular momentum transfer to a circumstellar disk is an extremely efficient mechanism for slowing the rotation of stars as they contract to the main sequence. This mechanism does require that the star have a convective envelope for the generation of a magnetic field, but the field strength

---

[1]Comparing the observations of effective temperature ($T_{eff} = 7630 \pm 300$K) and surface gravity ($\log g = 4.09 \pm 0.1$) directly to our models yields a mass estimate of $1.55 \pm 0.10 M_\odot$, independent of distance, in reasonable agreement with the determination of Shara et al. – see Figure 2.2.

required to shed a given amount of angular momentum is not necessarily as high as that needed for a wind-driven mechanism. Angular momentum transfer to a nearby companion has the advantage that a convective envelope is not required and demands that many blue stragglers be in binary systems, as is observed. During the distended contraction phase of the blue straggler's evolution, a nearby companion could exert a considerable torque on the star, forcing the stars to approach tidal lock. The angular momentum transfer to the companion will tend to force it into a larger orbit and reduce any initial eccentricity in the orbit, as well as slowing the rotation of the blue straggler.

3.3.1.2 Surface Abundances.

Although it is questionable whether surface convection is sufficient to explain the moderate rotation rates of most blue stragglers, any amount of surface convection could act to alter the surface abundances of these stars. Since we find that surface convection does not occur in many of the more massive merger remnants, it is possible that abundance anomalies might be a way in which to distinguish between the formation mechanisms, as suggested by Sills *et al.* (1997) — but only for the most massive stragglers. The convective zones in some of our lower mass models ($M \lesssim 1.40 \times M_{TO}$) can penetrate to depths where the temperature is high enough to destroy the more fragile elements, such as lithium (Pritchet & Glaspey 1991, Hobbs & Mathieu 1991, Glaspey *et al.* 1994). However, although the amount of hydrodynamical mixing which occurs during a collision appears to be small, sufficient mixing should occur in the envelope during the merger that some chemical anomalies might be expected, even in the absence of convection. Additionally, merid-

ional currents, which should occur to some extent in rapidly rotating stars, will also mix the surface layers even if the core is not penetrated (Tassoul & Tassoul, 1984).

3.3.2 Core Convection.

In the normal main sequence stars of very metal-poor globular clusters and metal-rich globular clusters (i.e. those with metallicities indicated in Table 3.1), core convection should persist for the entire main sequence lifetime of stars with masses greater than $\sim 1.50 M_\odot$ and $\sim 1.20 M_\odot$, respectively. Core convection does not occur at any time in the turnoff mergers, whereas core convection appears in most of the metal-rich equal-mass models. No core convection occurs during the distended pre-main sequence phase, but rather starts when the model has contracted close to its main sequence.

That no core convection occurs in our turnoff mergers is not surprising due to the high central density and helium abundance. This is in contrast to the results of Sills *et al.* (1997) who find that turnoff mergers typically do develop core convection. The simulations of Sills *et al.*, however, are based on models produced using the end-products of polytropic collisions, which, as shown earlier in the discussion on hydrodynamic stratification, will tend to have hydrogen-rich cores. The increased hydrogen abundance in the core results in a higher central opacity, making the central layers convectively unstable.

The differences in the amount of convection seen between the metal-poor and metal-rich models are a consequence of the fact that the metal-poor mergers were chosen to have a metallicity which is ~ 15 times lower

than that of the metal-rich mergers, reducing the efficiency of the CNO cycle for masses less than $\sim 1.50 M_\odot$. At that mass the metal-poor equal-mass mergers $(M_{TO} \sim 0.77 M_\odot)$ have sufficiently low central hydrogen content that convective transport is not necessary.

3.3.3 Consequences of Calculated Mixing Scales.

According to the Vogt-Russell Theorem, the structure of a star in hydrostatic and thermal equilibrium is determined by its mass and composition profile, which maps into a point on the CMD. We would expect that a star which is perturbed slightly from its position of equilibrium on the CMD would relax back to the same equilibrium position and structure. If the star is perturbed from its equilibrium state to a greater extent, such that no additional convection occurs which might change its chemical profile significantly, and such that no mass is lost during the perturbation, we would still expect it to relax back to the same equilibrium state on a timescale equal to the star's Kelvin-Helmholtz time scale. Similarly, two merger remnants produced in collisions involving identical sets of stars and having identical masses and chemical profiles, but which are initially at different points in the H-R diagram, should produce identical blue stragglers if no significant mixing occurs during their pre-main sequence phase.

This same argument was used earlier to explain why the exact details of the mechanism used to expand the blue straggler models to their initial pre-main sequence position are unimportant. However, here it has the additional implication that two theoretical merger remnant models which have identical masses and chemical profiles, but were produced using different assumptions

about their structure, should produce identical blue stragglers if no significant convective mixing occurs during their pre-main sequence phase. For this reason, we expect the evolution of the models of Sills & Lombardi (1997) and of Sills *et al.* (1997) to be similar to the evolution of our own turnoff merger models and equal-mass merger models, respectively.

3.4   Fully-mixed Models

Blue stragglers resulting from binary mass transfer (Section 2.2.4) should appear to be highly mixed due to the high surface helium abundance which is a consequence of the mass transfer. However, since mass transfer will often leave a remnant of the mass-donor, in the form of an inert helium or carbon-oxygen white dwarf, the surface abundances of the newly formed blue straggler are highly dependent upon the amount of nuclear-processed material which was actually transferred, and the amount of mixing which occurred in the mass-acceptor. As a result, a blue straggler formed by binary mass-transfer will lie somewhere between fully-mixed models (in which the material from both parent stars is completely homogenised throughout the new star) and unmixed models (such as the turnoff and equal-mass collisional merger remnants discussed in the previous sections). Blue stragglers formed through binary coalescence (Section 2.2.5) should also appear to scatter between the two extremes of unmixed and fully-mixed models, although one might expect the resulting merged star to appear slightly more evolved (on average) than a newly formed mass-transfer blue straggler (in analogy with the collisional merger remnants, coalesced stars will appear to have a truncated main-sequence evolution, as do the turnoff mergers, whereas mass-

transfer blue stragglers will tend to have a longer main-sequence lifetime, as do the equal-mass mergers).

The exact amount of mixing which occurs during mass-transfer and coalescence will be very dependent upon the initial stellar masses, binary parameters, evolutionary states, etc. in the initial system. This, unfortunately, means that there is likely no single family of models which will adequately represent the remnants of these processes. It may be possible, by creating models for these merger remnants over a wide range in mass, semi-major axis, age, etc., to produce an adequately general family of models which can be used to investigate populations of these remnants. However, in modelling such systems, one must deal with myriad effects which are poorly understood (e.g. the affect of accretion of material in a stream, rather than the simple approximation of uniform accretion, Sarna 1992); shock-heating of the envelope of the accretor ; mass-loss from the system; see Iben & Livio, 1993, for a review of binary coalescence).

Rather than attempt to model binary mergers over the full range in allowable parameters — which would be prohibitively time-consuming — the fact that these merger remnants will exhibit a comparatively high degree of mixing (relative to collisional mergers) will be used to make a general approximation. As was stated above, the remnants of binary mass-transfer and binary coalescence should scatter between fully-mixed and unmixed models: with the turnoff and equal-mass collisional merger models representing the unmixed extreme, turnoff and equal-mass fully-mixed models will be used to represent the other extreme. While neither set of models will adequately represent binary mergers, the assumption is that the increased helium con-

tent in these stars' atmospheres will allow reasonable agreement with the fully-mixed models.

As with the collisional merger models, the chemical content of the parent stars is used in the production of the fully-mixed models. However, the procedure used is quite simple in comparison. Given the average elemental abundances of the parent stars (i.e. hydrogen, helium, carbon, etc.), a mass-weighted average abundance[2] is calculated for each element: the elemental abundances in a chemically homogeneous model of the appropriate mass are replaced with these averaged abundances. In fact, the 'chemically homogeneous model' is a Hayashi (pre-main sequence) model of the desired mass: this does mean that the chemical abundances in the core will be modified by some small amount by the time the star has contracted to its main-sequence structure, but the change is small.

Figures 3.8 and 3.9 show evolutionary tracks of the fully-mixed merger remnants for both metal-rich and metal-poor clusters. To distinguish between these merger models and the equal-mass and turnoff merger models for collisional remnants, these models will be referred to as equal-mass and turnoff binary mergers. Turnoff binary mergers refer to the fully-mixed merger of a turnoff star and a lower mass star.

---

[2] The mass-weighted average uses the parent stars' masses for the weighting: $\bar{X} = (\bar{X}_1 M_1 + \bar{X}_2 M_2)/(M_1 + M_2)$ where X is the mass-fraction of the element and the subscripts 1 and 2 refer to the quantities for the primary and secondary stars.
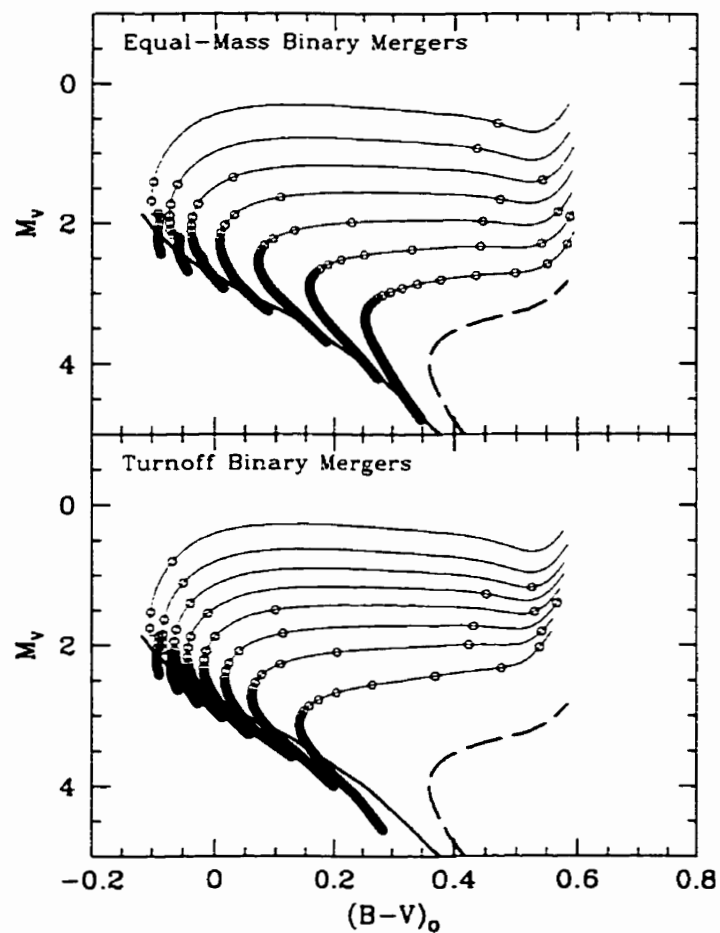
Figure 3.8: Evolutionary tracks for fully-mixed mergers. Masses for the mergers run from $0.90 M_\odot$ to $1.50 M_\odot$.
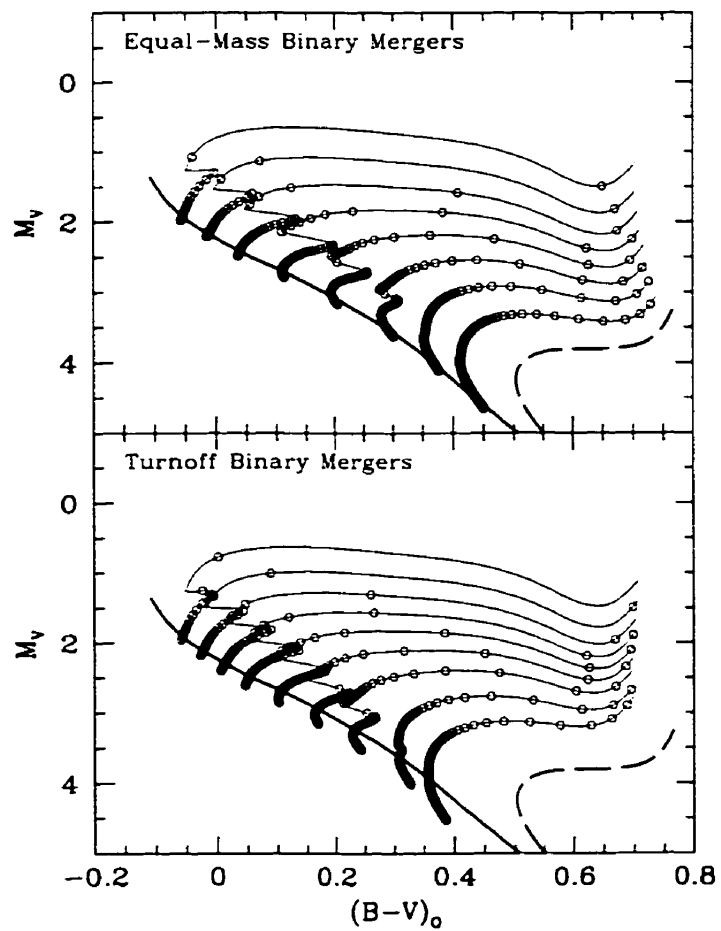
Figure 3.9: Same as Figure 3.8, except for metal-rich mergers. The range of masses is $1.10 M_\odot$ to $1.70 M_\odot$.

Chapter 4

Comparison with Observations

It was the goal of the previous chapter to present evolutionary models for the products of stellar collisions and binary mergers.[1] This chapter will compare these models with the observed distributions of blue stragglers in several clusters, with the hope of determining which most closely predicts the evolution, and hence formation mechanism, of the blue stragglers in these clusters.

Selection of the clusters to be examined was made using several criteria:

- *The cluster must have a significant population of blue stragglers.* With only a few blue stragglers, statistical comparisons with the models would be very uncertain.

- *The chosen dataset must have high photometric quality.* While this is an obvious criterion, its need is twofold. First, with large photometric errors, it will be hard to distinguish between the formation mechanisms

---

[1]As defined in the previous chapter, the remnants of stellar collisions are referred to as collisional mergers (**CM**), although this also refers to the collision itself. **Binary mergers (BM)** refer to the remnants of binary coalescence and binary mass-transfer which are, in this work, approximated by fully-mixed stellar models.

which may yield similar remnants. Second, the models must be carefully aligned with the cluster photometry (through alignment of the cluster fiducial and an appropriate isochrone in our case) to avoid any bias due to an error in the assumed cluster distance or reddening.

- *The cluster's Galactic latitude and longitude must be such that foreground contamination will be low.* Foreground stars will be easily mistaken for real blue stragglers. If the cluster photometry contains enough real blue stragglers, then a small number of foreground stars can be tolerated.

- *The clusters must have metallicities and ages close to those assumed for the production of the models.* In fact, two clusters were chosen originally, NGC 6397 and 47 Tuc, and the models were developed for these clusters: the other clusters were chosen later, with this criterion in mind.

Based on these criteria, seven clusters were chosen. The cluster colour-magnitude diagrams (**CMDs**) are shown in Figures 4.1 to 4.7 and some of their published characteristics are shown in Table 4.1. It should be noted that the photometry shown in these figures, which constitute the datasets used for the following analysis, has been trimmed to exclude the worst photometry (those stars with photometric uncertainties greater than 2.5 times the median for stars of the same magnitude), and the photometry of NGC 2419 and NGC 5024 has been trimmed to exclude all stars within 50 arcseconds and 100 arcseconds, respectively, of the clusters' cores (the photometry within these radii is quite poor relative to the photometry in the outer regions). Also, the

Table 4.1: Selected Clusters

Cluster	l	b	[Fe/H]	Approx. # BS	Photometry Source
NGC 104 (47 Tuc)	305.9	-44.9	-0.83	55	Rich et al. (1997)
NGC 2419	180.4	25.2	-2.02	19	Harris et al. (1997)
NGC 5024 (M53)	333.0	79.8	-2.10	47	Rey et al. (1998)
NGC 6397	338.2	-12.0	-1.91	21	Kaluzny et al. (1997a)
NGC 6809 (M55)	8.8	23.3	-1.82	25	Mandushev et al. (1997)
NGC 7099 (M30)	27.2	-46.8	-2.13	39	Guhathakurta et al. (1998)

Table 4.2: Distance Moduli, Reddenings and Shifts for Selected Clusters.

Cluster	$(m-M)_V$	$E(B-V)$	$\Delta(m-M)$	$\Delta(B-V)$
NGC 104	13.38	0.04	13.454	0.038
NGC 2419	19.97	0.17[a]	19.935	0.182[a]
NGC 5024	16.38	0.02	16.315	0.039
NGC 6397	12.36	0.18	12.457	0.197
NGC 6809	13.87	0.07	14.010	0.142
			13.997	0.184[a]
NGC 7099	14.62	0.03	14.676	-0.009

[a]Reddening and colour shifts are in V-I, not B-V

photometry of NGC 6397 was trimmed of all stars further than 5 arcminutes away from the cluster center to lessen the contamination by field stars.

The metal-poor clusters were chosen with an additional constraint in mind, one intended to allow a direct comparison of the blue straggler populations without having to rely on the agreement (or lack thereof) with blue straggler models: *The metal-poor clusters, or at least a subset of these, must be demonstrably coeval.* The reasoning behind this criterion is that, since it is likely that blue straggler formation mechanisms are likely to be affected

Table 4.3: Cluster Structural and Dynamical Properties - I

Parameter	NGC 104	NGC 2419	NGC 5024
Cluster Mass, $\log(M_\odot)$	6.1	5.6	5.7[b]
Central Density, $\log(M_\odot/pc^3)$	5.1	1.4	3.18[a]
Central Velocity Dispersion σ_0, (km/s)	11.5	3.0	6.50[a]
Central Relaxation Time, log(yr)	7.99	10.02	8.9
Half-light Relaxation Time, log(yr)	9.24	10.28	9.42
Core Radius, (pc)	0.50	8.51	2.00
Half-mass Radius, (pc)	3.84	18.62	6.31
Central Concentration, $\log(R_{tidal}/R_{core})$	2.2	1.4	1.7[a]

All values are from Djorgovski, 1993, unless otherwise noted.
[a]From Webbink, 1985.
[b]Assuming a mass-to-light ratio (in V) of 2.0, and an integrated absolute magnitude of $M_V = -8.68$ (Djorgovski, 1993)

Table 4.4: Cluster Structural and Dynamical Properties - II

Parameter	NGC 6397	NGC 6809	NGC 7099
Cluster Mass, $\log(M_\odot)$	5.4	5.3	5.3
Central Density, $\log(M_\odot/pc^3)$	5.3	2.5	5.9
Central Velocity Dispersion, σ_0 (km/s)	4.5	4.9	5.6
Central Relaxation Time log(yr),	4.93	9.40	6.34
Half-mass Relaxation Time log(yr),	8.35	8.89	8.55
Core Radius, (pc)	0.03	3.98	0.12
Half-light Radius, (pc)	1.86	3.80	2.19
Central Concentration, $\log(R_{tidal}/R_{core})$	2.8	0.7	2.7

All values are from Djorgovski, 1993, unless otherwise noted.

Figure 4.1: Colour-magnitude diagram of 47 Tuc (Rich et al., 1997). Shown are the cluster data (dots), cluster fiducial (thick solid line), chosen isochrone (12Gyr, thick dashed line), blue straggler selection polygon (thin dashed line) and selected blue stragglers.
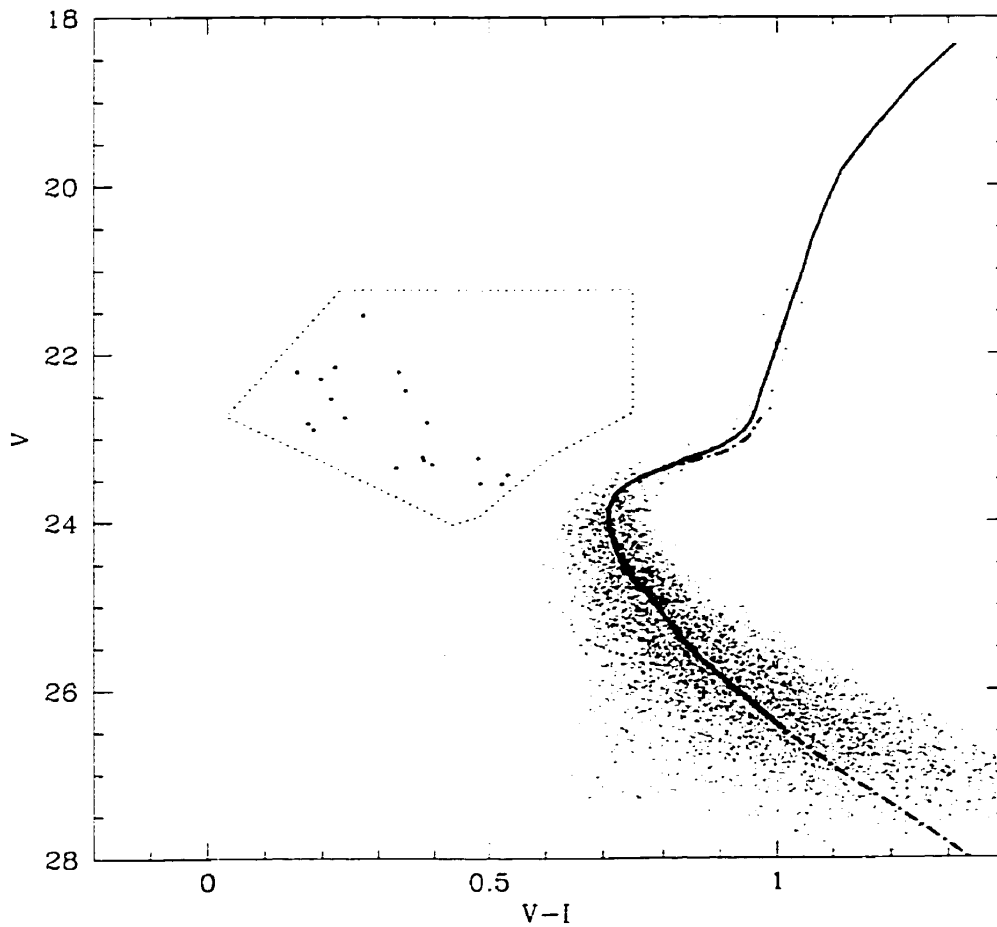
Figure 4.2: Colour-magnitude diagram of NGC 2419 (Harris et al., 1997). Lines and symbols have the same definitions as in Figure 4.1, except that the isochrone (thick dashed line) is a 14Gyr isochrone.
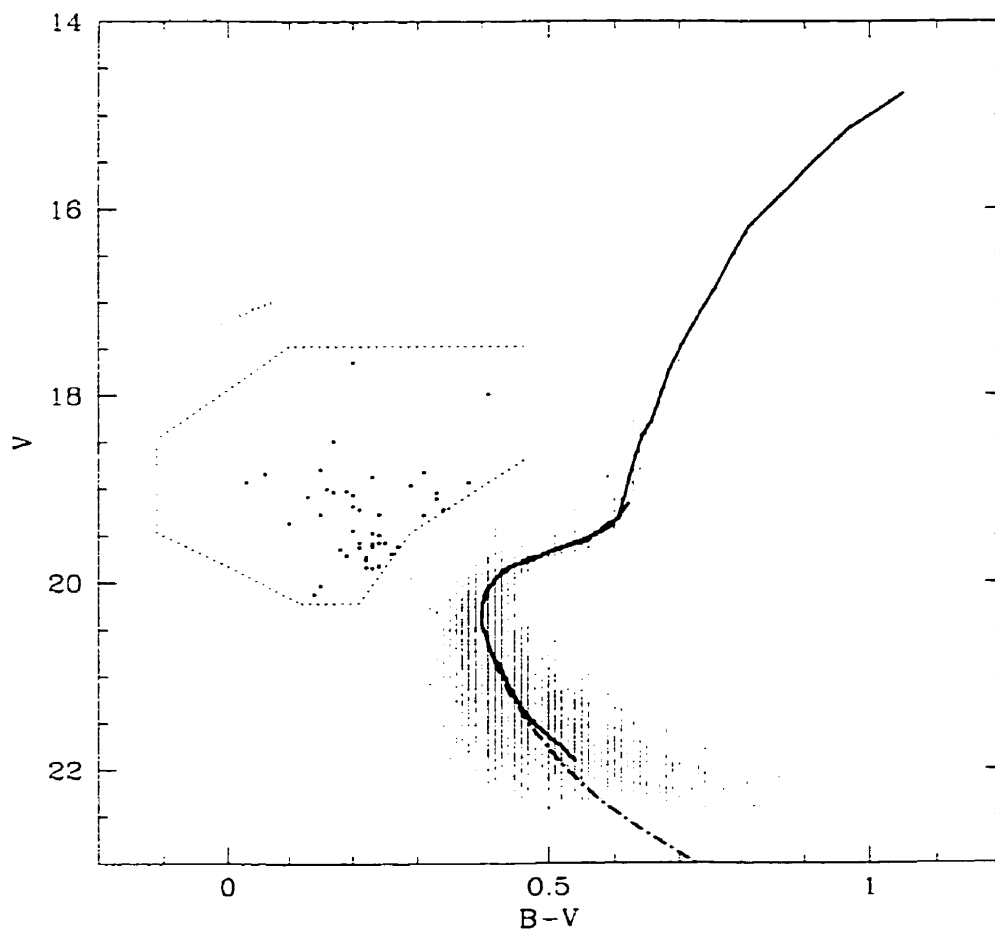
Figure 4.3: Colour-magnitude diagram of NGC 5024 (Rey et al., 1997). Lines and symbols have the same definitions as in Figure 4.2.
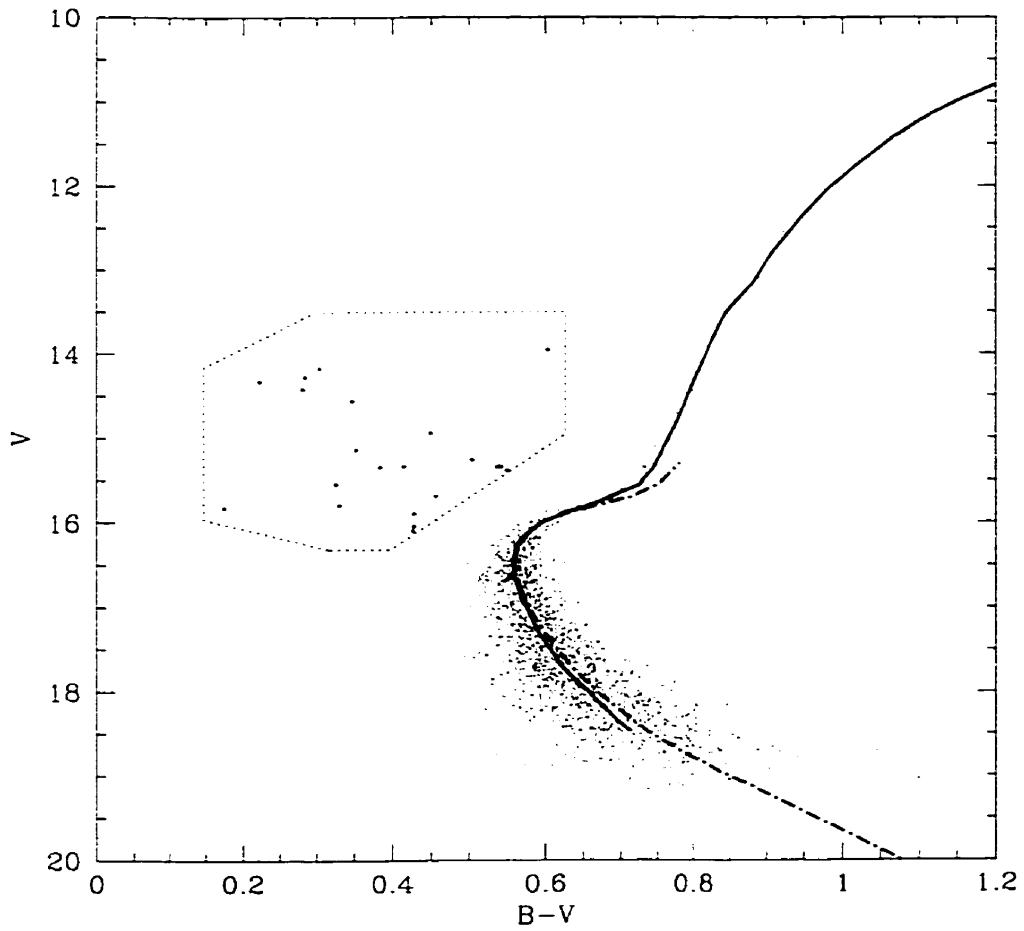
Figure 4.4: Colour-magnitude diagram of NGC 6397 (Kaluzny et al., 1997). Lines and symbols have the same definitions as in Figure 4.2.
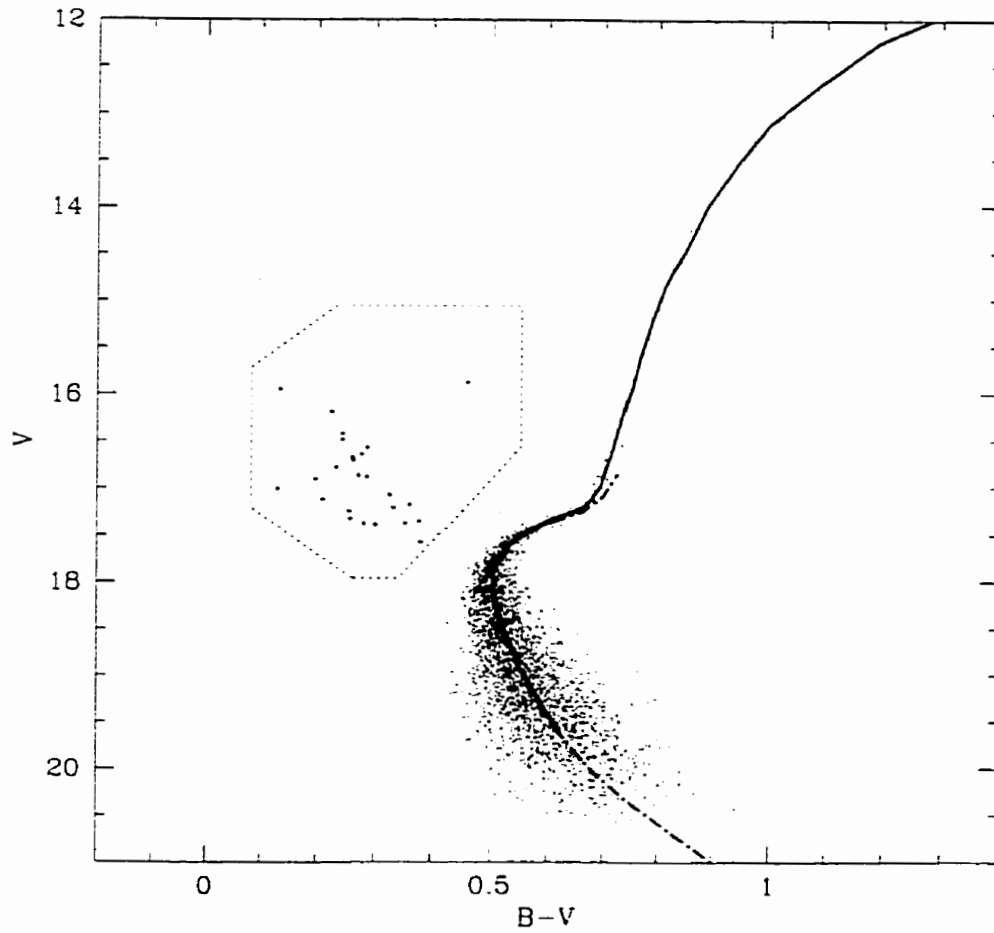
Figure 4.5: (V,B-V) Colour-magnitude diagram of NGC 6809 (Mandushev et al., 1997). Lines and symbols have the same definitions as in Figure 4.2.
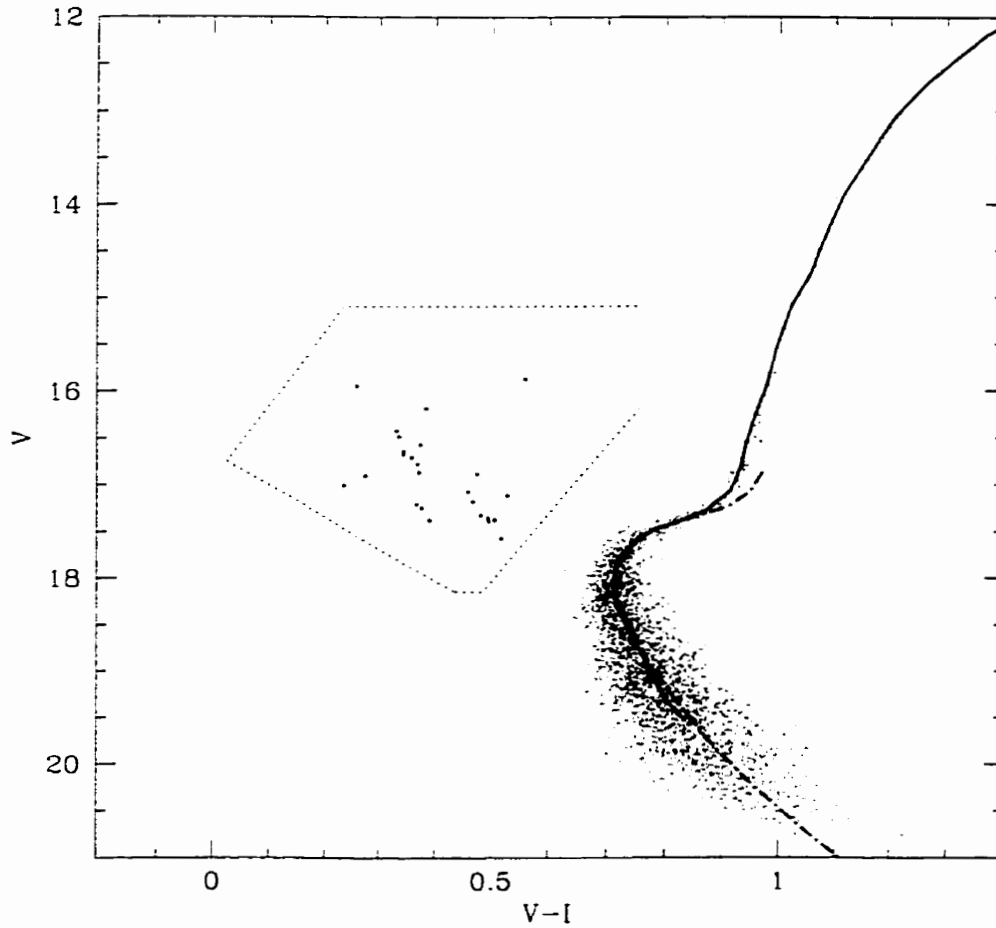
Figure 4.6: (V,V-I) Colour-magnitude diagram of NGC 6809 (Mandushev et al., 1997). Lines and symbols have the same definitions as in Figure 4.2.
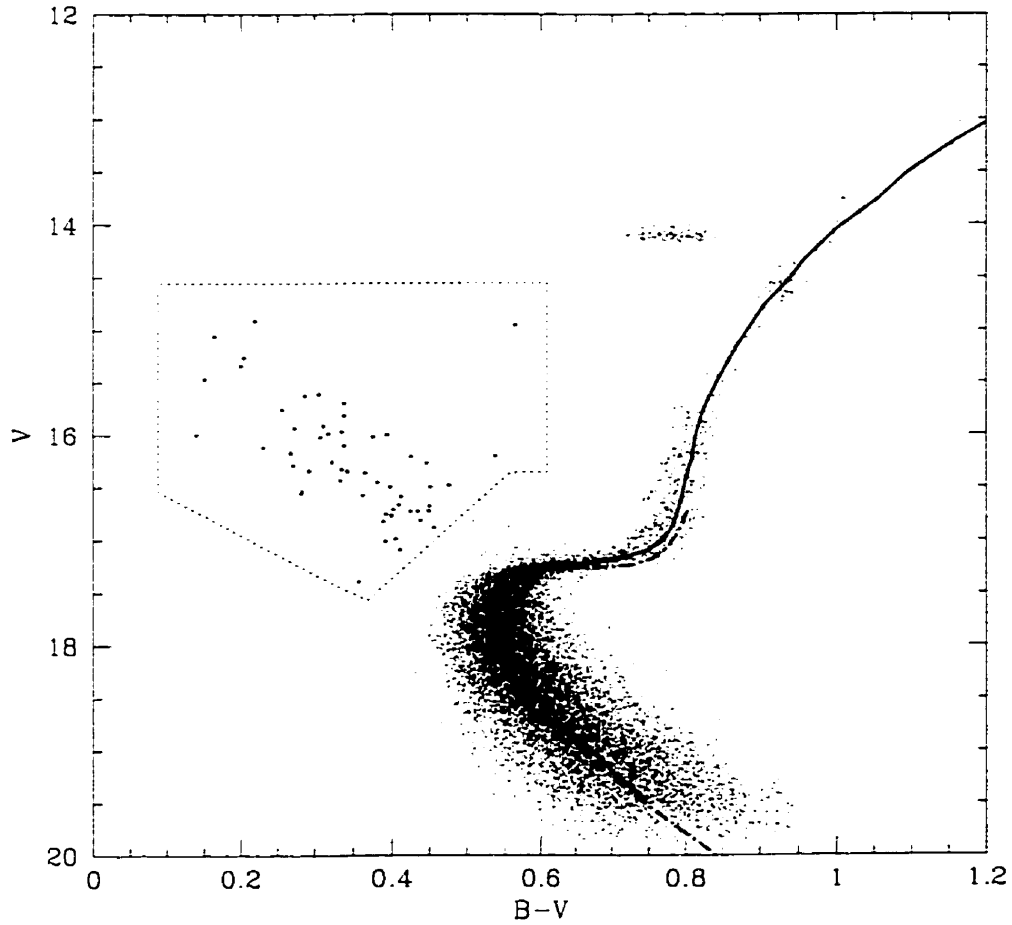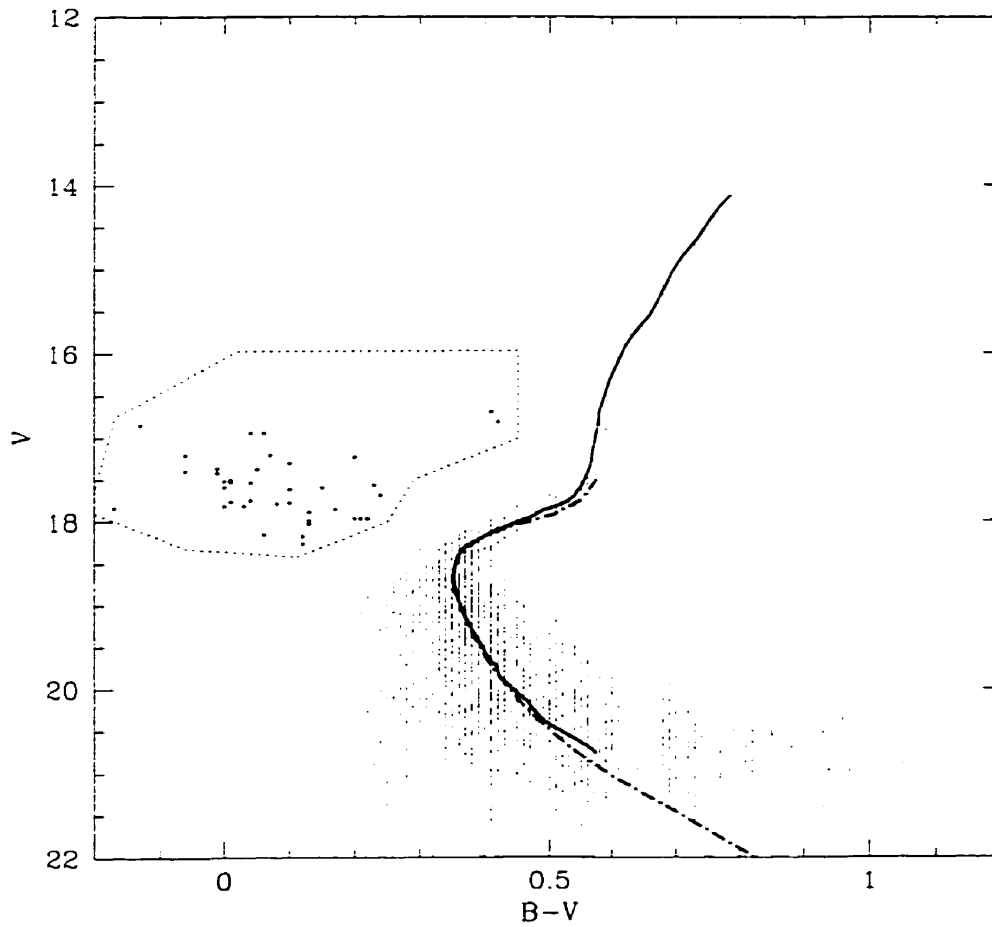
Figure 4.7: Colour-magnitude diagram of NGC 7099 (Guhathakurta et al., 1997). Shown are the cluster data (dots), cluster fiducial (thick solid line), chosen isochrone (14Gyr, thick dashed line), blue straggler selection polygon (thin dashed line) and selected blue stragglers.

by cluster dynamics, by ensuring that the clusters are coeval (or at least that their ages as determined from nuclear characteristics of the stars near the turnoff are similar), the only initial differences among the clusters should be dynamical (i.e. total cluster mass, concentration, binary fraction, etc). While it could be argued that the requirement of coevality is perhaps not necessary and that a similar comparison could be done using clusters of varying age and metallicity, doing so would add complexity and uncertainty into the comparison. For example: the distance of the point at which the termination of the main sequence is reached (i.e. central hydrogen exhaustion) from the zero-age main-sequence ($ZAMS$) is a function of metallicity for a fixed mass; it is likely that the blue straggler mass function is itself a function of age, since the formation of blue stragglers may often involve stars near the turnoff.

Figures 4.8 and 4.9 show the fiducials for the metal-poor clusters aligned in a manner similar to that of Chaboyer et al. (1996). As discussed by Chaboyer et al. (and VandenBerg, Bolte, & Stetson, 1990), the colour of the turnoff can be determined to high precision, given accurate photometry, but the magnitude of turnoff is more difficult to determine due to the shape of the turnoff itself. Chaboyer et al. suggest using, instead of the magnitude of the turnoff, the magnitude of the point on the cluster's subgiant branch which is 0.05dex redder than the turnoff colour. The nearly horizontal subgiant branch greatly simplifies the task of determining an accurate magnitude. Table 4.2 gives the shifts in colour and magnitude necessary to align the cluster fiducials to a 12 Gyr isochrone, for 47 Tuc, or a 14 Gyr isochrone, for the metal-poor clusters. An age spread of $\sim$ 2Gyr is arguable
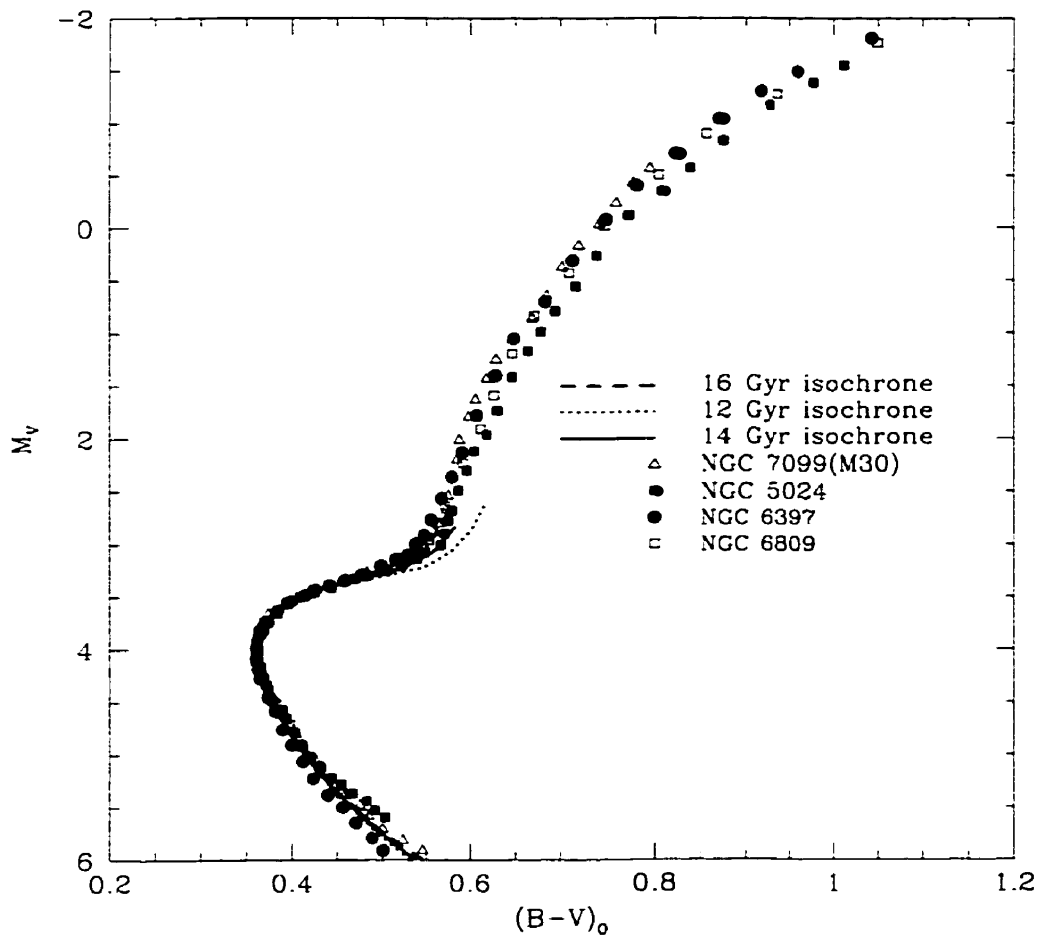
Figure 4.8: Fiducials of metal-poor clusters in (V,B-V), aligned in the manner of Chaboyer et al. (1996). The fiducials are all aligned with the 14 Gyr isochrone.
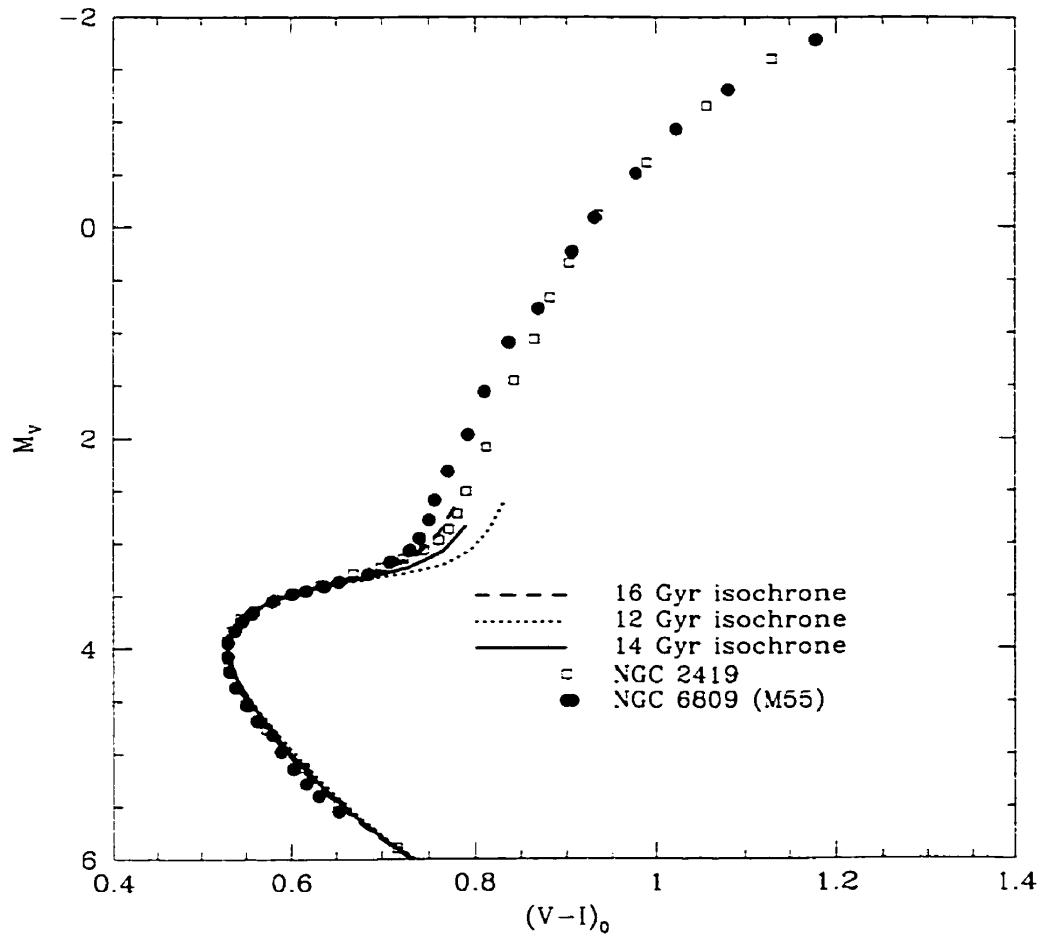
Figure 4.9: Fiducials of metal-poor clusters in (V,V-I), aligned in the manner of Chaboyer et al. (1996). The fiducials are all aligned with the 14 Gyr isochrone.

from the alignment of the fiducials but, for the sake of having a sample of clusters spanning a large range in dynamical properties, it will be accepted. A difference in ages of $\sim$ 2Gyr, relative to an age of 14Gyr, results in a difference in turnoff mass of only $\sim 0.03 M_\odot$. (NGC 2419 is the only cluster for which only Johnson V and Cousins I data are available; NGC 6809 has Johnson U, B, and V, and Cousins I data, whereas the rest of the clusters have only Johnson B and V data.)

In addition to selecting clusters, the blue stragglers within the cluster must be selected from the available photometry. As has been noted by many authors before, this is not always straightforward. Inspection of Figures 4.1 to 4.7 show distinct blue straggler sequences extending well beyond the main-sequence turnoff, so the selection of at least some blue stragglers in a cluster is an easy process: the difficulty is in drawing a boundary between the blue stragglers and the stars scattered from the other stellar sequences. The most difficult boundary to place is that between the blue stragglers and the stars scattered from the turnoff by photometric errors: if the boundary is placed too close to the turnoff, too many stars will be scattered into the blue straggler region; if it is placed too far away from the turnoff, many real blue stragglers will be missed. The chosen boundaries are indicated on the figures: they were chosen to be conservative, preferring not to risk including photometric interlopers at the expense of a few blue stragglers.

In selecting blue stragglers by placing sharp boundaries within the CMD, the interpretation of the blue straggler distribution may potentially be biased. The sections which follow present the results of Monte Carlo simulations in which fake blue stragglers have been created and compared to the real blue

stragglers in the clusters. In order to account for the potential biases intro-
duced by the selection of blue stragglers in the cluster, the same biases have
been introduced into the fake blue stragglers: that is, the same boundaries
which were used to select real blue stragglers are used to select viable fake
blue stragglers.

The following sections will introduce each of the clusters in turn, with 47
Tuc being chosen as the prototype with which to present the methods used
for the comparison of the models and cluster blue stragglers.

4.1 NGC 104 (47 Tuc)

4.1.1 Are Blue Stragglers Normal Stars?

In the Introduction it was hypothesised that the same assumptions which are
made when modelling the evolution of normal stars (i.e. hydrostatic equilib-
rium, sphericity, thermal equilibrium, etc.) can be made when modelling the
evolution of blue stragglers. Furthermore, it was hypothesised that processes
which might violate these assumptions (i.e. rotation, diffusion, binarity) do
not affect the evolution of blue stragglers any more than they affect the evo-
lution of normal stars. If these hypotheses are valid, then the evolutionary
differences between blue stragglers and normal stars are a consequence of
differences in their formation. Since the formation of a blue straggler could
cause its path through the CMD to differ from that of a normal star, this
final hypothesis can be tested by assuming that blue stragglers actually form
as normal stars, then comparing the predictions of this assumption to the
observations of blue stragglers.

Figure 4.10 shows the photometry for the GC 47 Tuc from Rich et al.
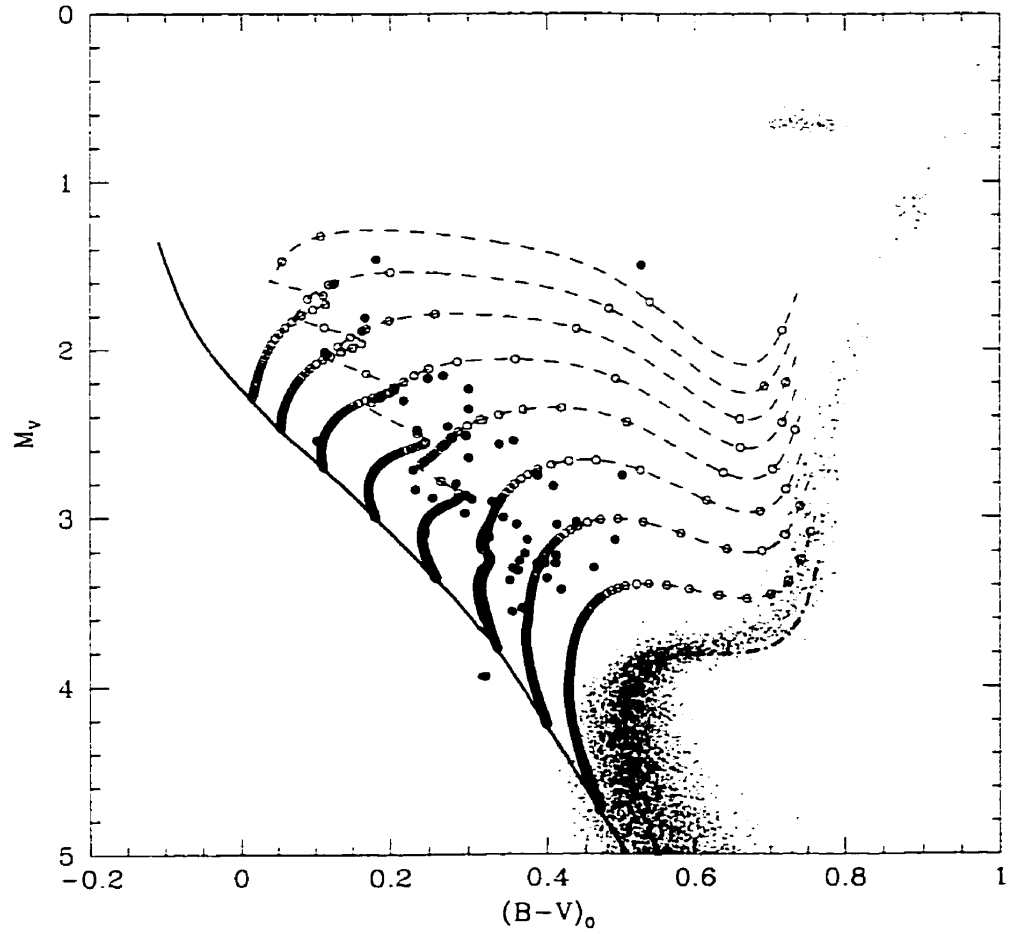
Figure 4.10: CMD of 47 Tuc, along with a 12 Gyr isochrone and evolutionary tracks. The masses of the tracks run from $1.0 M_\odot$ to $1.7 M_\odot$.

(1997) as well as an appropriate isochrone (12 Gyr), ZAMS, and evolutionary tracks of various masses. The marks along the tracks, which are spaced at equal intervals of 0.05Gyr, serve to indicate how we might expect to see blue stragglers distributed in the CMD if they form and evolve in a manner identical to normal stars. Since the marks are spaced equally in time along the tracks, the chance of a blue straggler, created at some random time in the past, being observed in any of the intervals between the marks is equal for every interval. Hence, we would expect to see blue stragglers clustered near to the ZAMS if the tracks adequately represented their formation and evolution: since the blue stragglers in 47 Tuc appear to avoid the ZAMS, it is obvious that the tracks are not adequate.

The conclusion that blue stragglers (at least those in 47 Tuc) are not normal stars is too qualitative to allow any real confidence. A statistical comparison between the tracks and blue stragglers requires knowing what the distribution of blue stragglers on the CMD would look like if they had been produced by the tracks in question. Since we have implicitly assumed that the blue stragglers have been created at random times in the past, the predicted distribution of stars from a single track can be found by simply drawing points from the tracks at random. Given the mass of a star, the predicted distribution of stars of this mass, created at random times, is easily found. For example, Figure 4.11a shows a $1.00M_\odot$ track with points spaced at equal 0.05Gyr intervals; Figure 4.11b shows the cumulative distribution of age as a function of model index along the track (the cumulative age distribution is defined here as

$$\sum_{i=0}^{n} \Delta t_i / \sum_{i=0}^{N} \Delta t_i,$$
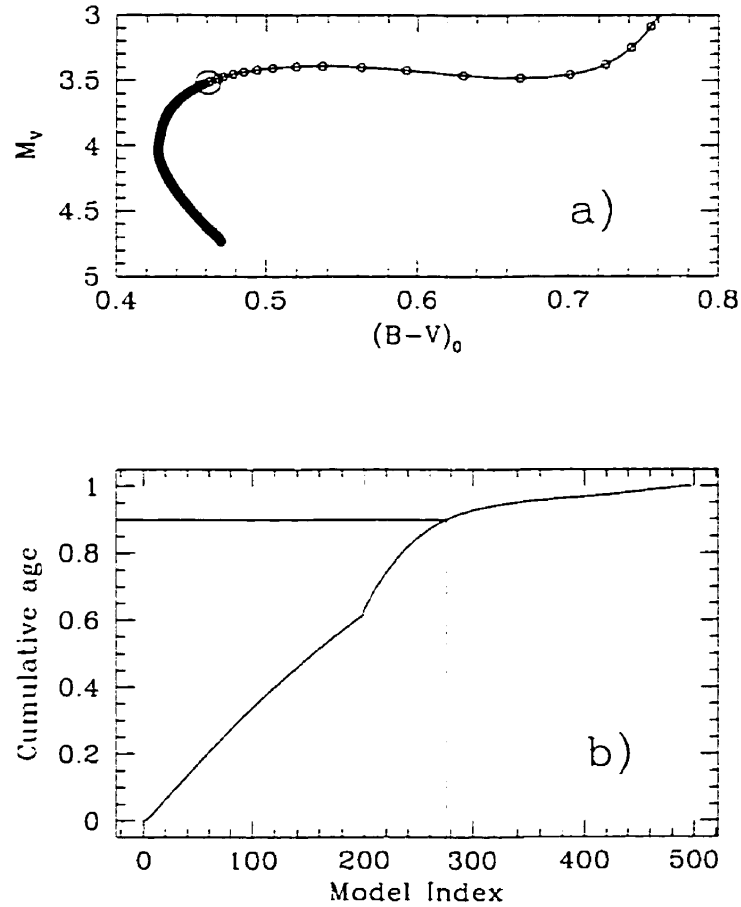
Figure 4.11: a) A standard 1.00M$_\odot$ track with equally spaced intervals of 0.05Gyr marked by the small open circles. The large open circle is a point drawn at random from the track using the cumulative age distribution. b) The cumulative age distribution of the track shown above. A random number was generated ($\sim$ 0.8991) and the corresponding index (276) in the track was found which then yielded the position of the star in the CMD. **Note:** The indices in Figure b) are not the indices of the equally spaced, 0.05 Gyr, points but rather are the indices of the computational models along the track. The spacing of the models is generally smaller than 0.05 Gyr.

where Δt_i is the difference in age between model i and model (i+1), N is the total number of models in the track, and n is the current model index). A random star can be drawn from this track by generating a random number between 0 and 1 as the random cumulative age, and taking the model index, n, which has that cumulative age. The only other requirement for producing a distribution of fake blue stragglers from a set of tracks is a distribution of masses for the blue stragglers.

There are two ways in which a mass distribution for a population of blue stragglers can be found: theoretically and observationally. The theoretical route requires a complete and accurate model for the cluster (including mass function, binary fraction, velocity dispersions, etc.) and the dynamics of the blue straggler formation mechanism (which may include interaction cross sections, binary semi-major axis distribution, binary eccentricity distribution, binary mass-ratio distribution, etc.). Given these, it is possible to model, through dynamical simulations, the expected blue straggler mass distribution. This is similar to what Sills & Bailyn (1999) did in their study of the blue straggler distribution of M3. Although this is indeed the preferred way in which to obtain the mass distribution, as it combines both the dynamical and evolutionary characteristics of a blue straggler formation mechanism, it has the potentially severe drawback that an incomplete understanding of any of the cluster dynamical properties could lead to an incorrect mass distribution. Also, any uncertainty in the blue straggler formation mechanisms (e.g. incorrect interaction cross-sections) could cause an error in the perceived rates of formation by those mechanisms, leading to a mis-interpretation of observations of blue stragglers.
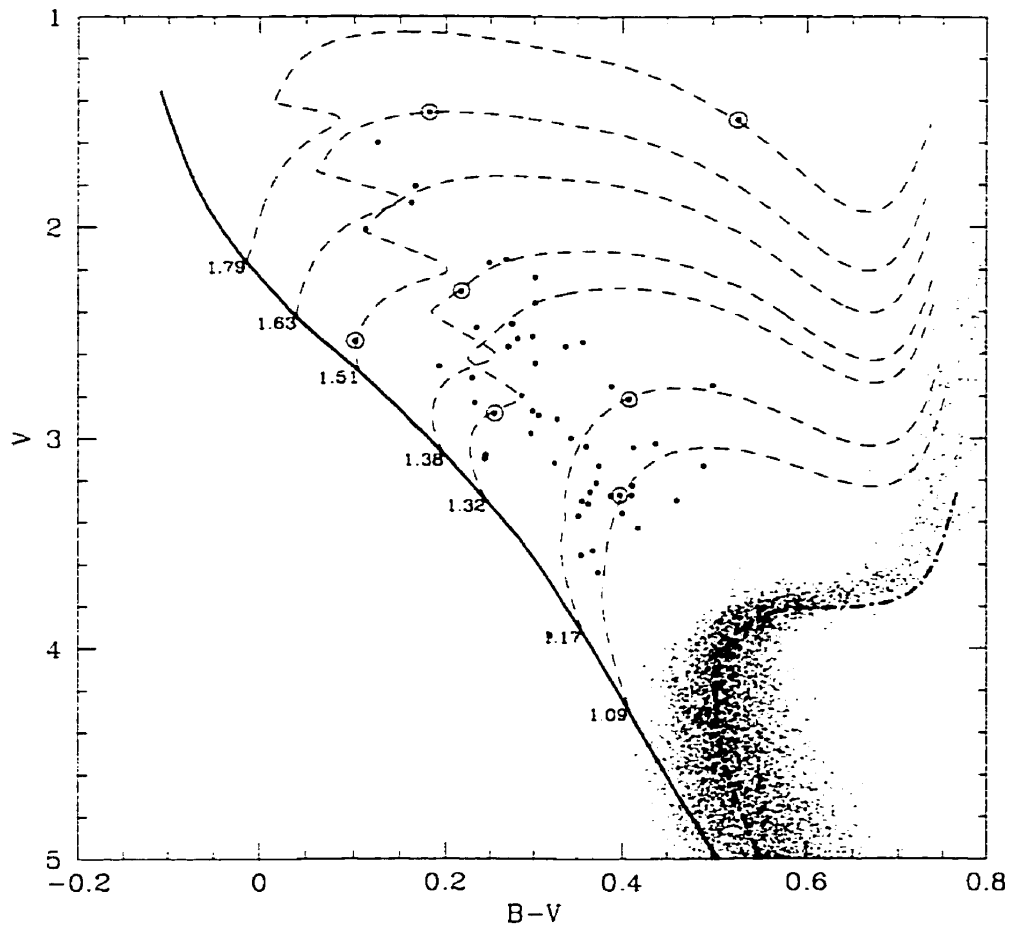
Figure 4.12: The photometric masses of the blue stragglers are found by finding the tracks which intersect the position of the star on the CMD. The tracks are spaced in mass at intervals of $0.01M_\odot$, so there is occasionally a slight shift between the position of the star and the closest point of the track.

The second route to obtaining the blue straggler mass distribution is to measure the masses of the blue stragglers through some observational method. There are several ways of observationally determining the mass of a star: gravitationally, spectroscopically, and photometrically. Gravitational (e.g. observations of eclipsing binaries) and spectroscopic (e.g. spectral estimates of surface temperature and gravity) mass determinations are potentially the most accurate of the three, but, unfortunately, both require extensive observations which have not been done for a large enough sample of blue stragglers to be of use here. Photometric mass determinations, while much less precise, are simply and readily done by finding the evolutionary tracks which most closely match the photometric properties of the stars. For example, using the same standard evolutionary tracks as those in Figure 4.10 the masses of the blue stragglers in 47 Tuc can be estimated by finding which tracks intersect the photometric positions of the blue stragglers, as shown in Figure 4.12. Obviously, different tracks from different blue straggler formation mechanisms will yield different mass estimates. This method of determining the blue straggler mass distribution has the advantage that no assumptions about cluster dynamics have to be made: the blue stragglers already include the effects of cluster dynamics, binary fractions, etc., and so no knowledge of these cluster properties is necessary to determine their masses in this way. A drawback of this method of determining stellar masses is that, for it to be accurate, the cluster distance and reddening must also be known accurately.

Rather than determine a distance and a reddening for each cluster and then determine an appropriate age through comparison with isochrones, the

reverse has been done here: an age has been assumed for the clusters, and the appropriate vertical and horizontal shifts necessary to align the cluster fiducial to the chosen isochrone were then found (Table 4.2). For the metal-poor clusters, one age was assumed for all (14 Gyr), while an age of 12 Gyr was assumed for 47 Tuc. While we do not assume that the shifts are viable estimates of the true distances and reddenings of the clusters, the derived shifts are reasonable and, if the chosen ages of the isochrones are reasonable (compared to the published distance moduli and reddenings), we can expect an error in the turnoff mass of only a few hundredths of a solar mass (as mentioned above). The effect of such a small error in turnoff mass, due to an incorrect assumed age, should merely be to shift the derived mass distribution to slightly higher or lower masses. Since the shape of evolutionary tracks which differ by only a few hundredths of a solar mass are very similar, it is unlikely that the comparison of the models to the observations will be strongly affected.

An additional concern with the photometric masses determined here is the uncertainty in mass due to the photometric uncertainty. Figure 4.13 shows essentially the same diagram as Figure 4.12, but the uncertainties (1σ) in colour and magnitude have been included for each blue straggler. Typically, the 1σ uncertainty in the masses of the blue stragglers is less than $\sim 0.05 M_{\odot}$, which is comparable to the error in turnoff mass if the assumed ages are off by $\sim$ 2Gyr. In the simulations which will be done to compare the predictions of the various formation mechanisms to the observations of blue stragglers, this uncertainty in the photometric mass of the stars will be taken into account.
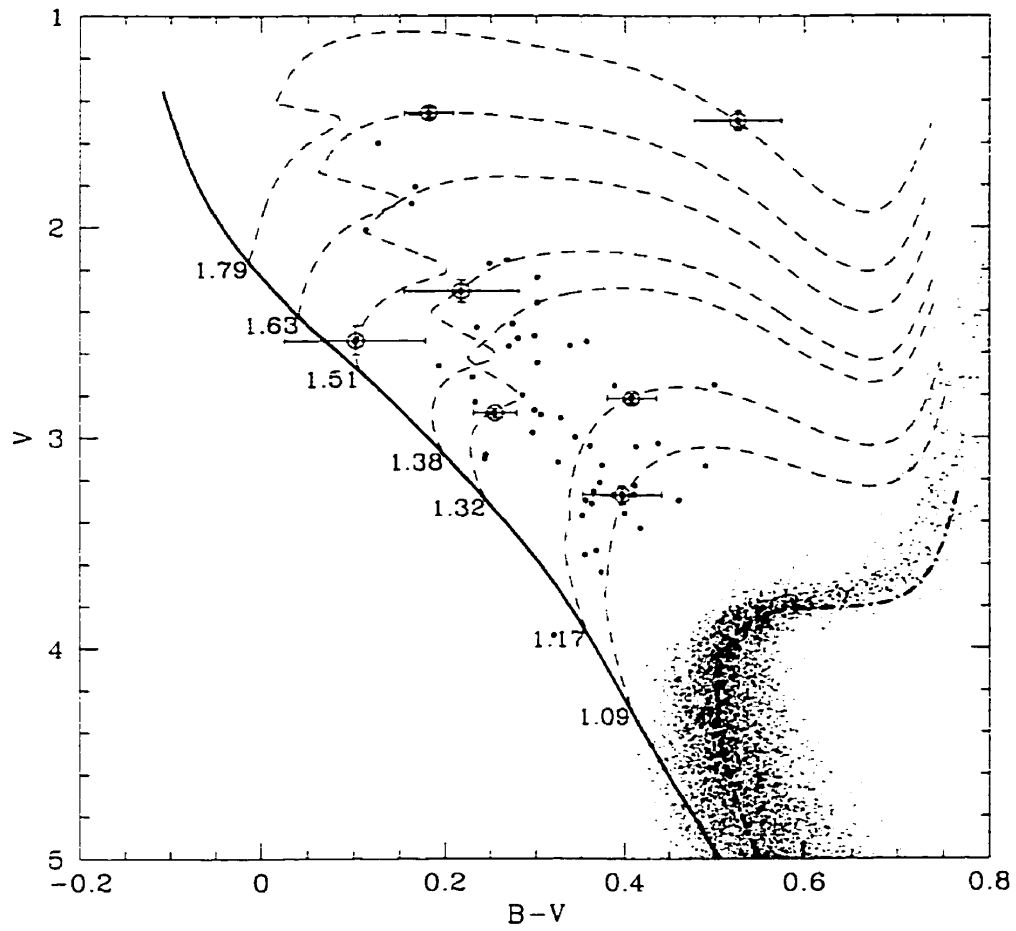
Figure 4.13: This figure is identical to Figure 4.13, except the photometric uncertainties of several of the blue stragglers are also shown.
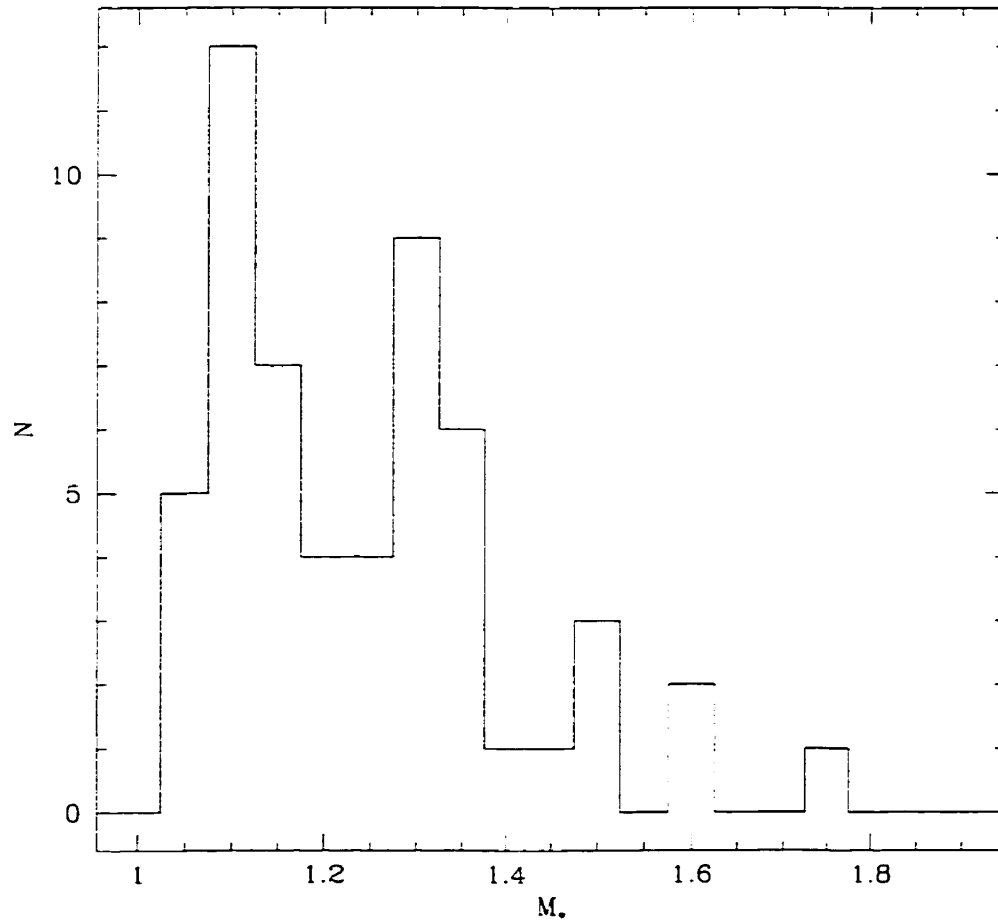
Figure 4.14: Distribution of photometric masses of the blue stragglers in 47 Tuc, assuming that they are normal stars. The masses are in solar units.
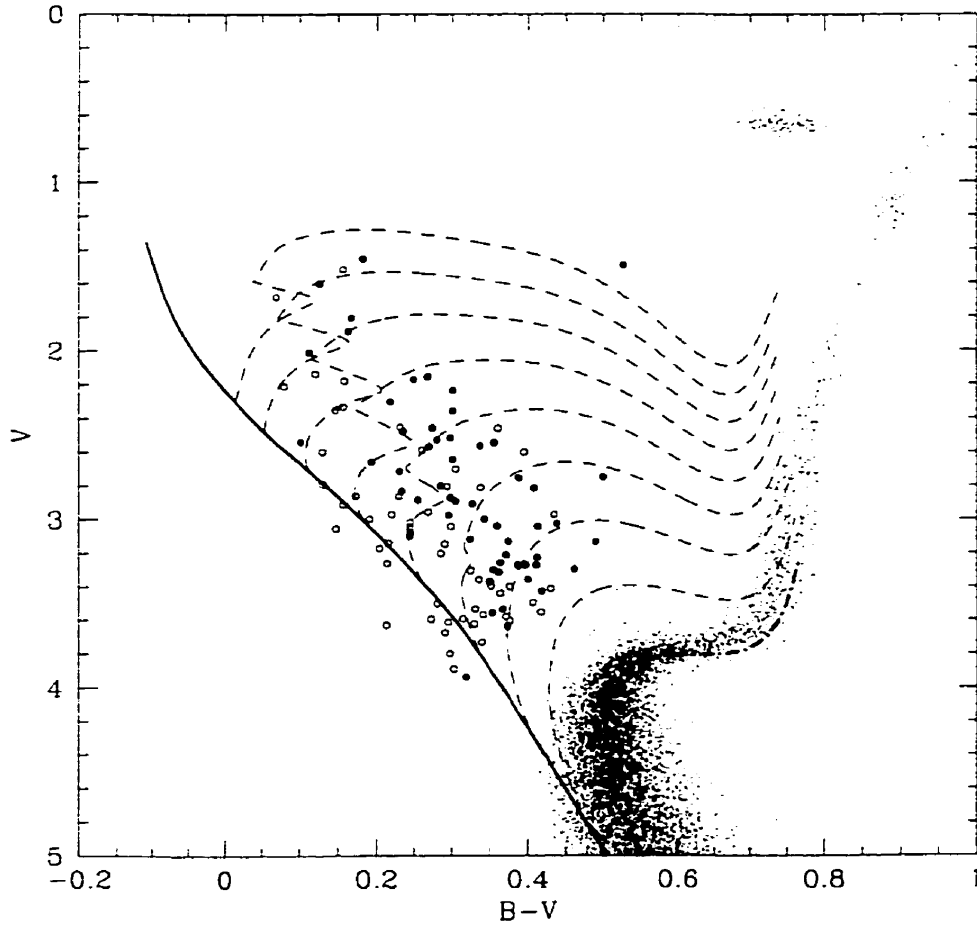
Figure 4.15: Comparison of fake blue stragglers (open circles), which have been drawn from standard tracks, and real blue stragglers (filled circles). The distribution of the fake blue stragglers is quite different from that of the real blue stragglers.

Now that we have a mass distribution for the blue stragglers in 47 Tuc, assuming they were formed as normal stars (Figure 4.14), fake blue stragglers can be drawn from these tracks and their distribution on the CMD compared with that of the observed blue stragglers. An example of such a fake distribution is shown in Figure 4.15 (the positions of the fake blue stragglers, after being drawn from the tracks, have had random photometric scatter added). Although there is some overlap between the two distributions of blue stragglers, the two populations appear to populate somewhat different regions relative to the ZAMS. At face value, this seems to suggest that blue stragglers are not normal stars. However, this statement is again based on a simple, qualitative comparison, and so needs some statistical verification.

4.1.1.1 Distance from the Zero-age Main Sequence – Δ_Z

A possible statistic for a more quantitative comparison between the models and blue stragglers is the distribution of the stars relative to the theoretical ZAMS. This statistic is an obvious choice since the models produced in Chapter 3 (collisional mergers, binary (fully-mixed) mergers) will obviously produce different distributions relative to the ZAMS, and the chosen clusters also have different distributions relative to the ZAMS (a similar statistic was used by Fusi Pecci et al., 1992, except that they used a straight line extension of the observed cluster main-sequence). The distance from the ZAMS is defined here as

$$\Delta_Z = \sqrt{(m_{1\bullet} - m_{1Z})^2 + (m_{2\bullet} - m_{2Z})^2}$$

where $m_{1\bullet}$ and $m_{2\bullet}$ are the independent magnitudes of the blue straggler (e.g. for BV data, $m_{1\bullet} \equiv$ B and $m_{2\bullet} \equiv$ V), and m_{1Z} and m_{2Z} are the equivalent
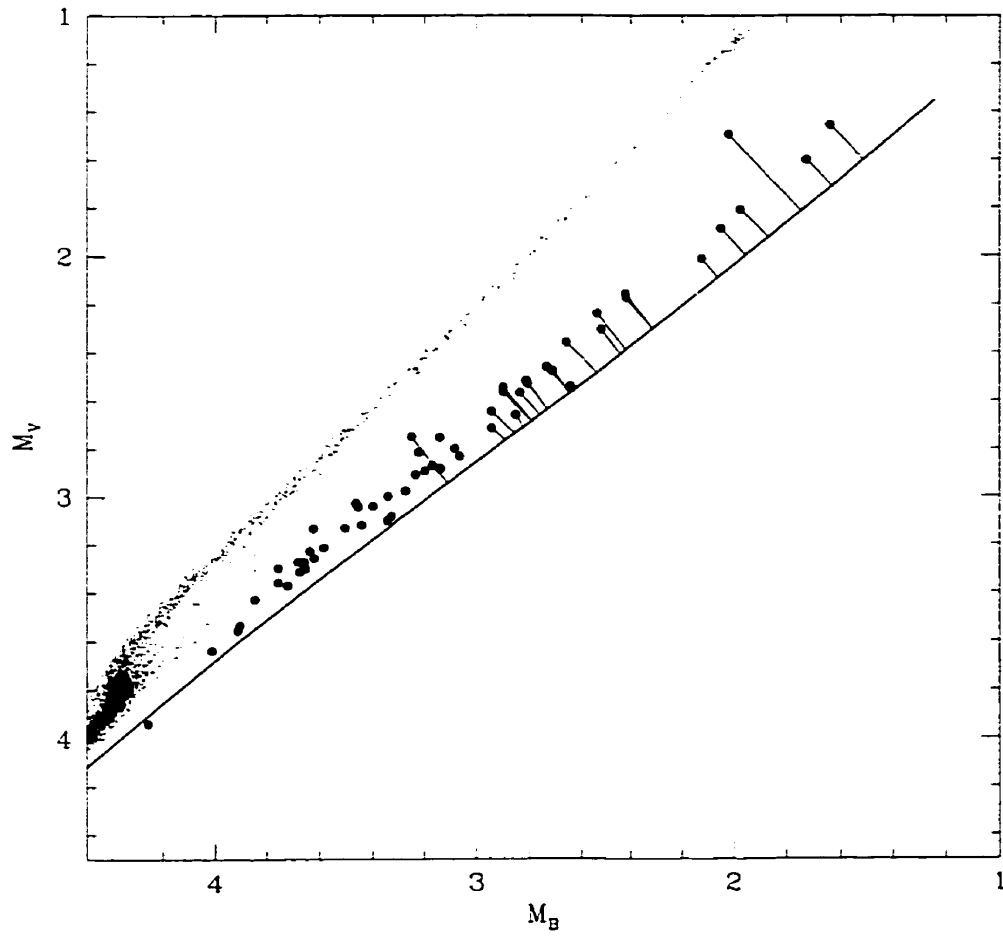
Figure 4.16: Shown is a M_B,M_V plot of the stars in 47 Tuc, along with the ZAMS for the cluster (thick line). The length of the thin lines connecting some of the blue stragglers to the ZAMS define the Δ_Z values for those stars.
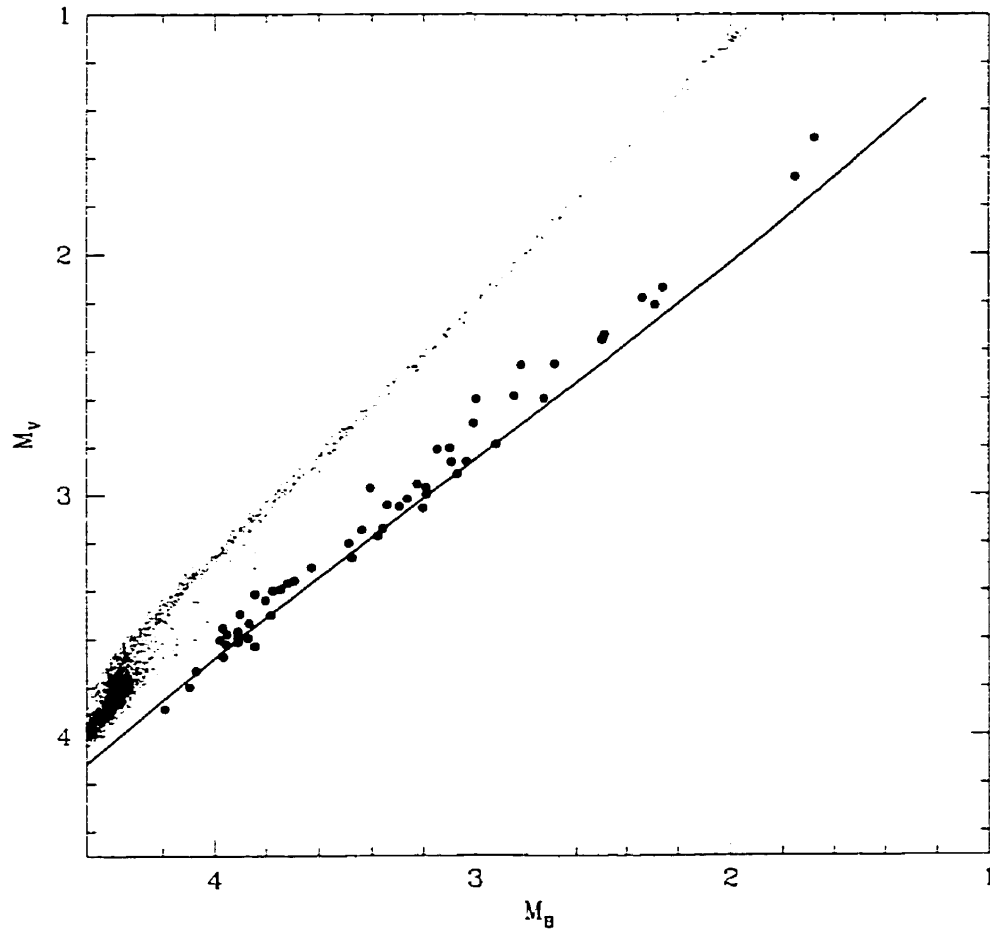
Figure 4.17: This figure is the same as Figure 4.16, except that the filled circles are the same fake blue stragglers shown in Figure 4.15. Compare the distribution of fake blue stragglers to that of the real blue stragglers in Figure 4.16.
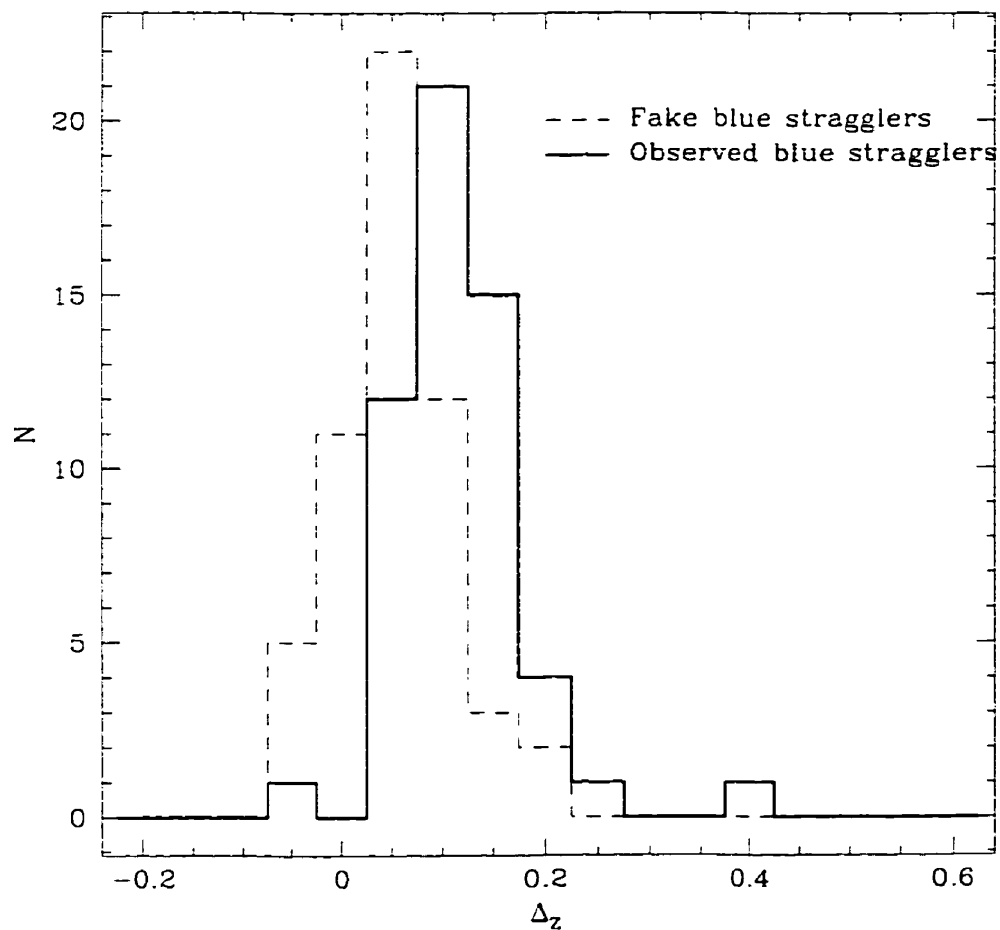
Figure 4.18: Histograms of the Δ_Z distribution of the real (thick line) and fake (thin dashed line) blue stragglers 47 Tuc. The fake blue stragglers are the same as those shown in Figure 4.15.

magnitudes for the nearest point on the ZAMS (Note: this is *not necessarily* the same as the ZAMS position of the blue straggler, it is merely the point on the ZAMS which minimises Δ_z). Δ_z is defined to be negative for stars blue-ward of the ZAMS. The independent magnitudes were used, rather than the colour and magnitude together, since this gives both coordinates the same scale (i.e. colours, such as B-V, are the logarithm of the ratio of two fluxes, whereas magnitudes are the logarithm of the flux itself) (Figure 4.16). Figure 4.18 shows the Δ_z distributions for the real and fake blue stragglers shown in Figure 4.15: the two distributions are obviously different and a Kolmogorov-Smirnoff (**KS**) test comparing the two distributions gives a probability of 0.05% that they were drawn from the same parent population.

The fake blue stragglers shown in Figure 4.15 have the same (photometrically determined) masses as the observed blue stragglers. However, since there is an uncertainty associated with each mass, the lack of agreement between the models and observations is also uncertain. In order to take the uncertainties in the masses into account, the observed position of each blue straggler was randomly scattered, using its photometric uncertainty in each magnitude, and the photometric mass of the blue straggler was re-determined using the chosen tracks.[2] Using this new mass, a new fake blue straggler was drawn from the track using the procedure described above. Photometric scatter was added to each fake blue straggler's magnitudes and the Δ_z distribution was again determined and compared to the observed distribution. This 'Monte Carlo' procedure was repeated, typically 10,000 times, and the

---

[2]The photometric scatter was added to $m_{1\bullet}$ and $m_{2\bullet}$, not to the corresponding colour.

median KS probability was accepted as the final value.

Each time a fake blue straggler was drawn from the tracks and photo-metric scatter added to the star's magnitudes, its location on the CMD was checked to determine if it was inside the boundary used to select the clus-ter stragglers. If the fake star had wandered out of the boundary, it was discarded and another fake star created.

There may be some concern about the above procedure for drawing fake blue stragglers from the chosen tracks. One might think that the magnitudes of the fake blue stragglers are convolved with the photometric uncertainty three times: once by the observations of the blue stragglers themselves, once when determining random masses, and once more to simulate observational scatter again. This is not so. It is true that the observed magnitudes of the blue stragglers are removed from their true values by some amount which is (hopefully) normally distributed with a standard deviation equal to the measured uncertainty: since we do not know these true values, we must assume that the observed values lie within 1σ of the true values $\sim$ 68% of the time, and within 2σ $\sim$ 95% of the time, etc. Having determined a photometric mass from the observed magnitudes of the blue straggler, and the equivalent uncertainties due to the photometric uncertainties, we can also only be certain of arriving at a mass close to the true value some fraction of the time. However, in arriving at an assumed mass and drawing a fake blue straggler from the appropriate track, *there is no uncertainty* in that fake star's magnitudes: we are assuming that the magnitudes drawn from the tracks define the values for a star formed with the appropriate mass, age, and formation mechanism. Hence, since these magnitudes are the true,

Table 4.5: 47 Tuc — Statistical comparison with models

Statistic	Standard Models	Turnoff Mergers	Equal-mass Mergers	Equal-mass Binary Mergers
$P(\Delta_Z)$	3.3×10^{-4}	0.245	0.032	8.0×10^{-5}
$\ln L_T$	-57.46	-46.45	-42.58	-60.00

error-free, values, we must add observational scatter as has been done to the observed blue stragglers by Nature.

The results of Monte Carlo simulations, as described above, are listed in Table 4.5 for standard evolutionary tracks, as well as for turnoff mergers, equal-mass mergers, and binary mergers. It can now be said, with some confidence, that blue stragglers, at least those in 47 Tuc, are not normal stars.

4.1.1.2 Maximum Likelihood – L_T

A concern raised by Sills & Bailyn (1999) was that, when comparing distributions of stars on the CMD, failing to use both magnitude and colour information could lead to a misinterpretation of the observations. In particular, they found that using only the magnitudes (e.g. Bailyn & Pinsonneault, 1995) or colours[3] by themselves could result in a false agreement when comparing model CMDs with observations. While this is most probably true, the Δ_Z statistic developed in the last section does incorporate all of the photometric information which is otherwise contained in a CMD; however, the one potential problem with using such a statistic is that the two-dimensional

---

[3]The authors imply that Ouellette & Pritchet (1996) used colour information only when comparing their models to the observed blue stragglers in M3: in fact, a quantity similar to Δ_Z, which incorporated both colour and luminosity information, was used.

photometric information is compressed into one dimension perpendicular to the ZAMS. It is possible that this will result in some loss of information and potentially bias the model-cluster comparisons.

Tolstoy & Saha (1996) have developed a robust method for comparing observed CMDs to theoretical CMDs, which we have decided to use here. In their method, each star in an observed CMD has some likelihood, $S(\xi_n)$[4], dependent upon the observational uncertainties and difference in magnitude, of being represented by each star in a theoretical CMD; the product of these likelihoods for the entire set of observed stars gives the likelihood that the observed ensemble is well represented by the theoretical CMD. Given a series of theoretical CMDs — each produced with different assumptions about formation history, mass functions, etc. — the one which maximises this likelihood is the best match to the data. Since not every possible permutation of input parameters can be explored (usually) when making the theoretical CMDs, the likelihoods are not normalised and so do not represent the absolute probability of a particular theoretical model being a match to the data; instead, the ranking of the theoretical CMDs from highest likelihood to the lowest gives the order of preference.

The likelihood of each star in the observed CMD being well-represented by a theoretical CMD is given by

$$S(\xi_n) = \frac{1}{N} \frac{1}{2\pi\sigma_{m_1\bullet}(n)\sigma_{m_2\bullet}(n)} \times$$
$$\sum_{i=1}^{N_T} \exp\left[-\frac{1}{2}\left(\frac{\left(m_{1\bullet}(n) - m_{1T}(i)\right)^2}{\sigma_{m_1\bullet}(n)^2} + \frac{\left(m_{2\bullet}(n) - m_{2T}(i)\right)^2}{\sigma_{m_2\bullet}(n)^2}\right)\right],$$
(4.1)

---

[4]ξ_n is simply the photometric position of the star, given its magnitudes m_1 and m_2: $\xi_n = (m_1, m_2)$.

where $\sigma_{m_{1*}}(n)$ and $\sigma_{m_{2*}}(n)$ are the observational uncertainties for observed star n, $m_{1*}(n)$ and $m_{2*}(n)$ are, as before, the independent magnitudes for star n, $\xi_n = \left(m_{1*}(n), m_{2*}(n)\right)$, and $m_{1T}(i)$ and $m_{2T}(i)$ are the independent magnitudes for star i in the theoretical CMD in which there are N_T stars. The combined likelihood of the the observed dataset being well represented by the theoretical CMD is the product of the N_* likelihoods for the observed stars:

$$L = \prod_{n=1}^{N_*} S(\xi_n)$$

or, as a logarithmic quantity:

$$\ln L = \sum_{n=1}^{N_*} \ln S(\xi_n). \tag{4.2}$$

A perfect match to the data would yield a likelihood which is dependent upon the observational uncertainties of the data. In fact, a perfect match to the data is the data itself: finding $\ln L$ for the data ($\ln L_d$, found by using the observed data as the 'theoretical data', $m_{1T}(i)$ and $m_{2T}(i)$, in Equations 4.1 and 4.2) allows us to express the likelihoods of the theoretical CMDs relative to this 'perfect' dataset:

$$\ln L_T = \ln L - \ln L_d. \tag{4.3}$$

Some statistical tests of the method are presented in Appendix A.

It should be noted that, in contrast to the simulations involving the distribution of Δ_Z, the fake blue stragglers in the theoretical CMDs used here are not scattered by their individual photometric uncertainties after they are drawn from the tracks: the observed blue stragglers are compared directly to the *models*, with the photometric uncertainties of the observations taken

into account in the calculation of the likelihoods (Equation 4.1). However, as it turns out, erroneously including the photometric scatter in the theoretical CMDs changes the likelihoods for each formation mechanism, but not the ranking.

The likelihoods given in Table 4.5 ($\ln L_T$) are the logarithmic likelihoods for the various formation mechanisms, and for the hypothesis that blue stragglers are normal stars. The highest likelihood for a best match to the observed blue stragglers in 47 Tuc are equal-mass mergers; the hypothesis of standard stellar formation gives a much lower likelihood, but it is apparently not as unlikely as all of the blue stragglers having formed by binary mergers. Again, the blue stragglers in 47 Tuc are not likely to be normal stars.

4.1.2 Other Possibilities

Using the Δ_Z distributions, turnoff mergers would appear to be the best match for the blue stragglers in 47 Tuc of the four formation mechanisms presented. Unfortunately, the probability of the observed Δ_Z distribution being drawn from a parent population of turnoff mergers is only 24.5%. This is not a significant rejection of the turnoff merger Δ_Z distribution as the parent distribution, but it is unsatisfactory. Statistically, this is in the 'grey' level of probability where one may not confidently reject or accept the chosen hypothesis, but it might indicate that something else is amiss.

The unsatisfactory agreement of the 47 Tuc blue stragglers with the turnoff mergers is somewhat puzzling. Ouellette & Pritchet (1998) used very similar models to find a very significant agreement of 96% between the two populations. Also, the probability that equal-mass mergers could be

the parent population for the blue stragglers in 47 Tuc is rejected here at a significant 3.2%, whereas it was only marginally rejected at the 18% level by Ouellette & Pritchet. At first glance, this is somewhat worrisome, but, in fact, it is quite understandable and the relative ranking of the formation mechanisms (equal-mass merger : turnoff merger : standard formation : binary merger) is acceptable, though not statistically significant.

Ouellette & Pritchet used the photometry from Guhathakurta et al. (1992) for their study of 47 Tuc. While this was the best photometry available for the blue stragglers in 47 Tuc at the time this study was done, the photometric uncertainties are larger (by a factor of ~ 2) than those in the data from the Rich et al. (1997) study; also, there were fewer stars in the sample (again, by a factor of ~ 2). The larger uncertainties in the Guhathakurta et al. study made it easier to achieve an agreement between the turnoff mergers and the 47 Tuc blue stragglers since slight differences were blurred. In Figure 4.19, which shows the Δz distributions for turnoff mergers and the blue stragglers in 47 Tuc, it is easy to see how larger uncertainties (in the observations, and incorporated into the theoretical data) could improve agreement significantly. With the higher quality data of Rich et al. it is obvious that the turnoff mergers are spread out too far to the red (positive Δz), although the reddest blue straggler in 47 Tuc is far too red to be in agreement with the models. Also, the blue straggler which falls blueward of the ZAMS (negative Δz) is poorly matched by the turnoff mergers. The distribution of real blue stragglers appears to be somewhat more narrow than that of the turnoff mergers, with a possible enhancement on the blue side of the theoretical distribution.
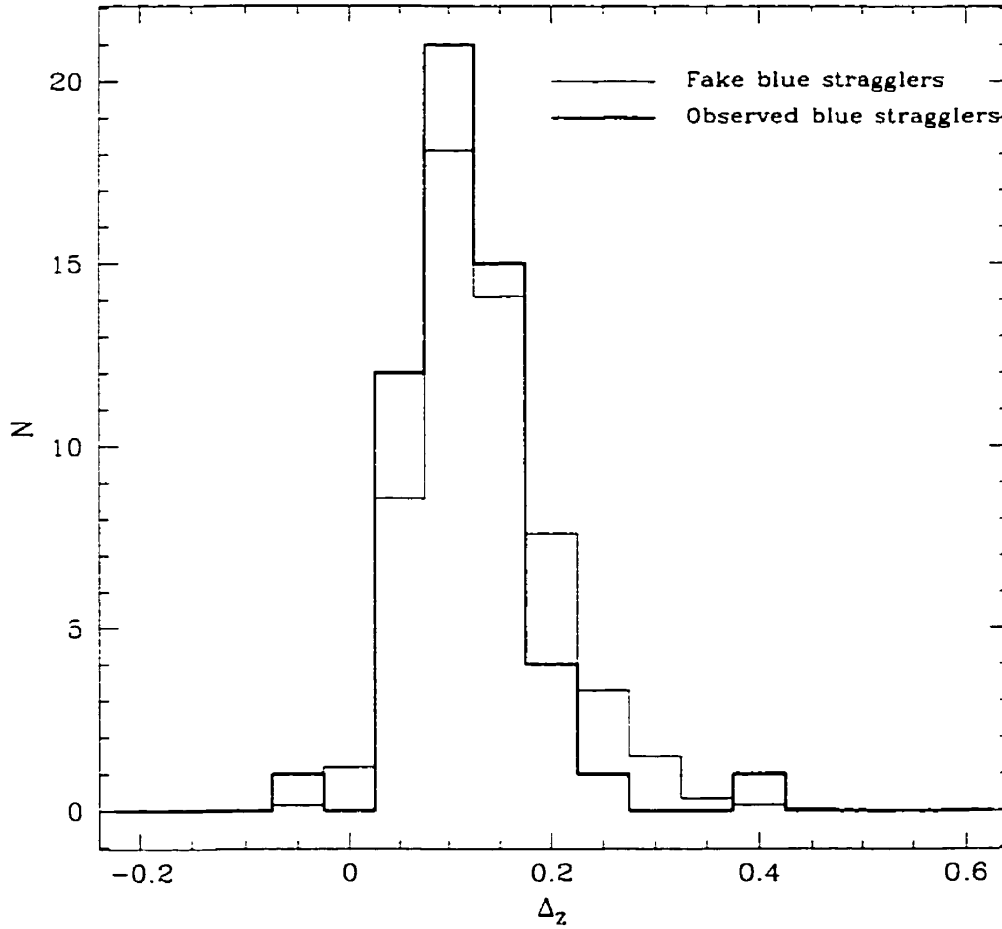
Figure 4.19: Histograms of the Δ_z distribution of the real (thick line) blue stragglers and turnoff merger remnants (thin solid line). The turnoff merger distribution has a broader distribution toward positive Δ_z, while the real blue stragglers have a slight enhancement toward small and negative Δ_z.

Table 4.6: 47 Tuc — Statistical comparison with models using data subset

Statistic	Standard Models	Turnoff Mergers	Equal-mass Mergers	Equal-mass Binary Mergers
$P(\Delta_Z)$	4.2×10^{-4}	0.220	0.029	1.2×10^{-4}
$\ln L_T$	-52.14	-35.75	-37.66	-57.03

Could the two stars in obviously poor agreement with the turnoff mergers — the two stars with the most negative and most positive Δ_Z values — be the culprits? Removing these from the data for 47 Tuc changes the probabilities from the KS comparison of the distributions to those shown in Table 4.6. While the significance of the agreement between the turnoff mergers and the observed blue stragglers has not improved, the relative ranking of the various formation mechanisms remains the same: turnoff mergers are apparently the most likely to have produced the blue stragglers in 47 Tuc, although little statistical confidence can be placed in the appearance.

The weak confidence in this result is further weakened by the fact that the most likely formation mechanism according to the ranking of L_T is equal-mass mergers (Table 4.5). Since this statistic is arguably more robust than the $P(\Delta_Z)$ statistic, we should be able to place somewhat more confidence in the results from L_T; however, as these are likelihoods and not probabilities, only the relative rankings of the formation mechanisms can be compared. On the other hand, could the Δ_Z statistic be such a poor indicator of the differences between the models that it would lead to a highly significant, but false, rejection of the true parent population? Since Δ_Z is an intuitively obvious way of comparing the models and blue stragglers, and since the Δ_Z distributions of the turnoff mergers and equal-mass mergers are so obviously

different from each other, this seems doubtful.

The source of the high likelihood of the equal-mass mergers can be examined more closely by looking at the likelihoods for the individual stars, the $S(\xi_n)$ values (Equation 4.1). Figure 4.20 shows the likelihoods for the observed blue stragglers $(S_d(\xi_n)$; i.e. the likelihood obtained by comparing each observed star to the entire observed dataset) plotted against the average likelihoods from the comparisons with the theoretical CMDs drawn from the turnoff merger and equal-mass merger tracks:

$$\bar{S}_n = \sum_{j=1}^{N_{MC}} S(\xi_n)_j - S_d(\xi_n), \tag{4.4}$$

where N_{MC} is the number of Monte Carlo simulations performed. One star — the star mentioned earlier as having a Δ_Z too negative to be adequately represented by the turnoff mergers — is assigned an extremely low likelihood relative to the rest of the observed blue stragglers: omitting this single star from the data set yields a likelihood of -35.75 of the remaining stars being adequately represented by turnoff mergers, while the likelihoods for the other formation mechanisms do not show as much of a change (Table 4.6). The extremely low value of $S(\xi_n)$ for this star, and the resulting low likelihood for turnoff mergers when it is included in the data, is easily explained by the fact that only very rarely will an turnoff merger be photometrically scattered near to its position on the CMD.

It *is* possible that the deleted star is merely a photometric interloper (its photometric uncertainties are not unusually large or small, compared to other stars of similar magnitude). If it has been scattered from the cluster turnoff, then it is also possible that other stars have been scattered from the turnoff region into the blue straggler region. It may be that the polygon used
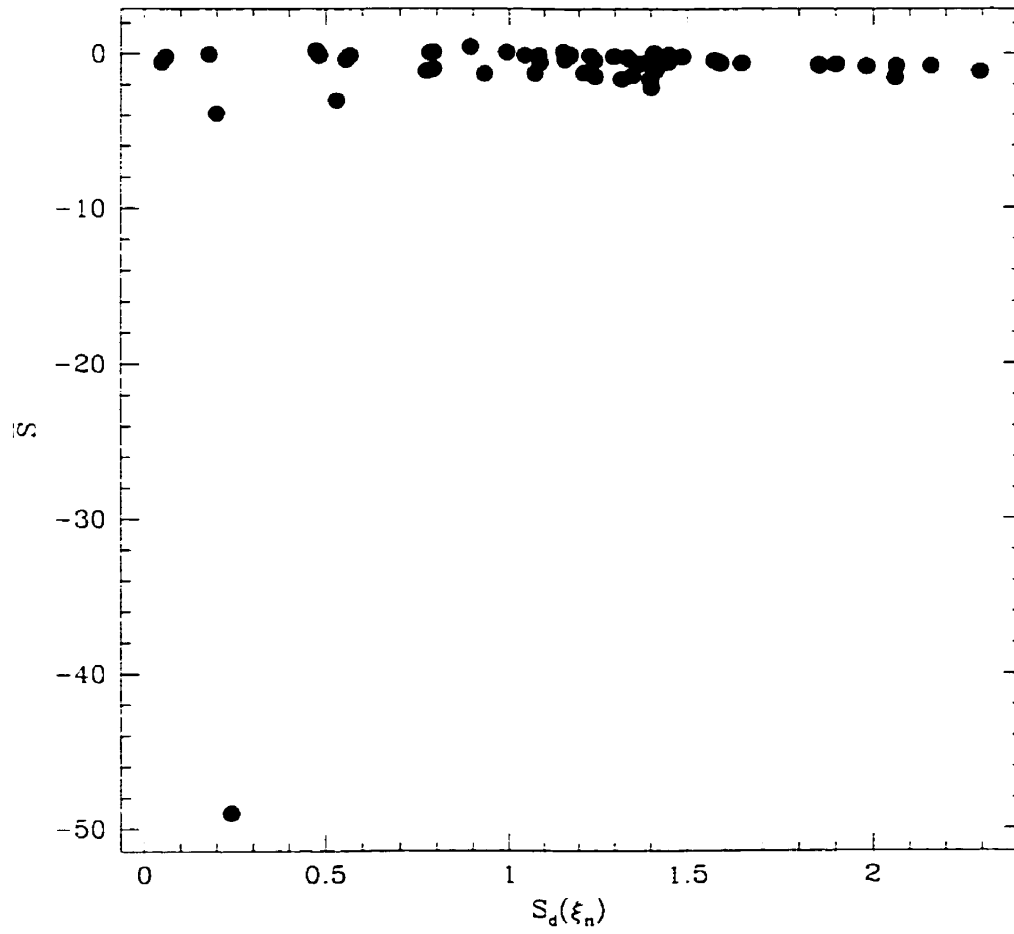
Figure 4.20: Individual likelihoods for the real blue stragglers in 47 Tuc, S_d, plotted against the likelihoods for turnoff mergers being an adequate match to the observations (see Text).

Table 4.7: 47 Tuc — Statistical comparison with models using restricted polygon

Statistic	Standard Models	Turnoff Mergers	Equal-mass Mergers	Equal-mass Binary Mergers
$P(\Delta_Z)$	5.9×10^{-4}	0.41	0.046	1.3×10^{-4}
$\ln L_T$	-45.54	-35.27	-32.28	-50.37

to select blue stragglers in the cluster is too generous and extends too close to the scattered stars around the turnoff. Using a somewhat different polygon with the redward side shifted ~ 0.05 bluer in B-V (rejecting 10 stars from the dataset), the rankings from the two tests (Table 4.7) are again what they were originally: the Δ_Z test shows that the most likely formation mechanism for the blue stragglers in 47 Tuc is turnoff mergers (with a probability that warrants a marginal acceptance of the result), whereas the L_T test now ranks equal-mass mergers as being the most likely mechanism.[5]

Although this minor fiddling with the data, which has produced significant changes in the ranking of the various formation mechanisms, might decrease the confidence in the methods being used to compare the models to the data, what it *should* do is indicate that the theoretical CMDs being used are inadequate. It is possible that there is more than one mechanism acting to produce blue stragglers in 47 Tuc: this would produce an unsatisfactory agreement between the models for an individual formation mechanism and the data, and it would also cause the results to be highly dependent upon the selection criteria (e.g. the polygon used to select the blue stragglers).

---

[5]Changing the dataset by including or excluding different stars changes the value of L_d, the likelihood found when the data is compared to itself. Because of this, the likelihoods in Tables 4.5, 4.6, and 4.7 cannot be compared directly.
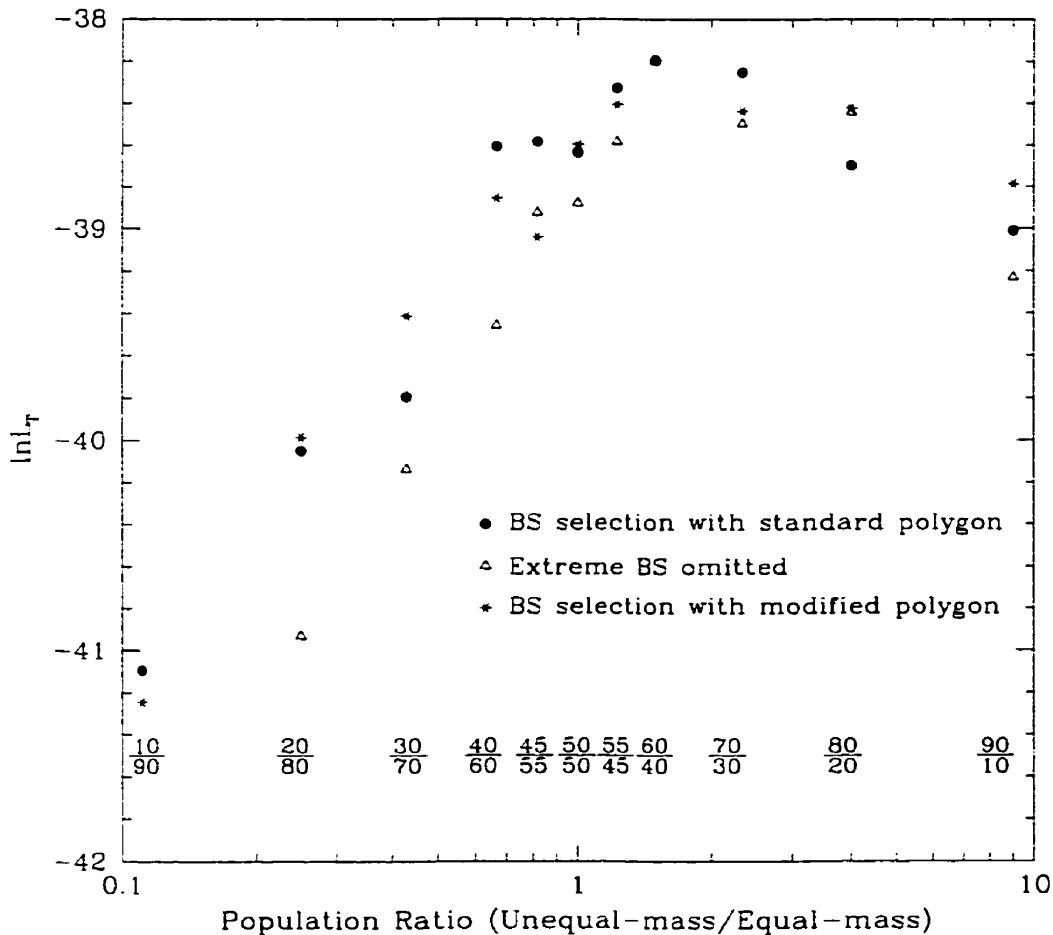
Figure 4.21: Likelihoods for varying turnoff merger/equal-mass merger population ratios in 47 Tuc. The three sets of population ratios were found using different sets of blue stragglers: one using the default selection polygon shown in Figure 4.1 (also used for the statistics in Table 4.5), one using a subset of the selected blue stragglers in which the two stars with the most extreme (positive and negative) Δ_z values have been omitted, and one using a modified selection polygon (also used for the statistics in Table 4.7). The three sets of likelihoods have been shifted so that the most likely population ratio — that with 60/40 turnoff mergers/equal-mass mergers — is equal in all sets. As explained in the text, only the likelihood rankings within each set are relevant. The likelihood values plotted are the median likelihoods from the Monte Carlo simulations.

One thing which the earlier data manipulations have shown is that the equal-mass and turnoff merger mechanisms are consistently the most likely formation mechanisms acting in 47 Tuc. Theoretical CMDs were created from both sets of tracks simultaneously by randomly assigning observed blue stragglers to one population or the other and drawing fake blue stragglers from the tracks (after determining the photometric masses with the assigned population's tracks); again, this procedure (including random assignment of the stragglers to the different populations) was repeated typically 10,000 times to generate the statistics. Figure 4.21 summarises the results of using hybrid populations of turnoff mergers and equal-mass mergers, with the relative populations of the merger remnants being varied from being nearly all turnoff mergers to nearly all equal-mass mergers. The population ratio with the highest likelihood of being the parent population for the blue stragglers in 47 Tuc is one which is 60% turnoff mergers and 40% equal-mass mergers. Performing the same data manipulations as were done when only single populations were being compared to the data (omitting the one discrepant straggler with the negative Δ_Z statistic and using a modified selection polygon) changes the likelihoods, but does not change the population ratio with the highest rank — this is what we expect to find when the theoretical CMDs representing the correct parent population are used.

Using the Δ_Z distributions of these hybrid populations results in a slightly different population receiving the highest probability of matching the observations: 50% turnoff mergers and 50% equal-mass mergers. However, although this population ratio is close to that found using $\ln L_T$ (Figure 4.21), the fact that Δ_Z compresses the information in the CMD into one dimen-

sion, rather than using the data in an unaltered form, lowers its perceived weight in the selection of the best-fitting population ratio. Since comparison of the Δ_Z distributions is nonetheless a viable method for weeding out population ratios which are poor matches to the data, a good match between the theoretical and observed Δ_Z distributions will be used as a necessary, but insufficient, criterion for an acceptable match between the the models and observations.

4.1.3 Discussion

Figure 4.22 shows the CMD of 47 Tuc, along with a hybrid population of fake blue stragglers composed of 60% turnoff and 40% equal-mass collisional mergers (CMs). This distribution of fake blue stragglers was selected from the theoretical CMDs generated for the Monte Carlo simulations with the quoted population ratio; it was selected at random from those sets of stars with likelihoods near to the median value for the entire run of 10,000 simulations $(\ln \widetilde{L_T} = -38.19)$. The likelihood assigned to this particular set of fake stars is $\ln L_T = -38.06$. Also, photometric scatter has been added to the stars shown (recall that, in the Tolstoy method, the theoretical CMDs do not have photometric scatter included before comparison to the observations). The visual agreement between the two (real and fake) distributions is quite good $(P(\Delta_Z) = 0.899)$. The obvious interpretation of this agreement is that the blue stragglers in 47 Tuc are being formed by collisional mergers.

4.1.3.1 Formation Rates

Sigurdsson & Phinney (1993) and Bacon, Sigurdsson & Davies (1996) have attempted to estimate the theoretical collisional formation rate of blue strag-
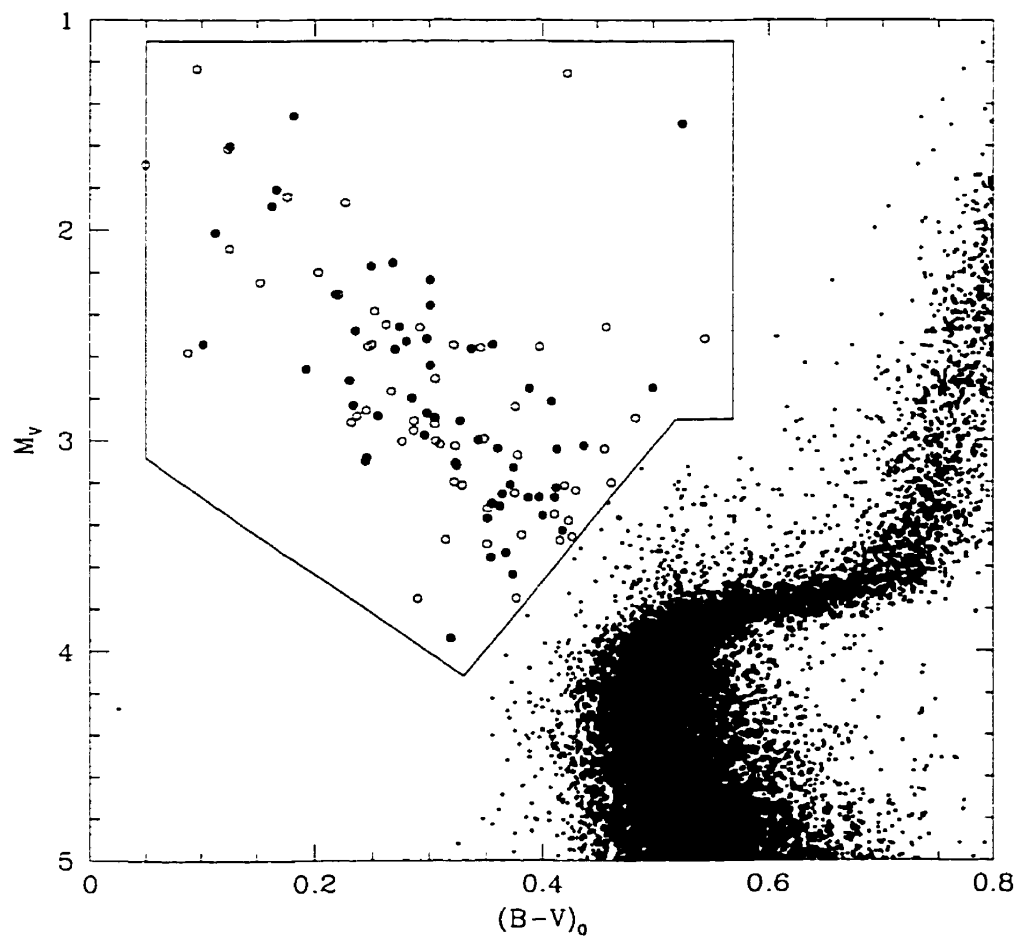
Figure 4.22: The open circles are fake blue stragglers drawn from a hybrid population composed of 60% turnoff mergers and 40% equal-mass mergers which best matches the observed distribution of blue stragglers in 47 Tuc (filled circles). The fake blue stragglers include the effects of observational uncertainty.
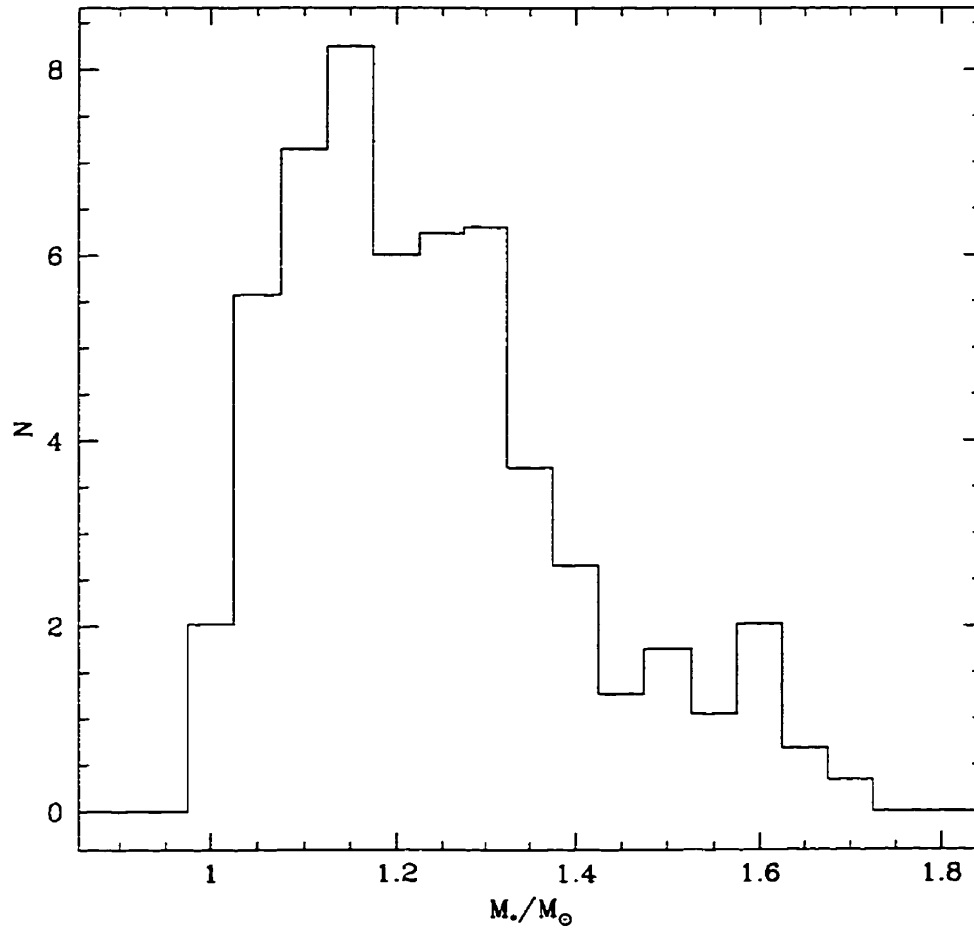
Figure 4.23: Distribution of the masses, in solar units, of the blue stragglers in 47 Tuc. The distribution shown is the average mass distribution from the Monte Carlo simulations.

glers in globular clusters by determining the collision cross-section through N-body simulations of binary-single star and binary-binary interactions. Given the cross-sections, the collision rate can be estimated using the observed stellar velocity dispersion and stellar number density in the cluster being examined. Using the relationships provided in those studies, the collision rate[6] in 47 Tuc should be one collision every $\sim 1.3 \times 10^7$ years for binary-binary collisions and one collision every $\sim 4.5 \times 10^6$ years for binary-single collisions, assuming an average binary semi-major axis of 0.1 astronomical unit (AU) and a binary fraction of $\sim 20\%$.

The blue straggler formation rate can be estimated from the models developed here by first finding the average time a star will spend as an observable blue straggler. For the merger population ratio found above for 47 Tuc, this average time is $\sim 1.8 \times 10^9$ years. In order to preserve the observed number of blue stragglers, the required production rate must be one blue straggler (collision) every $1.8 \times 10^9/55 \sim 3.3 \times 10^7$ years. For the calculated binary-binary and binary-single collision rates to agree with the necessary blue straggler formation rate, the binary fraction would have to be reduced to $\sim 10\%$.

The above average rate for the formation of blue stragglers is perhaps a bit simple. In 47 Tuc, the blue straggler population is most likely composed of roughly equal numbers of turnoff merger remnants and equal-mass merger remnants: this does not mean that the rates of formation of these remnants are the same. Turnoff merger remnants have an average lifetime in 47 Tuc of $\sim 1.1 \times 10^9$ years, whereas equal-mass merger remnants have an average

---

[6]These collision rates, and those calculated for the other clusters, are calculated using the parameters for the cluster core (Tables 4.3 and 4.4) and the observed numbers of stars.

lifetime of $\sim 2.8 \times 10^9$ years: maintaining the apparent population ratio requires collisions involving a turnoff star and a lower mass star to occur more than twice as often as collisions involving equal mass stars. In fact, during a dynamical interaction, a collision, if one occurs, is likely to involve the most massive star in the interacting systems, so a higher collision rate for turnoff stars is perhaps not unexpected. The relative rates at which turnoff and equal-mass collisions occur will be dependent upon the dynamical state of the cluster and the properties of the surviving binaries.

In the following sections, the models are compared with the blue stragglers in the remaining clusters. Since much of the discussion is analogous to that for 47 Tuc, these sections will concentrate on merely presenting the results of the analysis and making note of any special circumstances.

4.2 NGC 2419

The blue straggler population in NGC 2419 is distinctly different from that of 47 Tuc, perhaps a consequence of the much lower central density of NGC 2419 (Table 4.3). The population which best matched the blue stragglers in 47 Tuc — one composed of 60% turnoff collisional mergers and 40% equal-mass collisional mergers — is ranked quite low as a possible parent population for the blue stragglers in NGC2419 (Figure 4.24). In fact, there are three parent populations which are found to be almost equally likely to be able to reproduce the observations (Table 4.8): 10%:90% turnoff:equal-mass collisional mergers, a single population of equal-mass collisional mergers, and 90%:10% equal-mass collisional mergers:equal-mass binary (fully-mixed) mergers (BMs).

It is perhaps not too surprising that these three population ratios are

Table 4.8: NGC2419 — Statistics for most likely population ratios

Statistic	Turnoff/Equal-mass CM (10:90)	Equal-mass CM Only	Equal-mass CM/ Equal-mass BM (90:10)
$P(\Delta_Z)$	0.972	0.894	0.902
$\ln L_T$	-27.418	-27.579	-27.630

almost equally ranked: the difference between these populations amounts to two blue stragglers being formed by a different mechanism than the rest of the blue stragglers in the cluster. The Δ_Z distributions for these population ratios are also all well matched to the observations, but the population composed of 10% turnoff collisional mergers and 90% equal-mass collisional mergers provides the most probable match to the observed Δ_Z distribution. Figure 4.25 shows the observed blue stragglers in NGC 2419 and a population of fake blue stragglers with this population ratio: these fake stars were drawn at random from the theoretical CMDs which were used to generate the statistics shown in Figure 4.24 (which are the *median* likelihoods from the simulations) and include the effects of observational uncertainty.

The time-scale for binary-binary collisions in NGC 2419 is one collision every $\sim 1.7 \times 10^{10}$ years, while for binary-single collisions the time scale is one collision every $\sim 1.8 \times 10^8$ years, assuming a binary fraction of 20% and an average binary semi-major axis of 100 AU. In contrast, the average formation time required to maintain the observed numbers and population ratio is one blue straggler every $\sim 1.8 \times 10^8$ years. For the assumed binary parameters, the agreement between the rates calculated from the models and the rates calculated from N-body simulations is excellent.
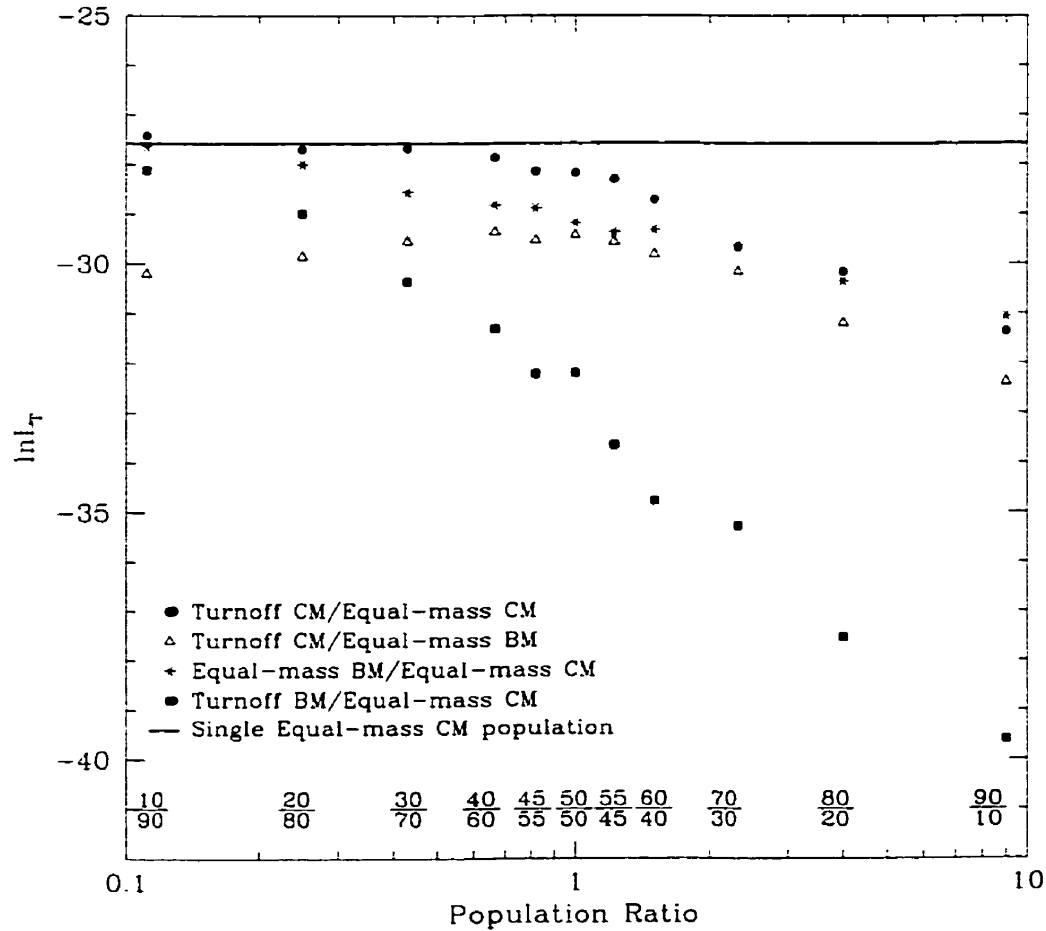
Figure 4.24: Likelihoods for different population ratios in NGC 2419. The likelihood values plotted are the median values from the Monte Carlo simulations: unlike the values plotted in Figure 4.21, these values have not been shifted to provide a match for the most likely population ratio.

Figure 4.25: CMD showing the observed blue stragglers in NGC 2419 (filled circles) and a hybrid population of blue stragglers composed of 10% turnoff CM and 90% equal-mass CM population (open circles).

As mentioned earlier, the relative collision rates between equal mass stars and between a turnoff star and a low mass star is likely to be dependent upon the characteristics of the binary population in the cluster, as well as the dynamics involved in the collisions. The turnoff merger rate in NGC 2419 should be one per $\sim 8 \times 10^8$ years, whereas the equal-mass merger rate should be one per $\sim 2 \times 10^8$ years. This is in contrast to the situation in 47 Tuc in which the formation rate for turnoff mergers is more than twice that of equal-mass mergers. While it is possible that this difference is due to the different cluster dynamics and binary populations, another possibility is that the blue stragglers in NGC 2419 are not being formed by collisions. Recalling the discussion in Section 3.4 regarding the fully-mixed models, it is possible that these blue stragglers are being formed via binary mass-transfer and/or coalescence: although we expect blue stragglers formed in this way to be in reasonable agreement with the fully-mixed models, it was recognised that they would, in fact, scatter between the fully-mixed (binary merger) models and the unmixed (collisional) models. However, without knowing more about the dynamics within the cluster it is difficult to say whether a population of almost solely equal-mass collisional mergers is likely — although Sigurdsson & Phinney (1993) find that, during collisions involving soft binaries, there is less of a bias toward collisions involving the most massive member of the system — and without knowing more about the amount of mixing which occurs during binary mass-transfer and coalescence, it is difficult to say whether such a population could mimic the population seen in NGC 2419. With the knowledge at hand, and the results of the simulations performed, we will accept that the blue stragglers in NGC 2419 are composed primarily of the

remnants of equal-mass collisional mergers.

4.3 NGC 5024

NGC 5024 has a central density which is intermediate between that of NGC 2419 and 47 Tuc — as it turns out, its blue straggler population is more similar to that of NGC 2419. It is possible that both NGC 2419 and NGC 5024 are in dynamically similar states, with similar binary populations and, hence, similar relative rates for the different blue straggler formation mechanisms.

As shown in Figure 4.27, two slightly different selection criteria were used for the blue stragglers: one polygon was chosen to include the two faint blue stragglers which lie just below the main population, and the other polygon was chosen to exclude them. These two blue stragglers, along with the two brightest blue stragglers, were consistently assigned low values of $\bar{S}$ (Equation 4.4, Figure 4.28). From the results of the comparisons with the models at various population ratios, including or excluding these two stars drastically changed the population ratio with the highest likelihood of matching the observed blue stragglers (Table 4.9), from a population consisting mostly of equal-mass binary mergers when the stars are included, to a population consisting mostly of equal-mass collisional mergers when the stars are excluded. However, when the stars are included in the blue straggler selection polygon, the highest ranked population provides a poor match to the observed Δ_Z distribution (Table 4.9): recall that a necessary condition for the acceptance of a given population was that it must not only receive a high likelihood of matching the observations, but that it must also provide a good match to the observed Δ_Z distribution. Whether these two faint blue
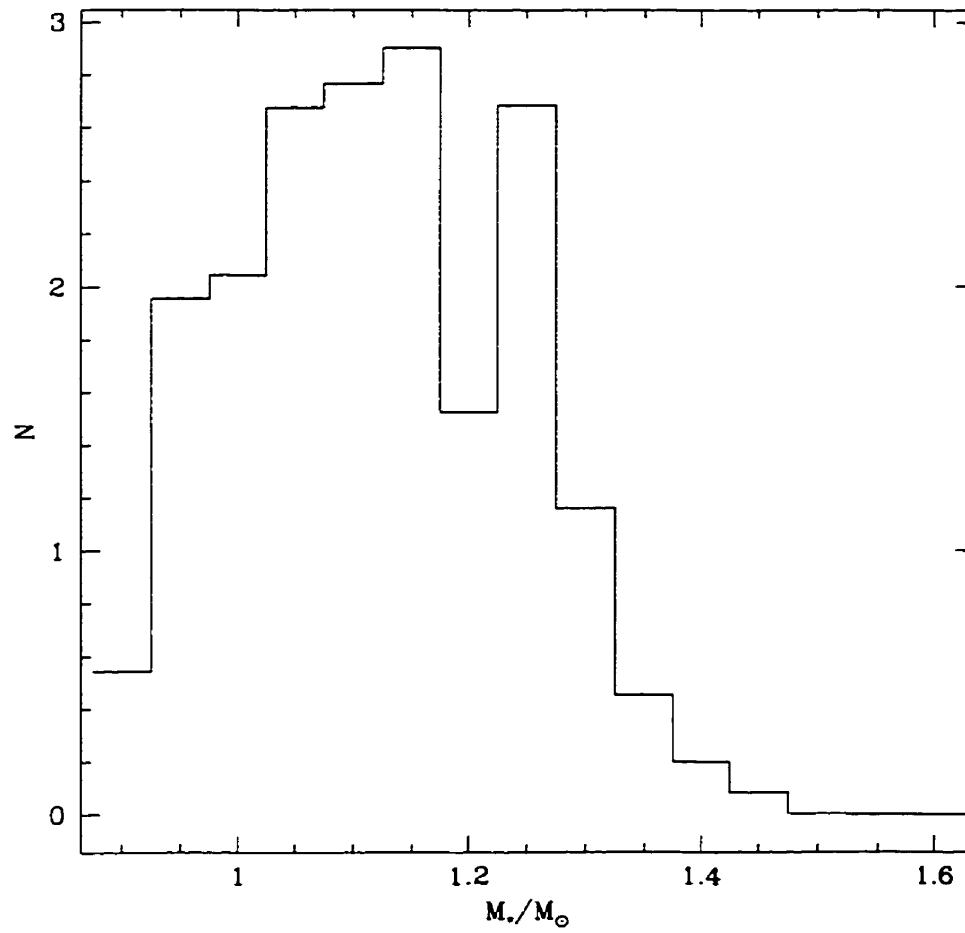
Figure 4.26: Distribution of the masses, in solar units, of the blue stragglers in NGC 2419.
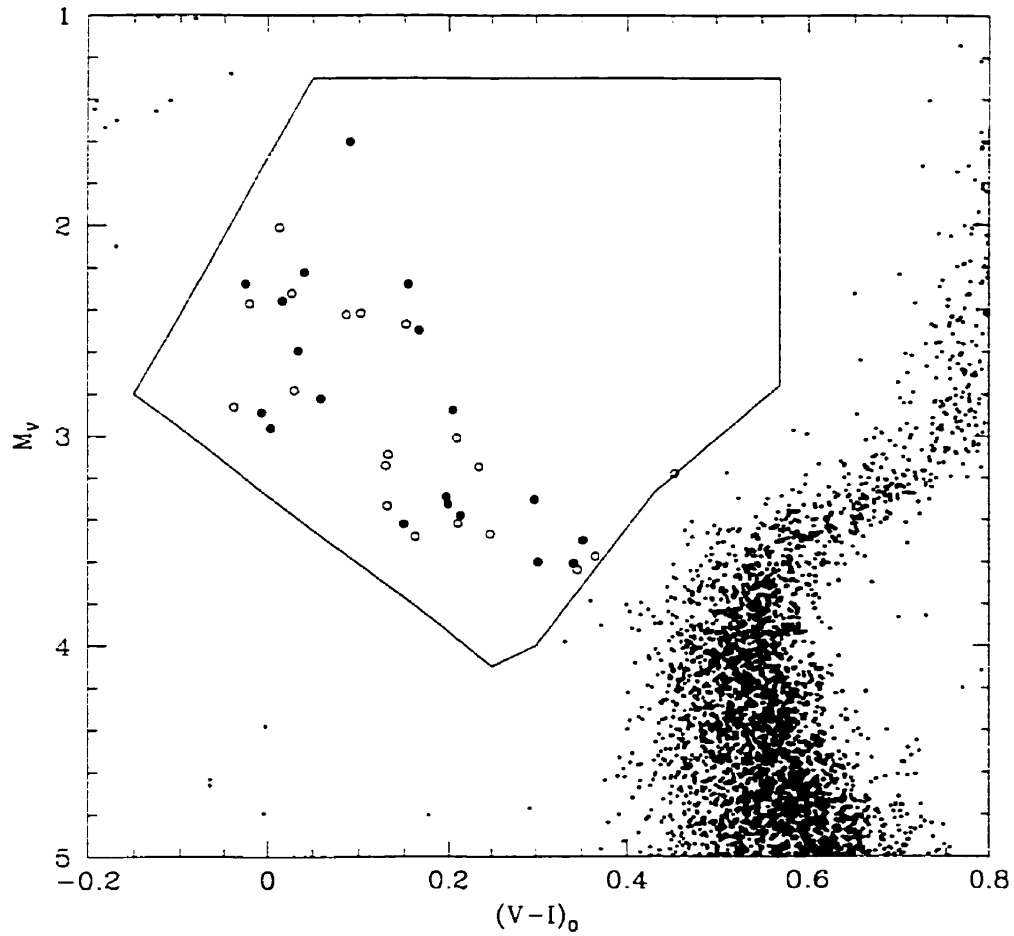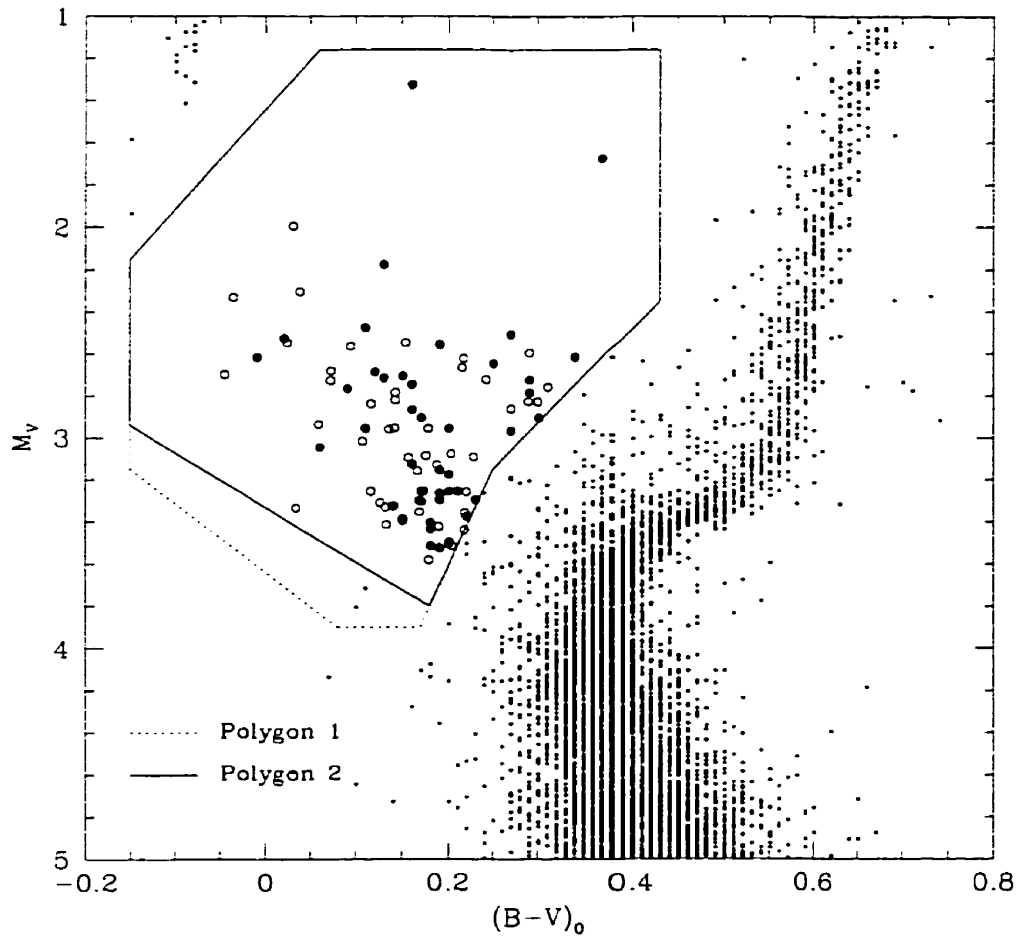
Figure 4.27: CMD showing the observed blue stragglers in NGC 5024 (filled circles) and a hybrid population of blue stragglers composed of 20% turnoff and 80% equal-mass collisional mergers (open circles). The two polygons show the slightly different blue straggler selection criteria described in the text.
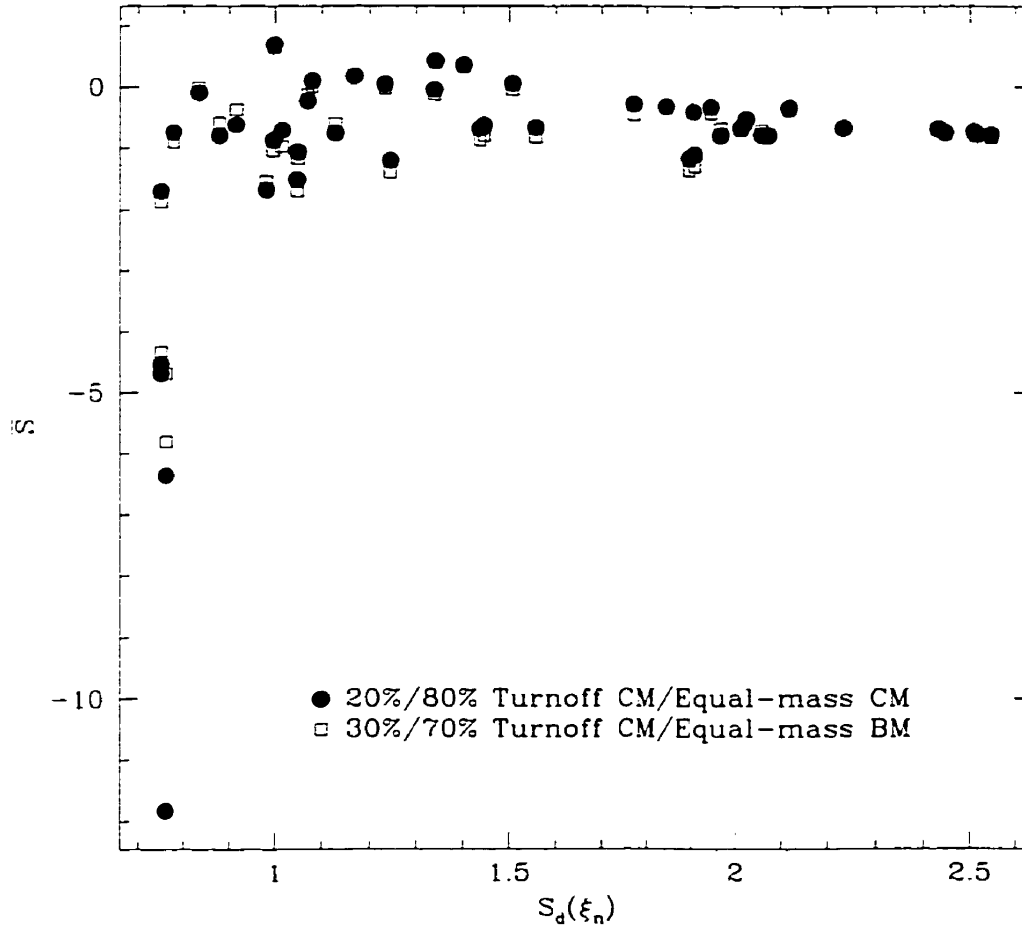
Figure 4.28: Individual likelihoods for the blue stragglers in NGC 5024 for the populations listed in Table 4.9 using Polygon 1. The two blue stragglers with the lowest values of $\bar{S}$ are the two faint blue stragglers which are excluded when Polygon 2 is used for candidate selection.

straggler candidates are included or not, a population consisting mostly of equal-mass binary mergers cannot satisfactorily reproduce the observed Δz distribution and so is likely not the parent population for the blue stragglers in NGC 5024.

Figure 4.29 and Table 4.9 show that, regardless of whether or not the two faint candidates are included, a population consisting of 20% turnoff collisional mergers and 80% equal-mass collisional mergers is consistently highly ranked (relative to other populations consisting only of collisional mergers) and also provides a good match to the observed Δz distribution.

The fact that the models do not provide a good match to the two faint candidates does not imply that they are not blue stragglers (although they may be photometric errors or foreground/background objects), but rather that they may come from a different population than the rest of the blue stragglers in the cluster. Including or excluding the two brightest blue stragglers does not change the relative ranking of the population ratios shown in Figure 4.29, despite the fact that these two blue straggler candidates receive values of $\bar{S}$ which are as low as those found for the two faint candidates. This is largely due to the fact that all of the models which have been used here are equally (un)likely to match the two bright candidates, whereas the collisional models are less likely to be able to provide a match to the faint candidates than are the models of binary mergers.

The blue straggler formation rate necessary to maintain the observed numbers is one blue straggler every $\sim 7.9 \times 10^7$ years, compared with the binary-binary collision rate of one collision every 1.4×10^7 years and the binary-single collision rate of one collision every 3.1×10^7 years assuming

Figure 4.29: Likelihoods for different population ratios in NGC 5024. The likelihood values plotted are the median values from the Monte Carlo simulations. The two data sets have been shifted so that the likelihoods for the highest ranked population ratio match.
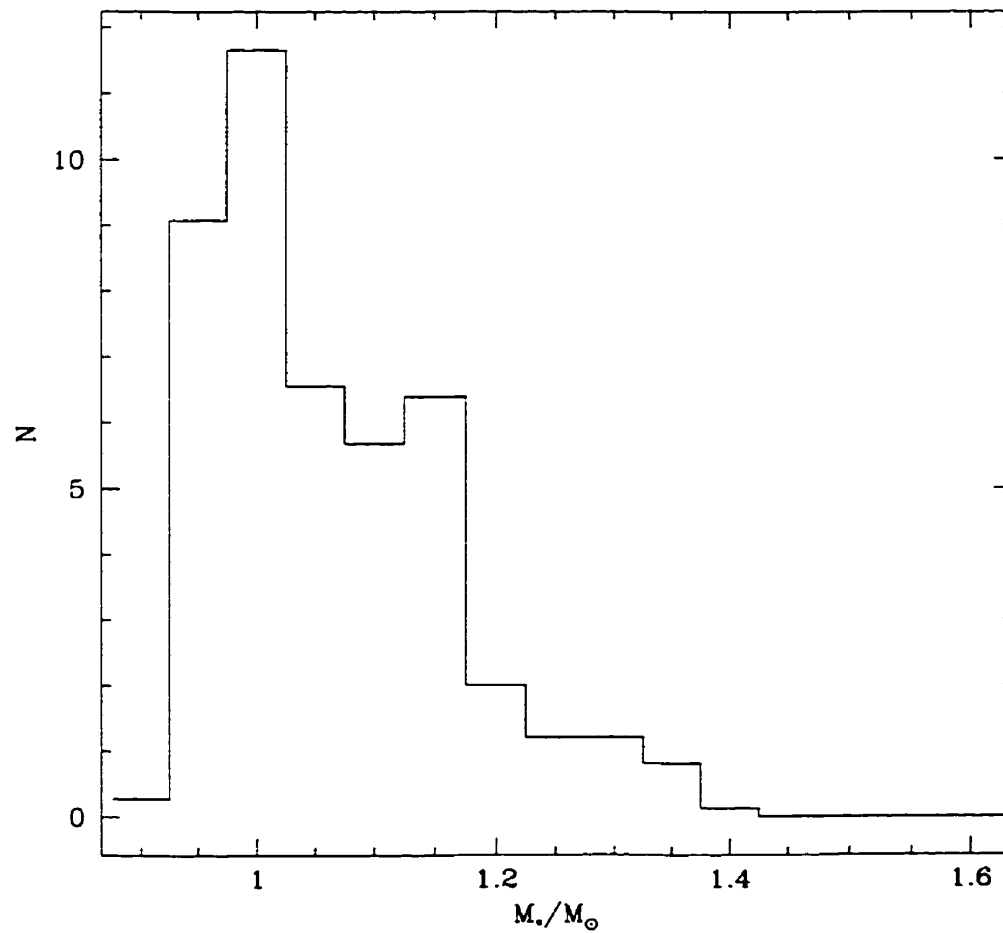
Figure 4.30: Distribution of the masses, in solar units, of the blue stragglers in NGC 5024.

Table 4.9: NGC 5024 — Statistics for the most likely population ratios

Statistic	Turnoff/Equal-mass CM (20:80)	Turnoff CM/ Equal-mass BM (30:70)
	Polygon 1	
$P(\Delta_z)$	0.84	0.36
ln L_T	-49.12	-43.08
	Polygon 2	
$P(\Delta_z)$	0.93	0.33
ln L_T	-35.66	-36.37

an average binary semi-major axis of 10AU and a binary fraction of 20% (following Bacon, Sigurdsson, & Davies, 1996). For the collision rates to agree with the necessary blue straggler formation rate, the binary fraction in the cluster would have to be ~ 10%.

4.4 NGC 6397

The blue straggler population in NGC 6397, along with that of 47 Tuc, was investigated by Ouellette & Pritchet (1998). It was found that turnoff collisional mergers provided a better match overall to the blue stragglers in NGC 6397, although with a low significance to the result. The match to the observations is greatly improved by using a hybrid population consisting of 80% turnoff collisional mergers and 20% equal-mass collisional mergers (Figure 4.31, Table 4.10).

As with NGC 5024, two blue straggler selection polygons were used to test the effect of including or excluding a blue straggler candidate which was consistently assigned a low value of $\bar{S}$ (Figure 4.32). With the star in
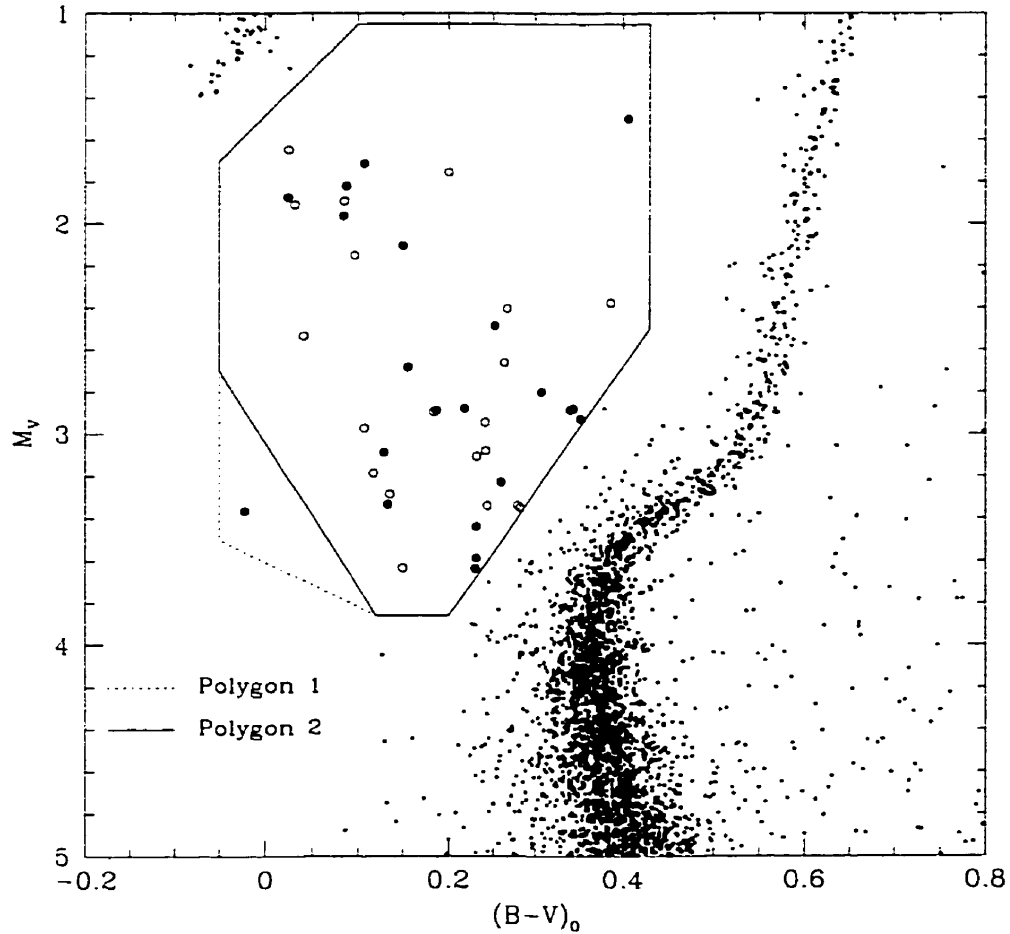
Figure 4.31: CMD showing the observed blue stragglers in NGC 6397 (filled circles) and a hybrid population of blue stragglers composed of 80% turnoff collisional mergers and 20% equal-mass collisional mergers (open circles). The two polygons show the slightly different blue straggler selection criteria described in the text.
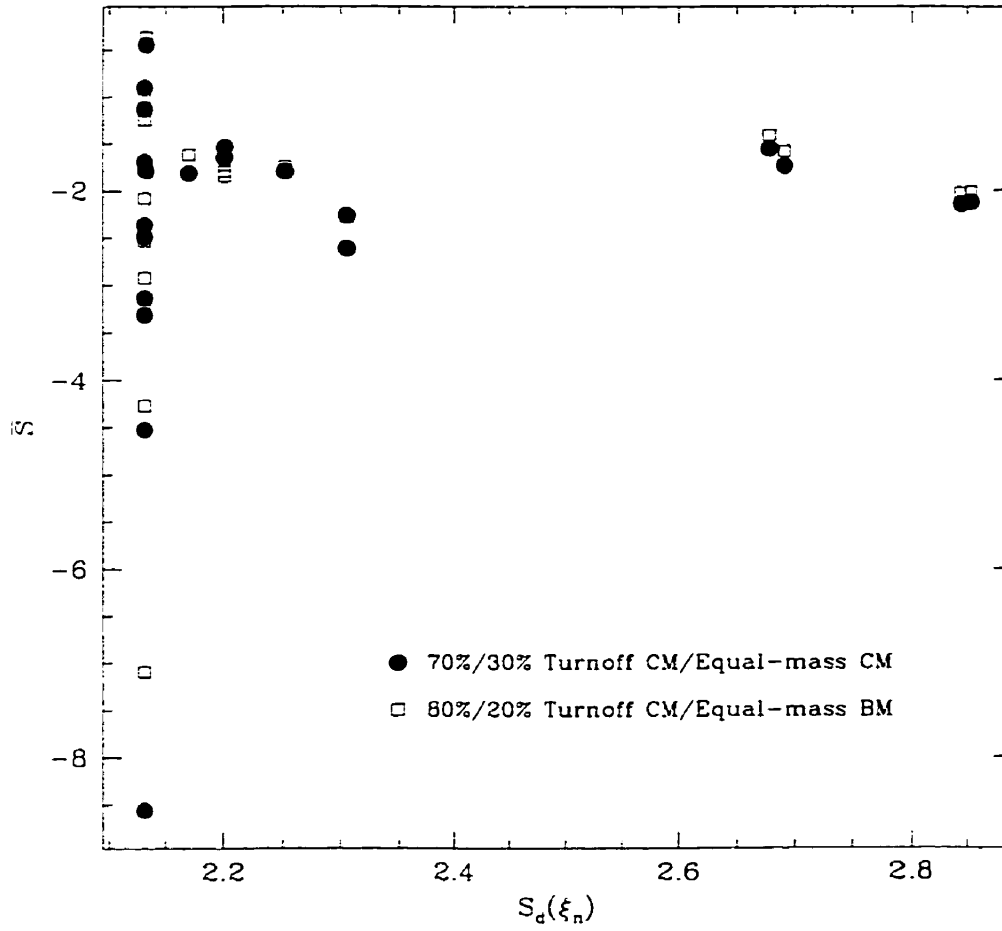
Figure 4.32: Individual likelihoods for the blue stragglers in NGC 6397 for the populations listed in Table 4.10 using Polygon 1.
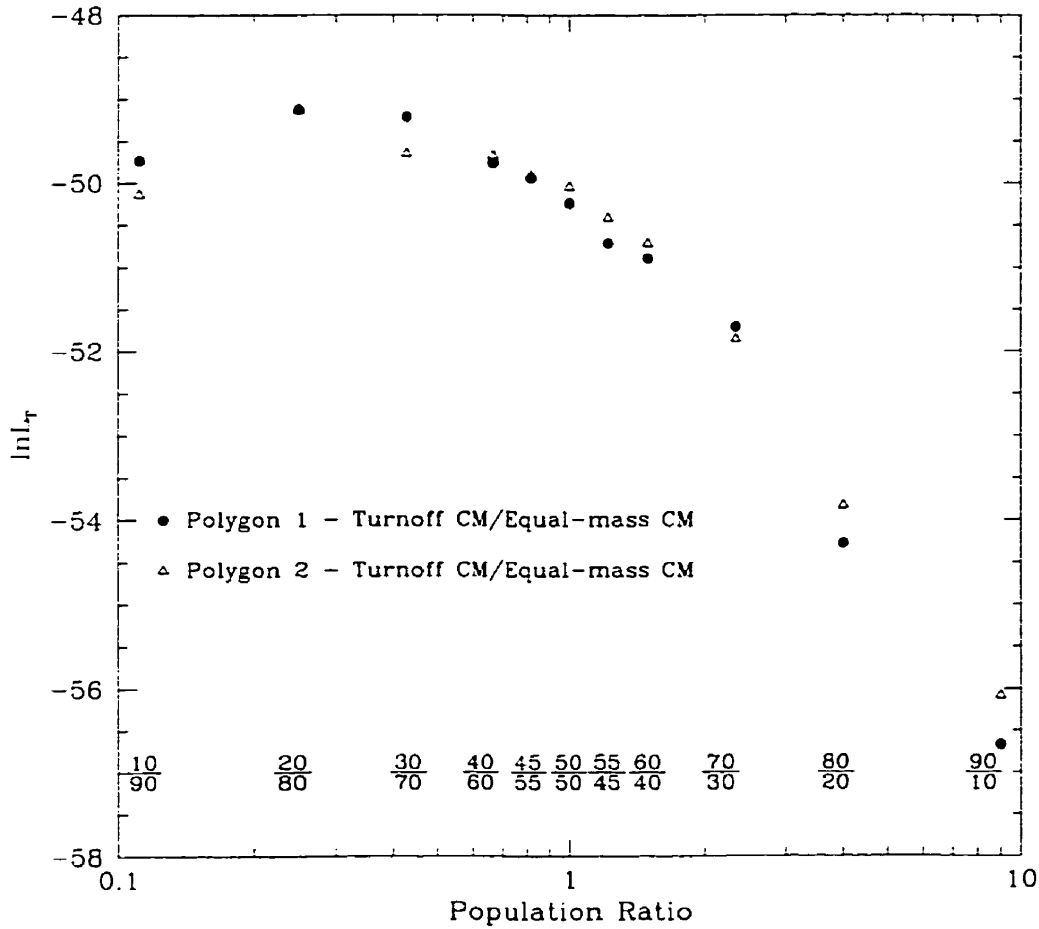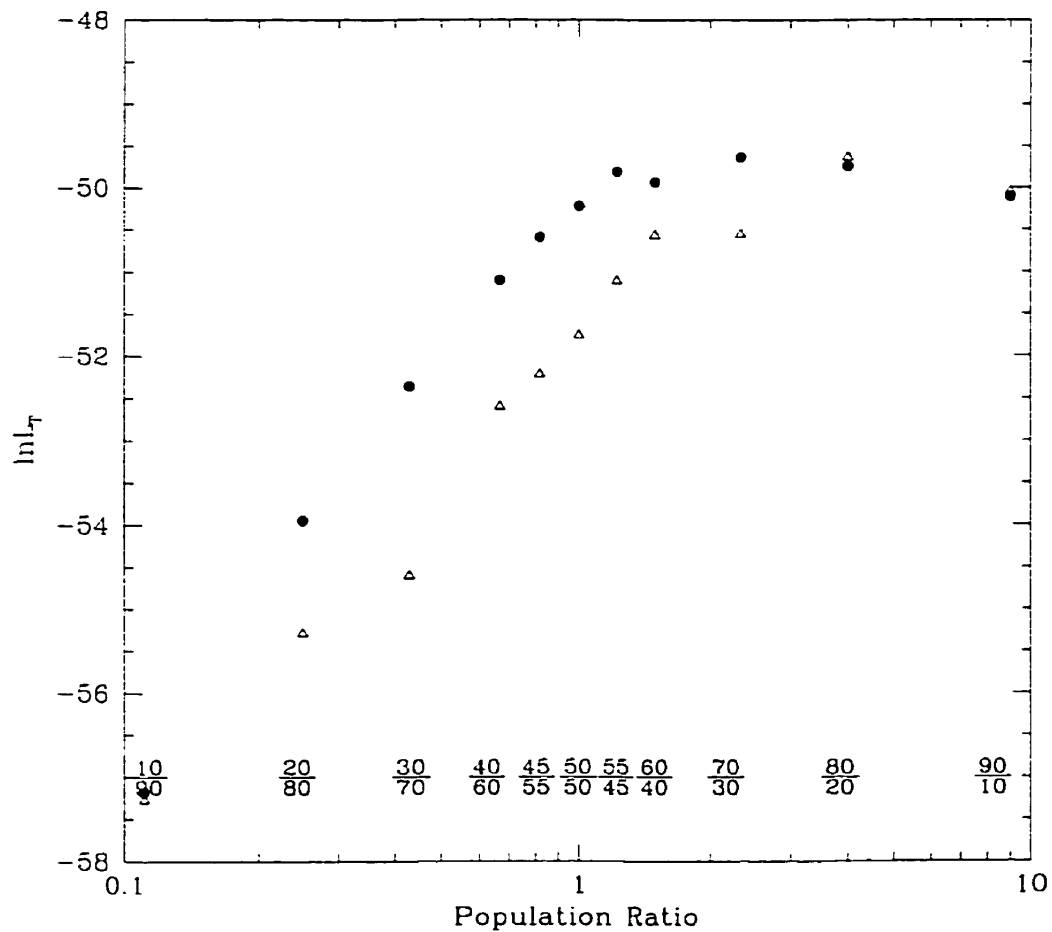
Figure 4.33: Likelihoods for different population ratios in NGC 6397. The likelihood values plotted are the median values from the Monte Carlo simulations. The two data sets have been shifted so that the likelihoods for the highest ranked population ratio match. Shown are the likelihoods when the blue straggler candidate discussed in the text is included (filled circles; Polygon 1) and when it is excluded (open triangles; Polygon 2).

Table 4.10: NGC 6397 — Statistics for the most likely population ratios

Statistic	Turnoff/Equal-mass CM	Turnoff CM/ Equal-mass BM
	Polygon 1	
$P(\Delta z)$	0.84	0.59
$\ln L_T$	-49.631	-47.24
Pop. Ratio	70:30	80:20
	Polygon 2	
$P(\Delta z)$	0.82	0.17
$\ln L_T$	-41.80	-44.18
Pop. Ratio	80:20	80:20

question included in the blue straggler sample, the population assigned the highest likelihood of being the parent population for NGC 6397 is one composed of 80% turnoff collisional mergers and 20% equal-mass binary mergers: however, this population has a very low probability of being able to match the observed Δz distribution (Table 4.10). Excluding this star decreases the relative ranking of the populations involving binary mergers: the most likely parent population for the blue stragglers in NGC 6397 is now one composed of 80% turnoff collisional mergers and 20% equal-mass collisional mergers. This final population provides a satisfactory match to the Δz distribution (Figure 4.33).

The average blue straggler formation rate in this cluster is one blue straggler every $\sim 1.1 \times 10^8$ years — the formation rate for turnoff mergers ($\sim 6.3 \times 10^7$ years) is nearly twenty times the formation rate for equal-mass mergers ($\sim 1.3 \times 10^9$ years). Assuming a binary fraction of 20% and an average binary semi-major axis of 0.1AU, the binary-binary collision rate is $\sim 6.8 \times 10^6$ years per collision and the binary-single collision rate is $\sim$
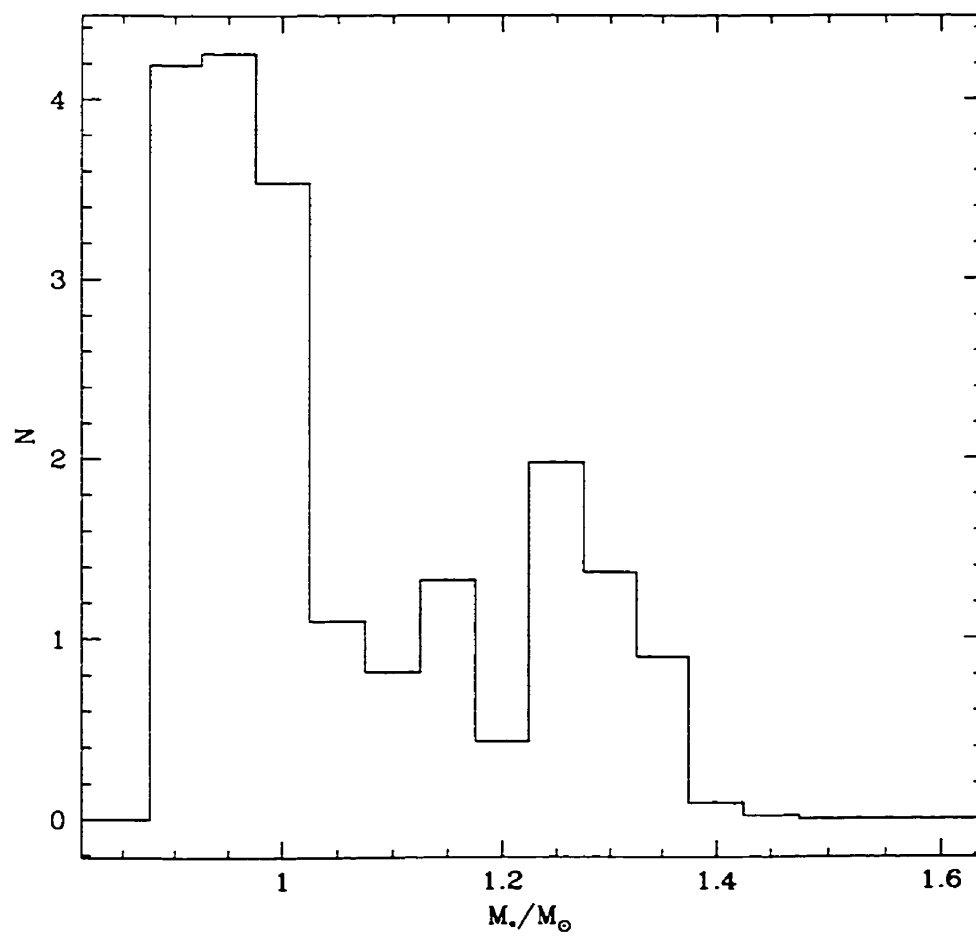
Figure 4.34: Distribution of the masses, in solar units, of the blue stragglers in NGC 6397.

4.7×10^5 years per collision. To bring the shorter binary-single collision rate into agreement with the necessary blue straggler formation rate, the binary fraction would have to be decreased to $\sim 1\%$.

4.5 NGC 6809

The photometry of NGC 6809 (Mandushev *et al.*, 1997) is unique among the datasets used here in that magnitudes in B, V, and I are available. This is convenient for two reasons: first, it allows us to test whether the same results are obtained if the B and V (Figure 4.35) photometry is used or if the V and I photometry (Figure 4.36) is used; second, it will allow a more direct comparison with NGC 2419 (for which V and I photometry, Harris *et al.* 1997, is used, whereas the datasets for the other clusters use B and V photometry).

Although care was taken to ensure that the same blue stragglers were used in each dataset, there is a slight discrepancy between the most likely populations for the BV and VI photometry of NGC 6809: for the BV photometry, the most likely parent population is one composed of 55% turnoff collisional mergers and 45% equal-mass collisional mergers ($P(\Delta_Z) = 0.84$), whereas for the VI photometry, the most likely parent population is one composed of 50% turnoff collisional mergers and 50% equal-mass collisional mergers ($P(\Delta_Z) = 0.93$); see Figure 4.37). Since this difference is equivalent to one or two blue stragglers having poor B or I photometry, this difference is perhaps acceptable.

The two datasets yield similar average blue straggler formation rates: 9.4×10^7 years for the BV dataset and 1.2×10^8 years for the VI dataset.

The difference between the two rates can be ascribed to the slightly different mass distributions found by comparing the models to the observations (Figure 4.38): the comparison with the BV dataset seems to assign slightly higher masses on average to the blue stragglers, which results in a shorter average formation rate. The difference in the median mass from the two datasets is $\sim 0.02 M_\odot$.

The expected collision rates for this cluster are one collision every $\sim 1.4 \times 10^{10}$ years for binary-binary collisions and one collision every $\sim 1.5 \times 10^8$ years for binary-single collisions. The shorter binary-single interaction rate is in good agreement with the blue straggler formation rate.

4.6 NGC 7099

NGC 7099 is dynamically quite similar to NGC 6397 (Table 4.4), although NGC 7099 is somewhat more dense. Because of this similarity, one might expect that the blue straggler populations would also be similar, assuming that dynamics play a role in determining the dominant blue straggler formation mechanism. As it turns out, the blue straggler populations in the two clusters are quite different, though this does not mean that cluster dynamics are not playing a role in determining the formation mechanism (discussed later).

The blue straggler population in NGC 7099 is best matched by a parent population composed of 30% turnoff collisional mergers and 70% turnoff binary mergers (Figure 4.40). Excluding the one isolated blue straggler candidate which lies blueward of the main population changes the likelihoods for the various model populations, but does not change the relative rank-

Figure 4.35: BV CMD showing the observed blue stragglers in NGC 6809 (filled circles) and a hybrid population of blue stragglers composed of 55% turnoff CM and 45% equal-mass CM (open circles).

Figure 4.36: VI CMD showing the observed blue stragglers in NGC 6809 (filled circles) and a hybrid population of blue stragglers composed of 50% turnoff CM and 50% equal-mass CM (open circles).

Figure 4.37: Likelihoods for different population ratios in NGC 6809, for both BV and VI datasets. The likelihood values plotted are the median values from the Monte Carlo simulations. Despite the fact that the two datasets contain the same blue stragglers, the value of $\ln L_d$ is different for the two datasets; this is the cause of the shift between the BV and VI likelihoods.
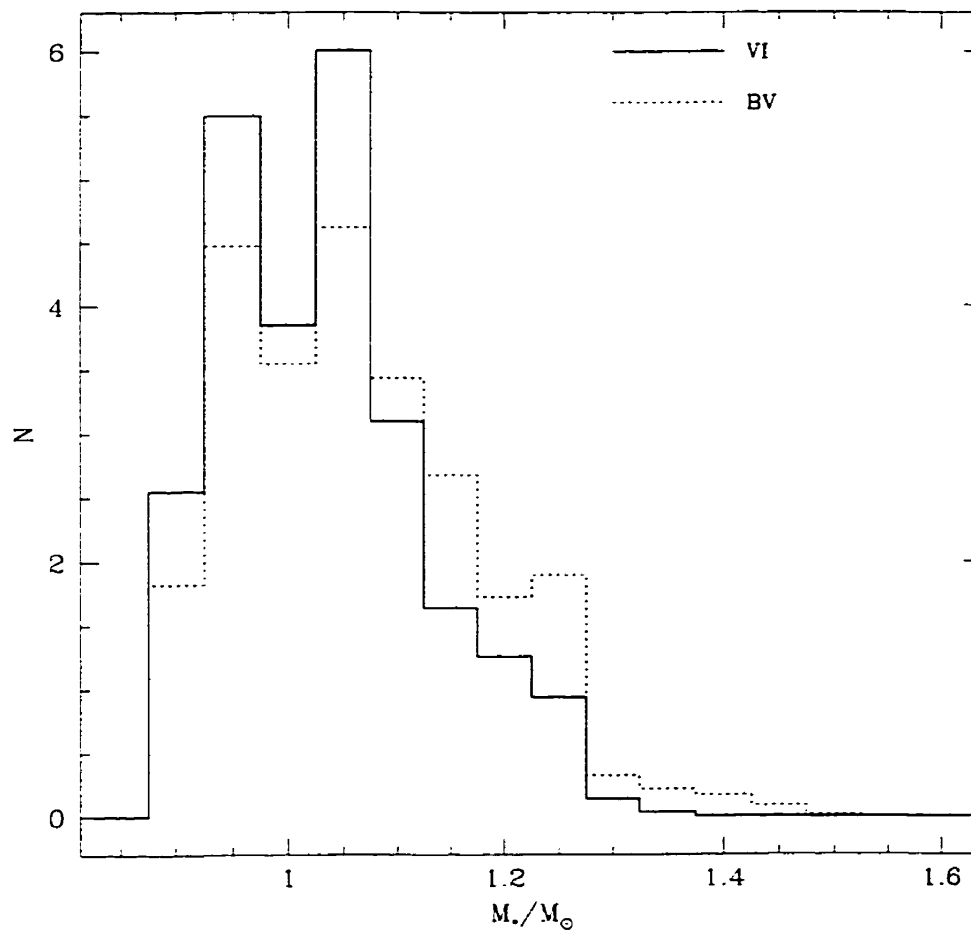
Figure 4.38: Distribution of the masses, in solar units, of the blue stragglers in NGC 6809. The derived mass distributions for both the BV and VI datasets are shown.

ings. However, excluding this star changes the probability that the above population matches the observed Δ_Z distribution from $P(\Delta_Z) = 0.89$ to $P(\Delta_Z) = 0.94$.

The fact that the dominant population in NGC 7099 appears to be composed of binary mergers may make it fruitless to consider the collision time-scales in this cluster. However, Sigurdsson & Phinney (1993) have shown that, when the average binary semi-major axis becomes small enough — through disruption or dynamical hardening of wider binaries — it is possible for the hardening time-scale to become shorter than the collision time-scale. Gradual hardening of the binaries in the cluster may accelerate the onset of mass-transfer or coalescence in already close binaries. Since NGC 7099 is a very dense cluster, it is possible that this stage has been reached in its binary population. An estimate of the hardening time-scale should be comparable to the collision time-scale (since the hardening time-scale only becomes much shorter than the collision time-scale at very small values for the average binary semi-major axis). Making the same assumptions for the binary population as for NGC 6397, the binary-binary collision time-scale is one per 9.4×10^6 years and the binary-single collision time-scale is one per 1.0×10^6 years. From the comparison with the models, the average blue straggler formation rate is one blue straggler every 5.7×10^7 years: reducing the binary fraction from 20% to $\sim 10\%$ would bring the binary-single formation rate into agreement with the blue straggler formation rate.
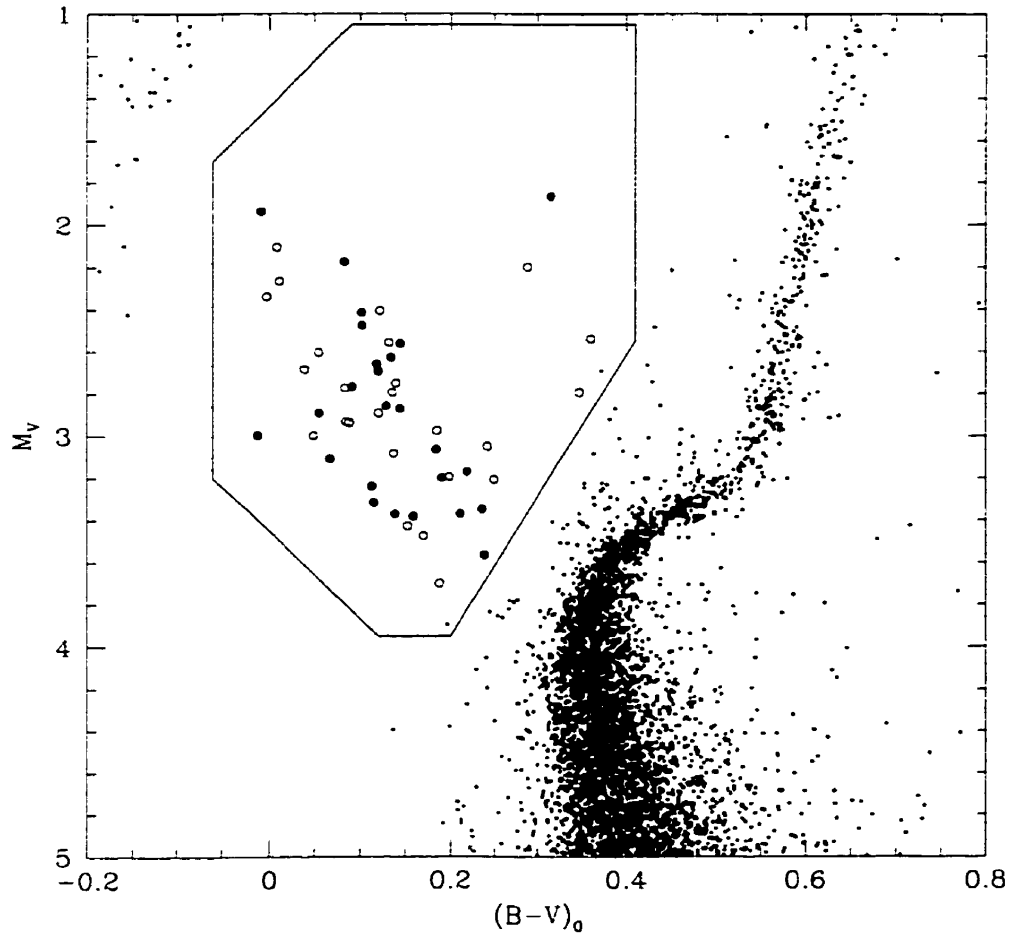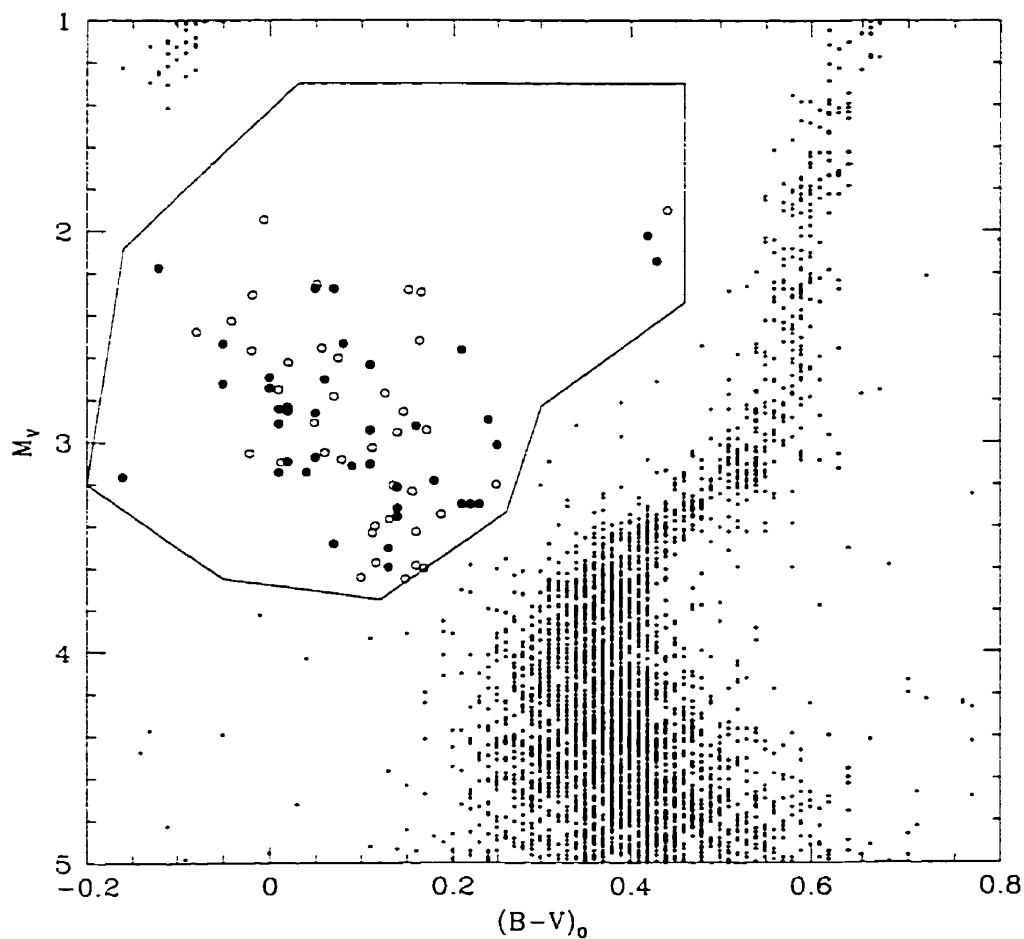
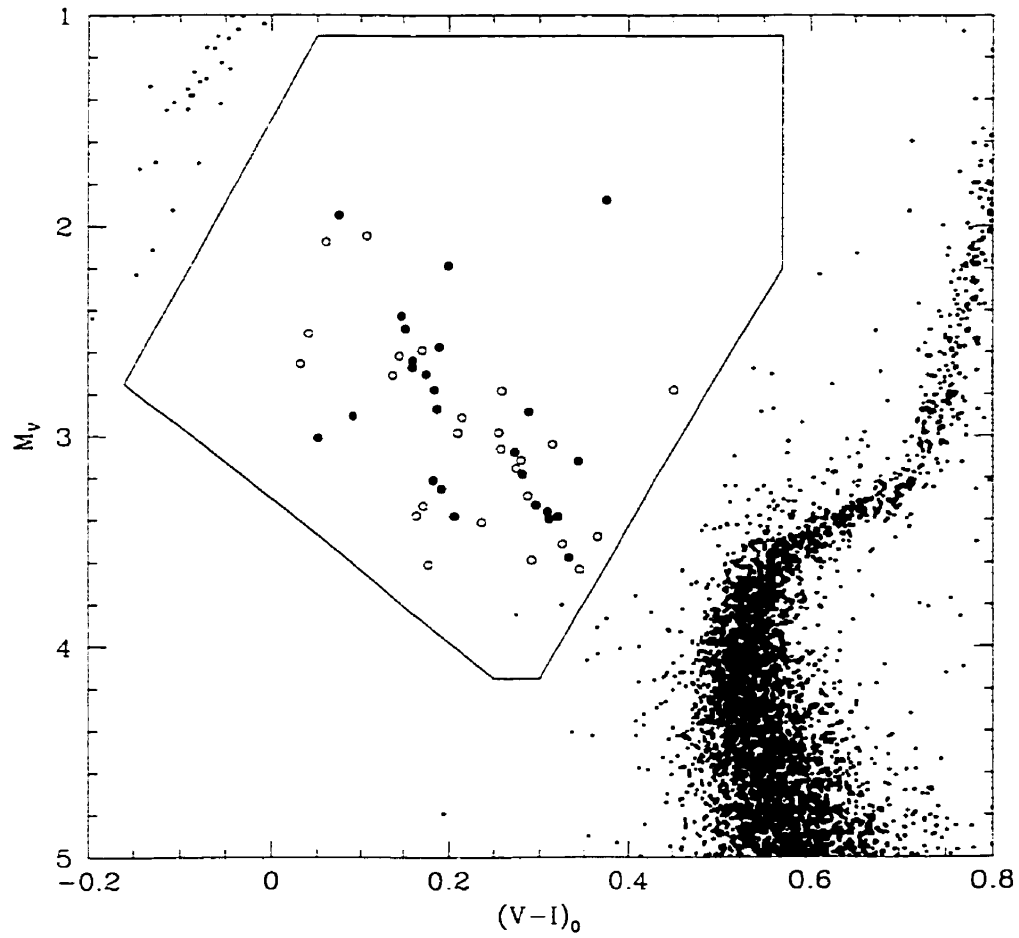Figure 4.39: CMD showing the observed blue stragglers in NGC 7099 (filled circles) and a hybrid population of blue stragglers composed of 30% turnoff CM and 70% turnoff BM (open circles).

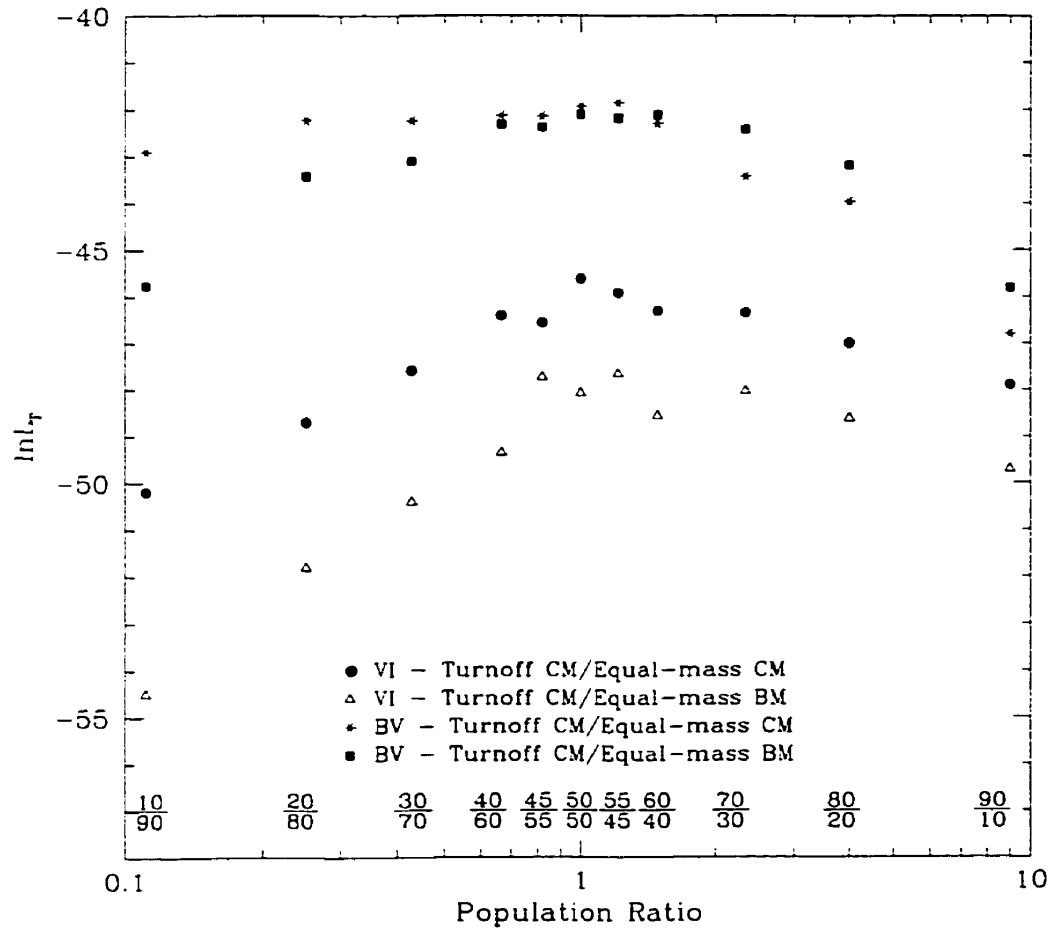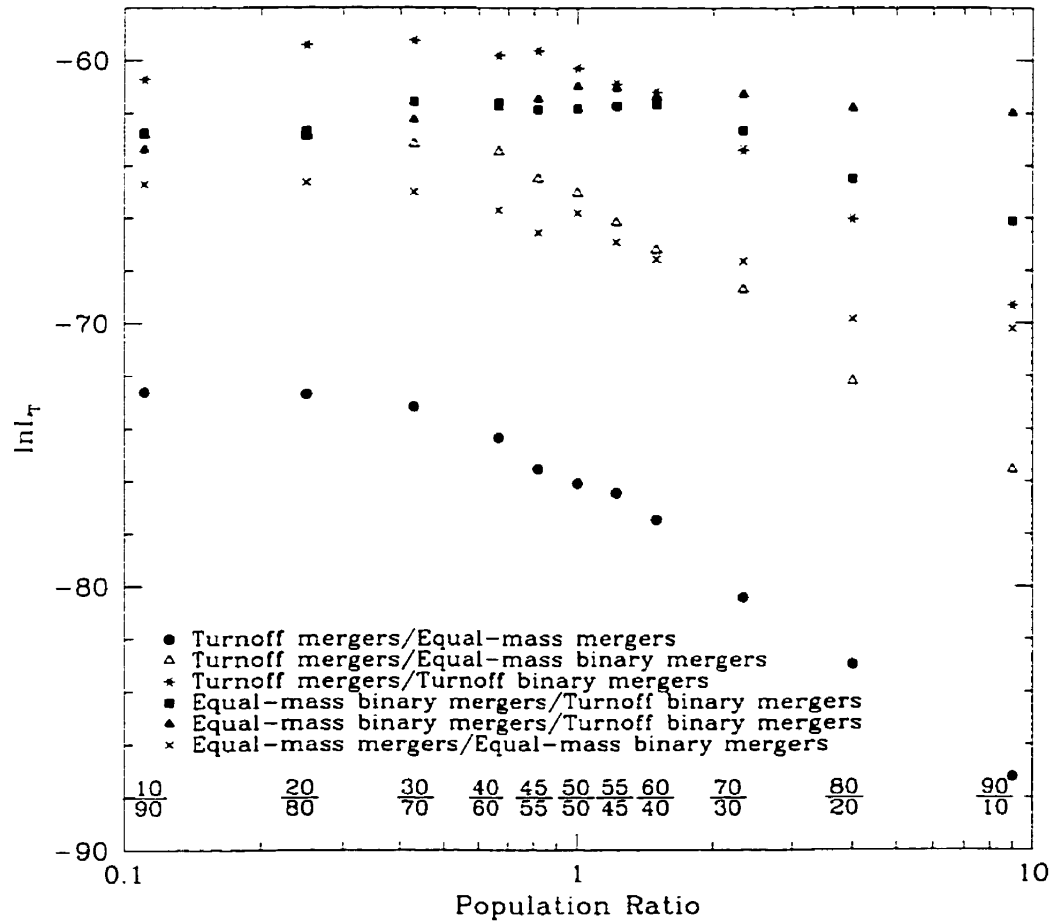Figure 4.40: Likelihoods for different population ratios in NGC 7099. The likelihood values plotted are the median values from the Monte Carlo simulations.
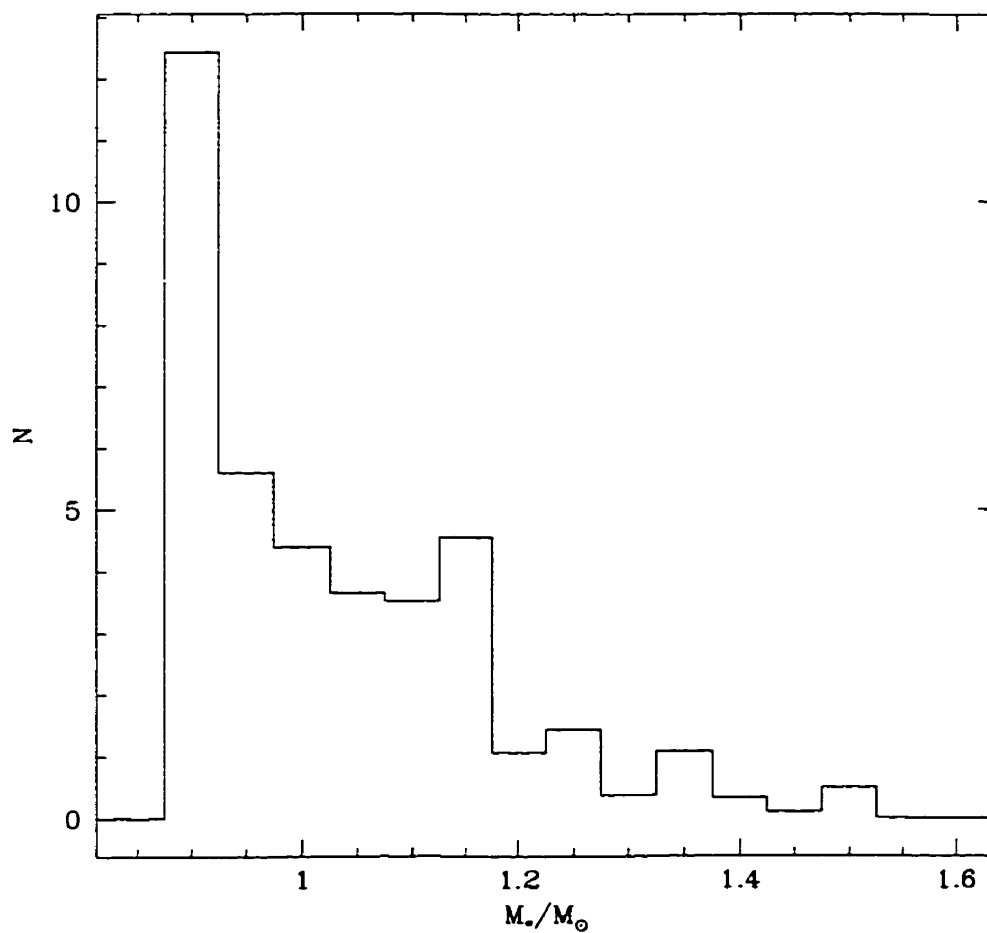
Figure 4.41: Distribution of the masses, in solar units, of the blue stragglers in NGC 7099.

Table 4.11: Summary of blue straggler formation rates

Cluster	BS Formation Rate (10^6 years)	Binary-binary Collision Rate (10^6 years)	Binary-single Collision Rate (10^6 years)	Approx. Binary Fraction[a]
NGC 104	33	13	4.5	> 10%
NGC 2419	180	1.7×10^4	180	20%
NGC 5024	79	14	31	< 10%
NGC 6397	110	6.8	0.47	~ 1%
NGC 6809[b]	~ 110	1.4×10^4	150	20%
NGC 7099	57	9.4	1.0	10%

[a]This is the approximate binary fraction necessary to bring the shorter collision rate into agreement with the observed formation rate.

[b]Blue straggler formation rate is an average of the values derived from the two datasets.

Table 4.12: Summary of blue straggler populations

Cluster	Parent Population Composition	Population Ratio
NGC 104	Turnoff CM:Equal-mass CM	60:40
NGC 2419	Turnoff CM:Equal-mass CM	10:90
NGC 5024	Turnoff CM:Equal-mass CM	20:80
NGC 6397	Turnoff CM:Equal-mass CM	80:20
NGC 6809	Turnoff CM:Equal-mass CM	~50:50
NGC 7099	Turnoff CM:Turnoff BM	30:70

CM - Collisional Merger
BM - Binary Merger

4.7 Summary and Discussion

Of the six clusters examined here, all but one have blue straggler populations which are consistent with having been formed via stellar collisions. The blue stragglers in the remaining cluster, NGC 7099, are more consistent with a population which is mostly composed of the remnants of binary mergers. One cluster, NGC 2419, is slightly unusual in that its blue stragglers are consistent with having been formed solely by equal-mass collisional mergers: however, since the binary merger models used here are admittedly over-simplified for the purpose of modelling the complex processes of binary mass-transfer and coalescence, it is possible that the blue stragglers in this cluster are being formed by binary mergers instead. Regardless, the overall agreement of the observations with the fairly simple models developed in Chapter 3 is impressive.

4.7.1 Uncertainty in derived population ratios

A word should be said on the confidence in the assignment of a given population ratio based on the calculated likelihoods. Given that on the order of 10,000 Monte Carlo simulations have been run for each population ratio and each combination of models for each cluster, the uncertainty in the likelihoods from the simulations is quite small; in fact, taking subsets (of, say, 1000 simulations) of the simulated data and comparing these subsets to the observations does not change the relative rankings of the various population ratios. However, as can be seen from the discussion of NGC 5024, NGC 6397, and NGC 7099, omitting even one blue straggler can change the likelihoods from the simulations significantly. In the analysis of these three

clusters, the blue straggler candidates which gave the lowest values of $\bar{S}$ were excluded from the datasets and the simulations were repeated with the reduced dataset. Since these candidates were the least well matched by the models, rejecting them produced the largest change in the calculated likelihoods for those blue straggler samples: rejecting any of the other candidates would still change the likelihoods, but not by as large an amount. For NGC 5024 and NGC 6397 the most likely parent populations were changed completely, from populations consisting of both collisional mergers and binary mergers, to populations consisting solely of collisional mergers. On the other hand, for NGC 7099, rejecting its one discrepant blue straggler candidate did not change the most likely parent population, but did change the overall likelihoods. If one looks only at the population ratio for the finally accepted populations (collisional mergers for NGC 5024 and NGC 6397, collisional mergers and binary mergers for NGC 7099), only for NGC 6397 does the apparent population ratio change with the modification in the accepted blue straggler sample (i.e. in NGC 6397, when the single errant blue straggler candidate is included, the most likely population ratio for collisional mergers only was 30% equal-mass and 70% turnoff collisional mergers; when this candidate was omitted, the collisional merger population ratio changed to 20% and 80%. For the other two clusters, the population ratio did not change.).

In addition to these changes in the likelihoods from omitting one or two blue straggler candidates, several of the clusters (in particular NGC 2419, NGC 6809, and NGC 7099) have rather flat distributions of likelihoods as a function of population ratio. While omitting the candidates which the models obviously fail to match produces the largest shifts in the likelihoods (although

not necessarily the relative ranking), it is possible that small changes in the remaining blue straggler sample could result in small changes in the relative likelihoods: with a flat distribution of likelihoods, it is possible that a significant change in population ratio could occur. Small changes in the blue straggler sample could occur, for instance, between different data sets of the same photometric quality simply due to the scatter in the observations (i.e. NGC 6809). Also, there is an inherent uncertainty in the blue straggler populations of many clusters simply due to the small number of stars.

The effect which uncertainties in the blue straggler population of a cluster have on the derived likelihoods and population ratios was investigated in the following manner for NGC 2419 and NGC 7099 (the L_T distributions of these clusters are flat near the most likely population ratio). For each blue straggler dataset consisting of N stars, N subsets were created by omitting each star in turn from the original data set (i.e. the ith subset consists of the stars numbered $1, 2, 3, .., i - 1, i + 1, ..., N$). Using these data subsets, a number of the original Monte Carlo simulations were redone (the simulations were redone only for those population ratios and models which gave high likelihoods in the original simulations). This procedure is similar to the jackknife method for estimating biases and standard errors in statistics drawn from limited samples (e.g. Efron & Tibshirani, 1993). The results of these investigations are summarised in Figures 4.42 and 4.43.

In the tests of the population ratio for NGC 2419, the accepted population — 10% equal-mass collisional mergers and 90% turnoff collisional mergers — is ranked the highest 10 out of 19 times (52%). Of the 9 times this population ratio is not ranked the highest, the population ratio of 20%turnoff

collisional mergers and 80% equal-mass collisional mergers is ranked the highest 7 times, a ratio of 30%turnoff collisional mergers and 70% equal-mass collisional mergers is ranked the highest once, and a population consisting solely of equal-mass mergers is ranked the highest once. While the accepted population ratio (10% equal-mass collisional mergers and 90% turnoff collisional mergers) is still the most likely to be the parent population for the blue stragglers in NGC 2419, it is possible that the population ratio has been underestimated.

From the original simulations for NGC 7099 (Figure 4.40), the accepted population composition — one of turnoff collisional mergers and turnoff binary mergers — was the only population composition tested as described above. The accepted ratio, 30:70, is ranked the highest 31 out of 39 times (79%). Of the 8 times the accepted population ratio is not ranked the highest, a population ratio of 20:80 is ranked the highest 5 times, and a population ratio of 40:60 is ranked the highest 3 times. These rankings are based solely on the likelihood estimates: if the probability of the given population ratio also being able to match the observed Δ_z distribution is used in conjunction with the likelihood values, the original population ratio of 30:70 is accepted in 37 of the 39 tests. As mentioned earlier, a necessary condition for accepting a given population of models as the parent population for the blue stragglers in a cluster was that it must provide a good match to the observed distribution of Δ_z.

It is apparent from these tests that the population ratios which were assigned to the various clusters are possibly uncertain by as much as 10% in either model population, although the uncertainty is probably smaller for
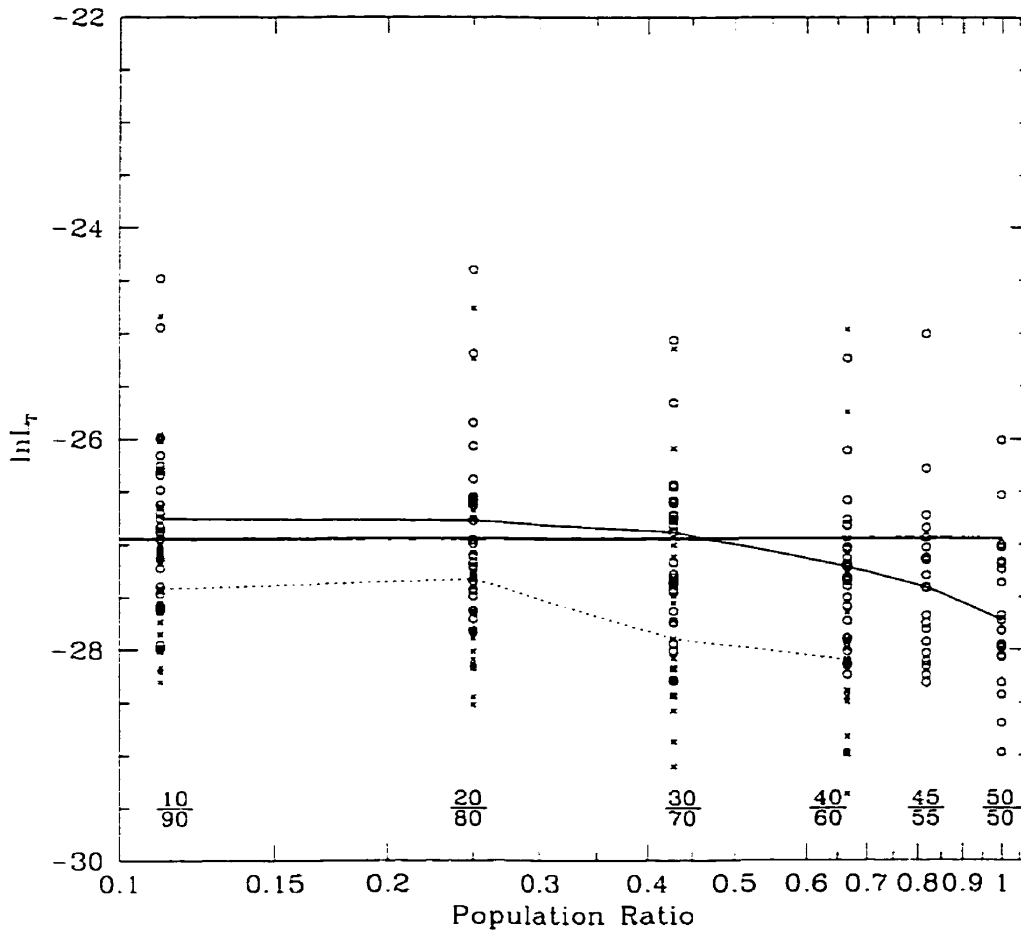
Figure 4.42: Uncertainties in the population ratios for NGC 2419. The open circles are the likelihood values for a population composed of Turnoff CM and equal-mass CM, in the ratios indicated (Turnoff/Equal-mass): the thin solid line connects the median values from these simulations. The crosses are the likelihood values for a population consisting of Equal-mass BM and Equal-mass CM (BM/CM): the thin dotted line connects the median values from these simulations. The thick solid line shows the median value of the simulations for a population consisting solely of equal-mass CM.
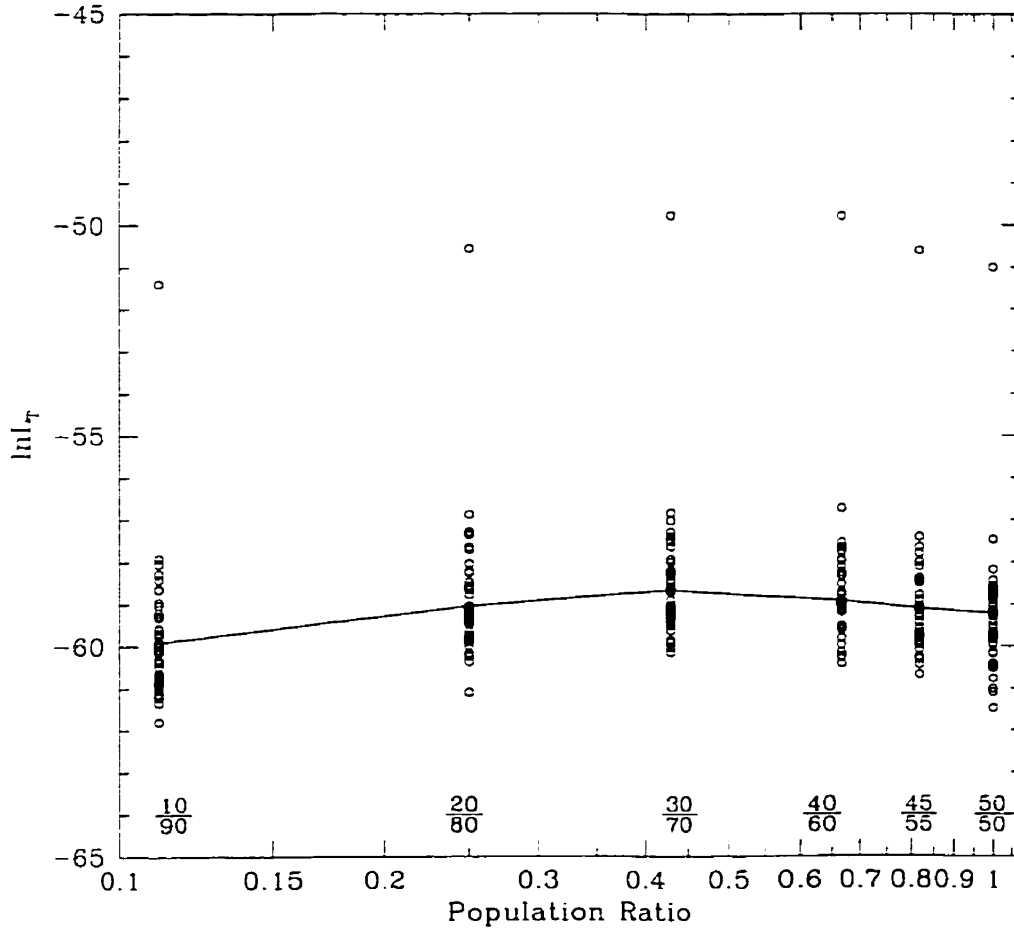
Figure 4.43: Uncertainties in the population ratios for NGC 7099. The open circles are the likelihood values for a population composed of Turnoff CM and Turnoff BM, in the ratios indicated (Turnoff CM/Turnoff BM): the thin solid line connects the median values from these simulations.

clusters for which the distribution of ln L_T is steep (e.g. 47 Tuc, Figure 4.21).

4.7.2 Rotation of Collisional Mergers

For those clusters with blue straggler populations consistent with having been formed by collisions, this apparent agreement with the models implies that the blue stragglers are not rapidly rotating, as is expected from the collision scenario. This is not to say that they do not have high rotation rates, as angular momentum conservation during a collision would require, but rather that the rotation rate cannot be high enough to affect significantly the evolution of the blue stragglers.

First, rapid rotation will affect the evolution of a star by providing a non-thermal form of pressure support, which will lower the demand for nuclear energy to support the star. This will not only extend the life of the star, but will also cause it to be redder and less luminous than it would otherwise be (Clement, 1994). If the change in evolutionary rate is significant, the distribution of stars in the CMD (in particular the Δ_Z distribution) will be altered from the predictions of the non-rotating collisional models. Nonetheless, this is a weak argument against rapid rotation since it is possible that such an alteration of the evolutionary rate could simply cause the blue straggler population to have a different population ratio when compared to the models.

A stronger argument against significant rotation among the blue stragglers studied is that a rapidly rotating population of stars (and the average rotation rate among collisionally formed blue stragglers should be quite high) should exhibit a broader distribution of stars along the subgiant branch

than is observed. After a star has exhausted the hydrogen in its core and has begun to burn hydrogen in a thick shell around an isothermal core, a larger core mass will be reached before the core begins to collapse, at which time the star will evolve rapidly across the subgiant branch (the Schönberg-Chandrasekhar mass, Schönberg & Chandrasekhar, 1942; Maeder, 1971). The collapse of the core, and the subsequent rapid evolution across the CMD toward the red giant branch, is what causes the apparent truncation in the number of blue stragglers which lie between the main blue straggler population and the giant branch (see Figure 4.22 for the best example of this). If the average collisionally formed blue straggler is rotating rapidly enough for the star's Schönberg-Chandrasekhar mass to increase, then this truncation will be moved redward, toward the giant branch: the agreement between the non-rotating models and the observations suggests that any change in the core mass cannot be large.

Additionally, rapid rotation could initiate meridional circulation currents in a star, potentially mixing helium-rich material to the surface of the star, which would cause it to be shifted toward the ZAMS. Meridional circulation currents are a consequence of the distortion of the star's gravitational potential by the rotation: the temperature gradient remains proportional to the potential gradient, resulting in a steeper temperature gradient at the poles than at the equator. If the temperature gradient is greater than thermal equilibrium requires, circulation currents may be initiated. If hydrogen-rich material is brought into the core of the star by the currents, the hydrogen-burning lifetime of the star, and so its lifetime as a blue straggler, could be greatly extended. Also, due to the increased central hydrogen abundance,

the position of the blue straggler on the CMD should be much closer to the ZAMS than it would be otherwise. It is possible that meridional circulation currents could be initiated in the envelope, with little or no helium-rich material being transported to the surface.

Blue stragglers formed by stellar collisions should, on average, be rotating quite rapidly, as demanded by angular momentum conservation during the collision. Since the comparison of the observations with the models would be quite sensitive to such a change in the average characteristics of a blue straggler population, the evolution of the stars is most likely not being strongly affected. One avenue for the effects of rotation to be mitigated is through angular momentum loss. As mentioned earlier (in Chapter 3), angular momentum loss by a magnetically driven wind is ruled out by the fact that only the lowest mass merger models ever develop convective envelopes, and these are too thin and short-lived to be effective conduits for angular momemtum loss. However, if the blue stragglers produced by collisions have bound companions, it is possible that angular momentum transfer to the companion stars could act to reduce the rotation of the stars. A consequence of a large binary population among the blue stragglers would be that they would appear brighter than the models predict, since it is the integrated light of the two stars which is measured. However, the agreement between the models and observations suggests that these companions, if present, must be much less luminous than the blue stragglers themselves.

4.7.3 Blue Stragglers as Dynamical Probes

Since the rate of stellar collisions and other strong dynamical interactions is highly dependent upon the local dynamics (Leonard & Fahlman, 1991 ; Sigurdsson & Phinney, 1993 ; Bacon, Sigurdsson, & Davies, 1996), the dominant process for blue straggler formation and the rate at which new blue stragglers are formed should also be dependent upon the cluster dynamics. As Table 4.11 summarises, the calculated collision rates for binary-binary and binary-single star interactions can be brought in to agreement with the observed blue straggler formation rates with reasonable values for the cluster binary fraction. Although the calculated collision time-scales are not precisely known due to the uncertainties in cluster dynamical quantities (e.g. cluster density, central mass density, the true binary fraction and binary parameters), the coincidence of the rates from the dynamical and evolutionary calculations allows us to speculate on the dynamical events occurring in the studied clusters.

In a dense cluster, collisions between stars are expected to be dominated by binary-single star interactions (Bacon, Sigurdsson & Davies, 1996), unless the binary fraction of the cluster is quite high ($f_b > 0.5$). Also, as the primordial binary population of the cluster is evolved by dynamical interactions, we would expect the softest binaries (those with binding energies less than or comparable to the average kinetic energy of a star in the cluster) to have been disrupted: it is the widest remaining binaries which are the most likely to undergo the dynamical interactions leading to a collision (Sigurdsson & Phinney, 1993; Leonard & Fahlman, 1991). In a dynamically evolved cluster, the binary population would have been significantly modified from

its primordial state — by disruption of the softest binaries, hardening of existing binaries, and exchanges of field stars into binaries. These dynamical effects will either modify the cluster potential or inject kinetic energy into the stellar population of the cluster, supporting the cluster from core-collapse. Because a dynamically evolved cluster should have only very hard binaries remaining, any interactions strong enough to produce a collision should also result in the binary (and the remaining field star or binary with which the interaction took place) receiving a large recoil velocity (Sigurdsson, Davies & Bolte, 1994): this recoil is larger for harder binaries and could kick the newly formed blue straggler out to the cluster periphery, or even completely out of the cluster.

During the initial dynamical evolution of a cluster toward equipartition of energies among its stellar populations, while its binary population is still relatively unmodified by dynamical interactions, a strong dynamical interaction between a binary and a cluster star is most likely to result in an exchange of stars – typically an exchange of the two most massive stars into a new binary – or a break-up rather than a strong hardening of the existing binary or a collision. As these exchanges progress in the binary population, and the cluster becomes dynamically more evolved, the time-scale for a collision decreases until collisions dominate over other interactions: as these collisions effectively remove the binary from the energy sink supplied by the binding energy of the binary population, the cluster may evolve toward core-collapse more rapidly, especially if the relaxation time in the cluster is shorter than or comparable to the time-scale for collisions. As the binaries with the largest collision cross sections are destroyed, the remaining binary population be-

comes hardened due to dissipative encounters with cluster field stars, further decreasing the cross section for collisions, but increasing the cross section for hardening interactions.

A strong interaction between a binary star and field star, or another binary, which results in significant hardening of the binary and a significant kick, but not a collision, can still produce a blue straggler. If a very hard binary is created (either by hardening an existing binary or creating a binary which is harder than any of the binaries involved in the interaction), mass transfer or coalescence may occur, probably after a delay. Since such hardenings are more likely in clusters with very hard binaries, such interactions should also produce large velocity kicks, propelling the hardened binary to the outskirts of the cluster. However, this does not mean that, in very dense, dynamically evolved clusters, we should expect to see an extended distribution of blue stragglers in the cluster halo: on the contrary, if the delay between the initial kick and the onset of mass transfer/coalescence is longer than or comparable to the relaxation time of the cluster, these blue stragglers may still be isolated in the core.

If the kicks being delivered to collisionally formed blue stragglers are large enough that there is a significant population of these stars in the outskirts of the cluster as well as in the core, there may be differences between the two populations. On average, the kicks delivered to the most massive blue stragglers will be smaller than the kicks delivered to the less massive blue stragglers, causing the most massive blue stragglers to be more centrally concentrated. Also, due to their larger mass, and the shorter relaxation time-scale near to the cluster core, any massive blue stragglers kicked out to

intermediate radii will quickly settle back into the core (similar to the scenario described by Sigurdsson, Davies, & Bolte, 1994, for the blue stragglers in M3). Because of this bias toward lower mass blue stragglers in the outskirts of clusters in which the formation mechanism is dominated by collisions, the blue straggler luminosity function will differ between the outskirts and the core. Interestingly, the luminosity function of M3 seems to exhibit this behaviour (Bailyn & Pinsonneault, 1995).

In low density clusters, the situation may be quite different. Although collisions may still occur, a binary is more likely to be broken up than to undergo a collision (Bacon, Sigurdsson, & Davies, 1996). Those binaries which survive, or are hardened by such encounters, may eventually undergo mass-transfer between the components, and the resulting blue straggler may look quite different than a collisionally formed one. In the lowest density clusters, only a few blue stragglers will ever be formed by collisions, especially after the softest binaries have been disrupted by a rare dynamical encounter. In this case, blue stragglers will form only by mass-transfer or coalescence, although the majority will form by mass-transfer, simply due to the fact that there should be more binaries with wide orbits. In somewhat denser clusters, the numbers of blue stragglers formed via stellar collisions will increase, but dynamical interactions will also have an effect on the general binary population in the cluster, accelerating the formation of blue stragglers by binary mergers. Increasing the binary fraction within a low density cluster will also have a dramatic affect on the formation of blue stragglers: since the collision rate is a non-linear function of the binary fraction (Bacon, Sigurdsson, & Davies, 1996; Sigurdsson & Phinney, 1993), whereas the binary

mass-transfer/coalescence rate will be unaffected by the binary fraction, increasing the binary fraction in a low density cluster will cause the relative fraction of collisionally formed blue stragglers to increase.

The lowest density cluster in the sample studied here, NGC 2419, has a blue straggler population which is consistent with formation by equal-mass collisional mergers, although there is a possibility of some having been formed by turnoff collisional mergers. For collisions to dominate in such a low density cluster the binary fraction would have to be quite high; nonetheless, there should still be strong evidence of binary (fully-mixed) mergers. Since there is no evidence of highly mixed stars — and the binary fraction necessary for a significant collision rate demands that there be some in evidence — it is likely that the binary mergers which are occurring are being confused for equal-mass collisional mergers. Since incomplete mass-transfer will leave the helium-rich core of the mass-donor orbiting the new blue straggler, it is possible that the surface helium abundance of the blue straggler will not be enhanced enough for it to look like a fully-mixed star, which is what our binary merger models are. If this is the case, the binary fraction in the cluster can be smaller than what has been estimated from comparison of the observed blue straggler formation rate and the expected collision rates (Table 4.11).

The next most dense cluster, NGC 6809, is likely being affected by a similar confusion between equal-mass collisional mergers and binary mergers which our fully-mixed models fail to match. The fact that there is strong evidence for a population of collisional mergers suggests that the binary population in this cluster must be large and fairly unevolved. The binary popula-

tion must be unevolved (dynamically) otherwise the average semi-major axis could have been reduced by gradual hardening to the point were collisions would be unlikely.

The fact that NGC 5024, an intermediate density cluster, has a blue straggler population which is heavily weighted toward equal-mass mergers, suggests that binary mergers may be contributing to the blue straggler population. However, the presence of a significant population of turnoff collisional mergers suggests that collisions are actually occurring at a significant rate in this cluster.

In 47 Tuc, however, the fact that there are few blue stragglers in the outskirts of the cluster (Kaluzny et al., 1998a) suggests either the kicks being dealt to the blue stragglers after formation by collisions are small on average, or that the scenario of delayed blue stragglers settling to the core is correct. Since the blue stragglers in 47 Tuc are apparently being formed by collisions, and since the lifetime of a collisionally formed blue straggler is comparable to the half-mass relaxation time of 47 Tuc (meaning that these blue stragglers would not have time to drift back to the core), the collisions forming the blue stragglers are dominated by wide binaries which are receiving relatively small kicks during the interaction. This, along with the fact that the blue stragglers in 47 Tuc are well-matched by the hypothesis that they form as collisionally merged stars, also suggests that the binary fraction of the cluster is not large: if it were, we would expect to see some fraction of the blue stragglers being formed by mass transfer or binary coalescence.

The fact that NGC 6397 has a fairly low blue straggler formation rate (one blue straggler every 1.1×10^8 years), and yet is one of the densest clusters

studied here, suggests that it must have a very low binary fraction. Also, unlike 47 Tuc, NGC 6397 does have blue stragglers in the cluster outskirts. This suggests that the blue stragglers in NGC 6397 are receiving sizeable kicks during formation, requiring the binary population in the cluster to be quite evolved.

NGC 7099 is perhaps the most interesting cluster studied here. Its blue stragglers are apparently formed very highly mixed, and so are likely to have been formed by binary mergers. Also, although there is a large population of blue stragglers in the core of the cluster (Guhathakurta et al., 1998), no blue stragglers are observed in the outskirts of the cluster (Sandquist et al., 1999). For the blue stragglers to be formed by binary mergers, the binary population must be fairly hard (blue straggler formation by mass transfer to very distant companions is ruled out: soft binaries would be rapidly destroyed in this cluster); on the other hand, the fact that no blue stragglers are observed in the cluster periphery means either that they are receiving small kicks during any strong interactions (which argues either that they are so dynamically hard that they very rarely undergo such interactions or that they are dynamically soft: the latter is extremely unlikely) or that the delay between the kick and blue straggler formation is much longer than the cluster relaxation time.

Chapter 5

Conclusions

In Chapter 3, the results of smoothed pariticle hydrodynamic (**SPH**) simulations of colliding polytropes (Lombardi, Rasio, & Shapiro, 1996) were used to create models appropriate for investigating the evolution of stellar collision remnants. In creating these models several assumptions were made in order to facilitate the incorporation of the results of the SPH simulations into the stellar models: the assumptions include neglecting mass loss, rotation, and shock heating during the collision. Because we have restricted our attention to head-on, parabolic collisions, these assumptions should be reasonably valid: mass loss and rotational velocity are small in this instance (Lombardi, Rasio, & Shapiro); shock heating, which could affect the distribution of material in the final remnant, is also negligible for the bulk of the star, although it is likely that some mixing due to shock heating will occur near the surface of the star. The form of the energy injection term ϵ_x, which was used to expand the merger remnant models to simulate the effect of the injection of orbital energy into the remnant during the collision, is shown to be unimportant as long as significant mixing is not artificially introduced

(Vogt, 1926; Russell, 1927).

Fully-mixed stellar models were also evolved, under the assumption that these would approximate the remnants of binary mass transfer and coalescence. These models are likely to be greatly over-simplified: in the case of mass transfer, if coalescence does not result, the helium-rich core of the mass-donor will be left orbiting the newly formed blue straggler and so little helium will be transferred; in the case of binary coalescence, mass is transferred from one star to the other, but the two stars will merge before complete mass transfer and mixing takes place. In either case, the remnants will be slightly evolved when they attain 'blue straggler-hood'. It was stressed that these stars would, in reality, most likely be confused with equal-mass collisional mergers. One possible way to differentiate between collisional mergers and these binary mergers is that in clusters in which collisions should dominate the blue straggler formation process, the 'contamination' by these stars should be small.

In Chapter 4, the evolutionary tracks created from the models were compared with observations of blue stragglers in six different clusters. The blue straggler populations in most of the clusters were best matched by hybrid populations of collisional turnoff mergers and equal-mass collisional mergers in various proportions. One cluster, NGC 7099, had a significant population of blue stragglers which was found to be consistent with the fully-mixed models, indicating that binary coalescence or mass transfer is the dominant blue straggler formation process. Despite the assumptions which went in to creating the models (those for both collsional mergers and binary mergers), the agreement between the predictions of the models and the observations is

remarkably good. The selection of the parent populations for the blue stragglers was done using two different statistical tests, but the greatest satisfaction comes from the visual agreement between the observed blue stragglers and fake blue stragglers on the CMDs of the clusters.

Based on the agreement between the models and the observations, it was speculated that the blue stragglers in these clusters are not being strongly affected by rotation. Since most of the blue stragglers were found to have been created by collisions, and since the collision scenario predicts that such blue stragglers should be rapidly rotating, the effects of rotation must be small; it is possible that angular momentum is being lost from the star, presumably to a nearby companion or circumstellar disk. However, it is also possible that the stars are actually affected by rotation but some conspiracy of effects is causing the apparent deviation from the predicted evolution to be small.

Since no assumptions were made about the cluster dynamics when the models were created, the comparisons between the models and observations is a potentially useful probe of the cluster dynamics. Unfortunately, the effects of cluster dynamics and the properties of the binaries in the cluster cannot be disentangled in any simple way. For NGC 7099, however, the fact that there is a large population of highly mixed blue stragglers suggests that binary coalescence is the dominant formation mechanism in this cluster. For coalescence to dominate in such a dense cluster must mean that the binaries in the cluster have been hardened to the point that they very rarely undergo collisions: any blue stragglers that are kicked out of the cluster core during a strong interaction are very quickly brought back into the core due to the

short relaxation time. NGC 7099 is unique among the clusters studied here and is obviously in a very interesting dynamical state.

5.1 Directions for Future Study

No astronomical thesis would be complete with out the cry for 'More data!' The statistical comparisons carried out here are, for many of the clusters, fairly tenuous due to the small number ($\sim$ 20) of blue stragglers with high quality photometry. Further observations to improve the quality of the photometry and to obtain a full census of the blue stragglers in a cluster would be invaluable. With blue stragglers, it seems that the harder one looks, the more one finds: NGC 7099 and NGC 6093 (M80) were, until recently, quite devoid of blue stragglers in the published photometry (e.g. Sandquist *et al.*, 1999; Brocato *et al.*1998). Guhathakurta *et al.*(1998) and Ferraro et al. (1999) have recently found very large populations of blue stragglers tucked away in the cores of these clusters. (The blue straggler population in M80 is so large that Ferraro et al. have, quite rightly, claimed that it is the largest sample of blue stragglers found in any cluster to date). Also NGC 288, which has shown only a few blue stragglers in its CMD (e.g. Alcaino *et al.*1997), has recently revealed a large population of blue stragglers in its core (Bellazzini & Messineo, 1999).

The primary source of these newly found blue stragglers has been the Hubble Space Telescope. Although similar spatial resolution can be obtained on the ground using adaptive optics, the Hubble is currently unparalleled when one considers both the size of its field of view ($\sim$ 4 arcminutes square, compared to ground-based adaptive optics cameras, $\sim$ 30 $-$ 60 arcseconds on

a side) and the spatial resolution it can achieve. Its place above the clouds is of minor importance since the large size of ground-based telescopes mostly compensates for atmospheric absorption (at visual wavelengths, anyway). On the other hand, the field of view of the Hubble is minuscule compared to the views obtainable with large format CCDs (charge-coupled devices) available at many telescopes. If a census of all blue stragglers in a cluster is to be made, and if photometric quality is not to be sacrificed at any point in the cluster, a programme which involves both the Hubble and ground-based telescopes is the only solution. Such a survey has only been started with M3 (Ferraro *et al.* 1995). A survey of the complete stellar content over several entire clusters would be invaluable to many aspects of the study of stellar evolution - *if* the photometric quality of the survey is made to be the best that is achievable with the instruments at hand. Poor photometry is of use to no one.

In addition to more photometry for blue stragglers, the type of photometry obtained should also be chosen to facilitate the study. As discussed earlier (Chapter 2), if gravity and temperature estimates could be obtained for the blue stragglers in a cluster, the data could be compared directly with evolutionary calculations. While it would be quite expensive, in terms of telescope time, to measure the surface gravity and temperature of a large sample of blue stragglers via spectroscopy, the Strömgren photometric system offers an alternative. The Strömgren filters are narrow band filters which have been chosen to maximise the sensitivity of the photometric system to stellar gravity and temperature. Since this photometric system provides more sensitivity to stellar surface parameters than do the usual broad-band filters,

comparisons between models and Strömgren data would similarly be more sensitive.

On the theoretical side, the inclusion of rotation into the model calculations would allow an important test of the collisional scenario. Although it was speculated that the predicted rotational velocity of collisionally formed blue stragglers is not affecting the apparent evolution of the stars, the extent of the effect of rotation on the models would allow some quantification of this speculation and may allow a more precise determination of the population ratios.

Gilliland *et al.*(1998) have used data from a photometric time-series of 47 Tuc to obtain pulsational mass estimates for several blue stragglers in 47 Tuc. In particular, they have computed theoretical pulsational periods for stellar evolutionary tracks for masses roughly corresponding to presumed masses for the blue stragglers in 47 Tuc and compared these theoretical predictions with their observations. While their use of this pulsational analysis was primarily to assign pulsational mass estimates to the blue stragglers and to determine pulsational modes, this method has the potential to be able to constrain the formation mechanism for the blue stragglers more precisely than the photometric analysis performed in this thesis. As an example, a similar set of pulsational calculations were done on the two tracks shown in Figure 5.1 using a version of the GONG (Global Oscillation Network Group) oscillation code (e.g. Christensen-Dalsgaard, 1993). For each point along the stellar tracks, the GONG code yielded pulsation periods for the first, second, and third radial modes: these pulsational periods are plotted in a Petersen Diagram (Figure 5.2). Of particular interest is the point at which

the two tracks cross in Figure 5.1, marked by the open circle: the same point in the tracks is marked in the Petersen diagrams in Figure 5.2. The points at which the evolutionary tracks coincided are well separated in the pulsational diagram. Given accurate time series for pulsating blue stragglers, it may be possible to use a similar method to attempt to differentiate between formation mechanisms.
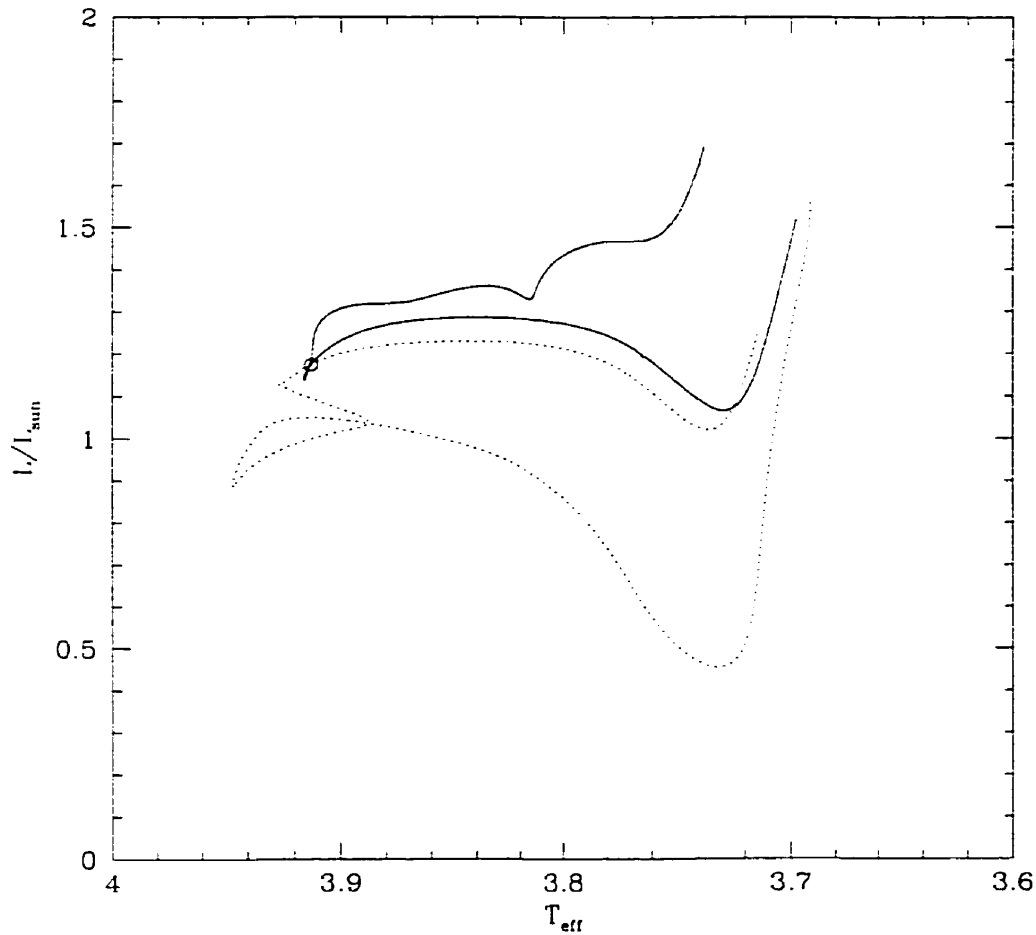
Figure 5.1: Evolutionary tracks for which pulsational periods have been computed. The solid line is a $1.60M_\odot$ collisional turnoff merger. The dotted line is $1.415M_\odot$ binary turnoff merger. The open circle indicates a point at which the two tracks cross. A similar pair of tracks could be found for a pulsating blue straggler in a CMD: period calculations, such as those in Figure 5.2 might help determine the star's origin.

Figure 5.2: Petersen diagrams for the two tracks shown in Figure 5.1. The figure on the top shows the Petersen diagram — which is a plot of period versus period ratio — for the first and second radial modes. The figure on the bottom shows the Petersen diagram for the second and third radial modes. The lines, and the open circle, have the same meanings as they do in Figure 5.1.

Bibliography

Abt, H. A.: 1979, *Astron. J.* **84**, 1591

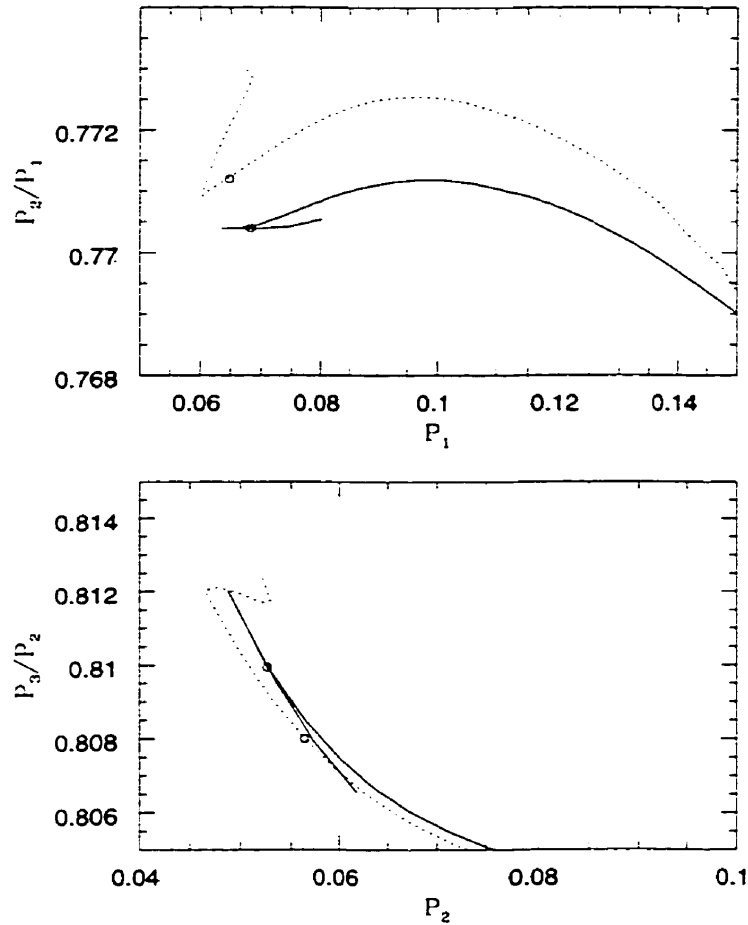Alcaino, G., Buonanno, R., Caloi, V., Castellani, V., Corsi, C. E., Iannicola, G., and Liller, W.: 1987, *Astron. J.* **94**, 917

Alcaino, G., Liller, W., and Alvarado, F.: 1997, *Astron. J.* **114**, 2626

Bacon, D., Sigurdsson, S., and Davies, M. B.: 1996, *Mon. Not. R. Astron. Soc.* **281**, 830

Bahcall, J. N. and Soneira, R. M.: 1984, *Astrophys. J., Suppl. Ser.* **55**, 67

Bailyn, C. D. and Pinsonneault, M. H.: 1995, *Astrophys. J.* **439**, 705

Bellazzini, M. and Messineo, M.: 1999, *Preprint* astro-ph/9910522

Benz, W. and Hills, J. G.: 1987, *Astrophys. J.* **323**, 614

Benz, W. and Hills, J. G.: 1992, *Astrophys. J.* **389**, 546

Boesgaard, A. M.: 1987, *Astrophys. J.* **321**, 967

Bond, H. E. and McConnell, D. J.: 1971, *Astrophys. J.* **165**, 51

Bond, H. E. and Perry, C. L.: 1971, *Publ. Astron. Soc. Pac.* **83**, 638

Borkowski, K. J. and Harrington, J. P.: 1991, *Astrophys. J.* **379**, 168

Bowers, P. F., Kerr, F. J., Knapp, G. R., Gallagher, J. S., and Hunter, D. A.: 1979, *Astrophys. J.* **233**, 553

Breger, M.: 1979, *Publ. Astron. Soc. Pac.* **91**, 5

Brocato, E., Castellani, V., Scotti, G. A., Saviane, I., Piotto, G., and Ferraro, F. R.: 1998, *Astron. Astrophys.* **335**, 929

Chaboyer, B., Demarque, P., Kernan, P. J., Krauss, L. M., and Sarajedini, A.: 1996, *Mon. Not. R. Astron. Soc.* **283**, 683

Christensen-Dalsgaard, J.: 1993, in *GONG 1992. Seismic Investigation of the Sun and Stars. Proceedings of a Conference held in Boulder, Colorado, August 11-14, 1993. Editor, Timothy M. Brown; Publisher, Astronomical Society of the Pacific #42, 1993.ISBN # 0-937707-61-9. LC # QB539.O83 G66 1992, P. 347, 1993*, p. 347

Clement, M. J.: 1994, *Astrophys. J.* **420**, 797

Cote, P., Pryor, C., McClure, R. D., Fletcher, J. M., and Hesser, J. E.: 1996, *Astron. J.* **112**, 574

Cote, P., Richer, H. B., and Fahlman, G. G.: 1991, *Astron. J.* **102**, 1358

Cote, P., Welch, D. L., Fischer, P., Da Costa, G. S., Tamblyn, P., Seitzer, P., and Irwin, M. J.: 1994, *Astrophys. J., Suppl. Ser.* **90**, 83

Cox, J. P. and Giuli, R. T.: 1968, in *Principles of stellar structure*, New York, Gordon and Breach [1968]

Da Costa, G. S., Norris, J., and Villumsen, J. V.: 1986, *Astrophys. J.* **308**, 743

Drissen, L. and Shara, M. M.: 1998, *Astron. J.* **115**, 725

Edmonds, P. D., Gilliland, R. L., Guhathakurta, P., Petro, L. D., Saha, A., and Shara, M. M.: 1996, *Astrophys. J.* **468**, 241

Efron, B. and Tibshirani, R. J.: 1993, in *An Introduction to the Bootstrap*, Chapman and Hall [1993]

Ferraro, F. R., Fusi Pecci, F., and Buonanno, R.: 1992, *Mon. Not. R. Astron. Soc.* **256**, 376

Giannuzzi, M. A.: 1984, *Astron. Astrophys.* **140**, 373

Gilliland, R. L., Bono, G., Edmonds, P. D., Caputo, F., Cassisi, S., Petro, L. D., Saha, A., and Shara, M. M.: 1998, *Astrophys. J.* **507**, 818

Gilliland, R. L., Brown, T. M., Duncan, D. K., Suntzeff, N. B., Lockwood, G. W., Thompson, D. T., Schild, R. E., Jeffrey, W. A., and Penprase, B. E.: 1991, *Astron. J.* **101**, 541

Girard, T. M., Grundy, W. M., Lopez, C. E., and Van Altena, W. F.: 1989, *Astron. J.* **98**, 227

Glaspey, J. W., Pritchet, C. J., and Stetson, P. B.: 1994, *Astron. J.* **108**, 271

Guhathakurta, P., Webster, Z. T., Yanny, B., Schneider, D. P., and Bahcall, J. N.: 1998, *Astron. J.* **116**, 1757

Guhathakurta, P., Yanny, B., Bahcall, J. N., and Schneider, D. P.: 1994, *Astron. J.* **108**, 1786

Guhathakurta, P., Yanny, B., Schneider, D. P., and Bahcall, J. N.: 1992, *Astron. J.* **104**, 1790

Harris, H. C.: 1993, *Astron. J.* **106**, 604

Harris, W. E., Bell, R. A., VandenBerg, D. A., Bolte, M., Stetson, P. B., Hesser, J. E., Van Den Bergh, S., Bond, H. E., Fahlman, G. G., and Richer, H. B.: 1997, *Astron. J.* **114**, 1030

Hills, J. G. and Day, C. A.: 1976, *Astrophys. Lett.* **17**, 87

Hobbs, L. M. and Mathieu, R. D.: 1991, *Publ. Astron. Soc. Pac.* **103**, 431

Hoffer, J. B.: 1983, *Astron. J.* **88**, 1420

Hut, P., McMillan, S., Goodman, J., Mateo, M., Phinney, E. S., Pryor, C., Richer, H. B., Verbunt, F., and Weinberg, M.: 1992, *Publ. Astron. Soc. Pac.* **104**, 981

Iben, I. J. and Livio, M.: 1993, *Publ. Astron. Soc. Pac.* **105**, 1373

Johnson, H. L. and Sandage, A. R.: 1955, *Astrophys. J.* **121**, 616

Kaluzny, J., *Astron. Astrophys. Suppl. Ser.*

Kaluzny, J.: 1997a, *Astron. Astrophys. Suppl. Ser.* **122**, 1

Kaluzny, J., Krzeminski, W., and Mazur, B.: 1995, *Astron. J.* **110**, 2206

Kaluzny, J., Krzeminski, W., and Nalezyty, M.: 1997a, *Astron. Astrophys. Suppl. Ser.* **125**, 337

Kaluzny, J., Kubiak, M., Szymanski, M., Udalski, A., Krzeminski, W., and Mateo, M.: 1996a, *Astron. Astrophys. Suppl. Ser.* **120**, 139

Kaluzny, J., Kubiak, M., Szymanski, M., Udalski, A., Krzeminski, W., Mateo, M., and Stanek, K.: 1997b, *Astron. Astrophys. Suppl. Ser.* **122**, 471

Kaluzny, J., Mazur, B., and Krzeminski, W.: 1993, *Mon. Not. R. Astron. Soc.* **262**, 49

Kaluzny, J. and Shara, M. M.: 1987, *Astrophys. J.* **314**, 585

Kaluzny, J. and Shara, M. M.: 1988, *Astron. J.* **95**, 785

Kaluzny, J., Thompson, I. B., and Krzeminski, W.: 1997b, *Astron. J.* **113**, 2219

Kaluzny, J., Wysocka, A., Stanek, K. Z., and Krzeminski, W.: 1998, *Acta Astronomica* **48**, 439

Landsman, W., Aparicio, J., Bergeron, P., Di Stefano, R., and Stecher, T. P.: 1997, *Astrophys. J., Lett.* **481**, L93

Lang, K. R.: 1992, in *Astrophysical data*, New York : Springer-Verlag, c1992-

Latham, D. and Milone, A.: 1996, in E. F. Milone and J.-C. Mermilliod (eds.), *The Origins, Evolution, and Destinies of Binary Stars in Clusters.*, Vol. 90 of *ASP Conference Series*, p. 385

Lauzeral, C., Ortolani, S., Auriere, M., and Melnick, J.: 1992, *Astron. Astrophys.* **262**, 63

Leonard, P. J. T.: 1989, *Astron. J.* **98**, 217

Leonard, P. J. T.: 1996, *Astrophys. J.* **470**, 521

Leonard, P. J. T. and Fahlman, G. G.: 1991, *Astron. J.* **102**, 994

Leonard, P. J. T. and Linnell, A. P.: 1992, *Astron. J.* **103**, 1928

Leonard, P. J. T. and Livio, M.: 1995, *Astrophys. J., Lett.* **447**, L121

Lombardi, J. C. J., Rasio, F. A., and Shapiro, S. L.: 1996, *Astrophys. J.*

468, 797

Lynch, D. K. and Rossano, G. S.: 1990, *Astron. J.* **100**, 719

Maeder, A.: 1971, *Astron. Astrophys.* **14**, 351

Mandushev, G. I., Fahlman, G. G., Richer, H. B., and Thompson, I. B.: 1997, *Astron. J.* **114**, 1060

Mateo, M., Harris, H. C., Nemec, J., and Olszewski, E. W.: 1990, *Astron. J.* **100**, 469

Mathieu, R. D. and Latham, D. W.: 1986, *Astron. J.* **92**, 1364

Mathys, G.: 1991, *Astron. Astrophys.* **245**, 467

Mazur, B., Krzeminski, W., and Kaluzny, J.: 1995, *Mon. Not. R. Astron. Soc.* **273**, 59

McCrea, W. H.: 1964, *Mon. Not. R. Astron. Soc.* **128**, 147

Milone, A. A. E. and Latham, D. W.: 1994, *Astron. J.* **108**, 1828

Nemec, J. and Park, N.-K.: 1996, in E. F. Milone and J.-C. Mermilliod (eds.), *The Origins, Evolution, and Destinies of Binary Stars in Clusters.*, Vol. 90 of *ASP Conference Series*, p. 359

Nemec, J. M. and Harris, H. C.: 1987, *Astrophys. J.* **316**, 172

Nemec, J. M., Mateo, M., Burke, M., and Olszewski, E. W.: 1995, *Astron. J.* **110**, 1186

Ouellette, J. A. and Pritchet, C. J.: 1996, in E. F. Milone and J.-C. Mermilliod (eds.), *The Origins, Evolution, and Destinies of Binary Stars in Clusters.*, Vol. 90 of *ASP Conference Series*, p. 356

Ouellette, J. A. and Pritchet, C. J.: 1998, *Astron. J.* **115**, 2539

Paresce, F., Meylan, G., Shara, M., Baxter, D., and Greenfield, P.: 1991, *Nature* **352**, 297

Podsiadlowski, P.: 1996, *Mon. Not. R. Astron. Soc.* **279**, 1104

Pritchet, C. J. and Glaspey, J. W.: 1991, *Astrophys. J.* **373**, 105

Rasio, F. A.: 1995, *Astrophys. J., Lett.* **444**, L41

Rasio, F. A. and Heggie, D. C.: 1995, *Astrophys. J., Lett.* **445**, L133

Renzini, A. and Pecci, F. F.: 1988, *Ann. Rev. Astron. & Astrophys.* **26**, 199

Rey, S. C., Lee, Y. W., Byun, Y. I., and Chun, M. S.: 1998, *Astron. J.* **116**, 1775

Rich, R. M., Sosin, C., Djorgovski, S. G., Piotto, G., King, I. R., Renzini, A., Phinney, E. S., Dorman, B., Liebert, J., and Meylan, G.: 1997, *Astrophys. J., Lett.* **484**, L25

Robb, R., Cardinal, R., and Ouellette, J.: 1997, *Unpublished*

Rodgers, A. W. and Roberts, W. H.: 1995, *Astron. J.* **109**, 264

Rubenstein, E. P. and Bailyn, C. D.: 1996, *Astron. J.* **111**, 260

Rucinski, S. M., Kaluzny, J., and Hilditch, R. W.: 1996, *Mon. Not. R. Astron. Soc.* **282**, 705

Russell, H. N.: 1927, in Russell, Dugan, and Stewart (eds.), *Astronomy*, Vol. 2, p. 910

Saio, H. and Wheeler, J. C.: 1980, *Astrophys. J.* **242**, 1176

Sandage, A. R.: 1953, *Astron. J.* **58**, 61

Sandquist, E. L., Bolte, M., and Hernquist, L.: 1997, *Astrophys. J.* **477**, 335

Sandquist, E. L., Bolte, M., Langer, G. E., Hesser, J. E., and Mendes De Oliveira, C.: 1999, *Astrophys. J.* **518**, 262

Sandquist, E. L., Taam, R. E., Chen, X., Bodenheimer, P., and Burkert, A.: 1998, *Astrophys. J.* **500**, 909

Sarajedini, A.: 1994, *Publ. Astron. Soc. Pac.* **106**, 205

Sarajedini, A. and Forrester, W. L.: 1995, *Astron. J.* **109**, 1112

Sarna, M. J.: 1992, *Mon. Not. R. Astron. Soc.* **259**, 17

Schoenberner, D. and Napiwotzki, R.: 1994, *Astron. Astrophys.* **282**, 106

Schönberg, M. and Chandrasekhar, S.: 1942, *Astrophys. J.* **96**, 161

Shara, M. M., Saffer, R. A., and Livio, M.: 1997, *Astrophys. J., Lett.* **489**, 59

Sigurdsson, S., Davies, M. B., and Bolte, M.: 1994, *Astrophys. J., Lett.* **431**, L115

Sigurdsson, S. and Phinney, E. S.: 1993, *Astrophys. J.* **415**, 631

Sills, A. and Bailyn, C. D.: 1999, *Astrophys. J.* **513**, 428

Sills, A., Bailyn, C. D., and Demarque, P.: 1995, *Astrophys. J., Lett.* **455**, L163

Sills, A., Lombardi, J. C., J., Bailyn, C. D., Demarque, P., Rasio, F. A., and Shapiro, S. L.: 1997, *Astrophys. J.* **487**, 290

Sills, A. and Lombardi, James C., J.: 1997, *Astrophys. J., Lett.* **484**, L51

Smith, G. H., Woodsworth, A. W., and Hesser, J. E.: 1995, *Mon. Not. R. Astron. Soc.* **273**, 632

Solano, E. and Fernley, J.: 1997, *Astron. Astrophys. Suppl. Ser.* **122**, 131

Strom, K. M. and Strom, S. E.: 1970, *Astrophys. J.* **162**, 523

Stryker, L. L. and Hrivnak, B. J.: 1984, *Astrophys. J.* **278**, 215

Terman, J. L. and Taam, R. E.: 1996, *Astrophys. J.* **458**, 692

Tolstoy, E. and Saha, A.: 1996, *Astrophys. J.* **462**, 672

Troland, T. H., Hesser, J. E., and Heiles, C.: 1978, *Astrophys. J.* **219**, 873

VandenBerg, D. A. and Bell, R. A.: 1985, *Astrophys. J., Suppl. Ser.* **58**, 561

VandenBerg, D. A., Bolte, M., and Stetson, P. B.: 1990, *Astron. J.* **100**, 445

VandenBerg, D. A., Larson, A. M., and De Propris, R.: 1998, *Publ. Astron.*

Soc. Pac. **110**, 98

VandenBerg, D. A., Swenson, F. J., Rogers, F. J., Iglesias, C. A., and Alexander, D. R.: 1999, *In preparation*

Vogt, H.: 1926, *Aston. Nachr.* **226**, 301

Webbink, R. F.: 1976, *Astrophys. J.* **209**, 829

Webbink, R. F.: 1977a, *Astrophys. J.* **211**, 486

Webbink, R. F.: 1977b, *Astrophys. J.* **211**, 881

Webbink, R. F.: 1977c, *Astrophys. J.* **215**, 851

Wheeler, J. C.: 1979, *Astrophys. J.* **234**, 569

Yan, L. and Mateo, M.: 1994, *Astron. J.* **108**, 1810

Yan, L. and Reid, I. N.: 1996, *Mon. Not. R. Astron. Soc.* **279**, 751

Glossary of Abbreviations and Astronomical Terms

AML: Angular Momentum Loss

AU: Astronomical Unit $(1.496 \times 10^{11} m)$

BM: Binary (fully-mixed) merger

BS: Blue Straggler

CM: Collisional merger

CMD: Colour-Magnitude Diagram

DC: Dwarf Cepheid

GC: Globular Cluster

Gyr: Giga-year $= 1 \times 10^9$ years

HB: Horizontal Branch

KS: Kolmogorov-Smirnoff

LRS: Lombardi, Rasio & Shapiro (1996)

$M_{\odot}$: solar mass $= 1.989 \times 10^{30}$ kg

MS: Main Sequence

MS TO: Main Sequence Turn Off

NGC: New General Catalogue

OC: Open Cluster

RGB: Red Giant Branch

SGB: Sub-Giant Branch

SPH: Smoothed Particle Hydrodynamics

TMS: Termination of the Main Sequence

TO: Turn Off

WD: White Dwarf

WUMa: W Ursae Majoris

ZAMS: Zero-Age Main Sequence

absolute magnitude: The *magnitude* an object would have if it were at a standard distance of 10 *parsecs*. The difference in absolute magnitude between two stars is a measure of the ratio of their true luminosities: a difference in *apparent magnitude* will include effects on the apparent brightness such as distance and interstellar absorption, and so is not, necessarily, a true relative luminosity indicator.

apparent magnitude: The *magnitude* of an object at its true distance. Unless otherwise indicated, this magnitude will often include the effect of interstellar absorption.

colour-magnitude diagram (CMD): A plot of magnitude (absolute or apparent) versus colour (the difference in magnitude measured through two different passbands). The colour of a star is a temperature indicator, as is *spectral type*, though the sensitivity of colour to temperature is dependent upon the passbands used and the spectral type.

distance modulus: $m - M = 5 \log D - 5$, where m is the apparent magnitude, M is the absolute magnitude, and D is the distance in parsecs. The magnitudes must, of course, be measured in the same photometric band, and the apparent magnitude may have to be corrected for interstellar absorption.

evolution (stellar): The gradual change of a star from one class, or phase, to another (e.g. main sequence to subgiant to red giant).

equal-mass merger: In this work, an equal-mass merger refers to the both the event and the remnant of a collision between two identical stars. Compare with *turnoff merger*.

giant: See red giant.

Hertzsprung-Russell Diagram (H-R Diagram): A plot of stellar absolute magnitude versus spectral type. Similar in information content to a CMD.

interstellar reddening: The result of short wavelength (blue) photons being preferentially scattered from the line of sight to an object due to interstellar gas and dust. Mainly due to Mie scattering. Since the scattering cross-section of Mie scattering is inversely proportional to the wavelength of the light ($\sigma_\lambda \propto \lambda^{-1}$), the number of short wavelength photons is decreased more than the number of long wavelength photons, causing an apparent reddening of the light emitted from distant objects.

isochrone: From Greek: isos (equal) + khronos (time). A line of constant time extracted from theoretical tracks of stellar evolution. Given a sequence of evolutionary tracks for stars of the same initial composition, but differing mass, the point on each track which corresponds to the desired age is extracted and retained; this sequence of points is the isochrone. An isochrone could be thought of as a theoretical H-R Diagram or CMD for an ideal cluster: abundances, age, distance, reddening are all constant, the only parameter which is allowed to vary is mass.

main sequence (MS): The band running across the H-R Diagram in which most stars, in the field and in clusters, are found. Also refers to the phase (core hydrogen burning) of evolution in which stars spend most of their lifetime.

magnitude: Defined as $m_\lambda = -2.5 \log_{10} f_\lambda + C$, where f_λ is the flux measured in a wavelength region centred on the wavelength λ, and C is a constant necessary to bring the magnitude onto a standard system. For example, the brightest star (to the eye) in the constellation Orion, Rigel (β Ori), has an apparent V ($\lambda \sim 550\text{nm}$) magnitude of $\sim +0.14$. The faintest stars visible to the naked eye have a magnitude of $\sim 5-6$.

parallax: The annual parallax of a star is its apparent motion relative to the background stars caused by the motion of the Earth around the Sun. One arcsecond of parallax would place the star at a distance of one parsec.

parsec(pc): The distance at which one astronomical unit (AU) subtends one arcsecond (206,264.8 AU).

reddening: See interstellar reddening.

red giant: The phase of stellar evolution following the main sequence and subgiant phases. Characterised by an inert helium core,a thin hydrogen burning shell, and a thick convective envelope.

spectral type: Originally, a classification of stellar types based upon the strengths of the hydrogen lines observed in stellar spectra, with spectral type 'A' having the strongest hydrogen lines, 'B' the next strongest, etc. Later, these spectral types were rearranged by Annie Jump Cannon(*circa* 1901) to correspond to a sequence of increasing temperature: OBAFGKM (mnemonic: in reverse, *"Mentioning Kepler's Great Finds, Astronomers Bore Others"*).

subgiant: The phase of evolution immediately after the main sequence during which the star is beginning hydrogen shell burning (initially thick shell burning). The star moves rapidly across the H-R Diagram to cooler spectral types, at nearly constant luminosity; in massive stars, the evolution is so rapid it leaves an apparent gap in the H-R Diagram of young clusters (the Hertzsprung Gap).

turnoff merger: Throughout this work, a turnoff merger refers to the collision between a star at the main-sequence turnoff (i.e. just having reached central hydrogen exhaustion) and a star of lesser mass.

Appendix A

The maximum likelihood method of Tolstoy & Saha (1996) is used in Chapter 4 to compare the observed distribution of blue stragglers in the colour-magnitude diagram (CMD) with the predicted distribution from the models in Chapter 3. In particular, the method is used to determine if a hybrid population of the models is a better match to the data than a single population. This Appendix presents the results of tests designed to determine whether the population ratio with the maximum likelihood of matching the observations is a reasonable indicator of the true population ratio.

If the maximum likelihood, L_T (Equation 4.3), is to be used to recover the population ratios for observed blue stragglers, it should be sensitive enough to recover the composition of fake blue straggler populations drawn from the models using a known population ratio. To test this, two sets of fake blue stragglers were drawn from the models and were analysed in a manner identical to that used with the observed blue stragglers. The fake blue stragglers to be used were chosen from the sets of theoretical CMDs generated for the comparison of the models with the observations of 47 Tuc, and so have the same masses as the blue stragglers in 47 Tuc. However, these fake blue stragglers were drawn from population ratios which did not necessarily match the observations of 47 Tuc (compare Figures 5.3 and 5.5 to Figure 4.22).
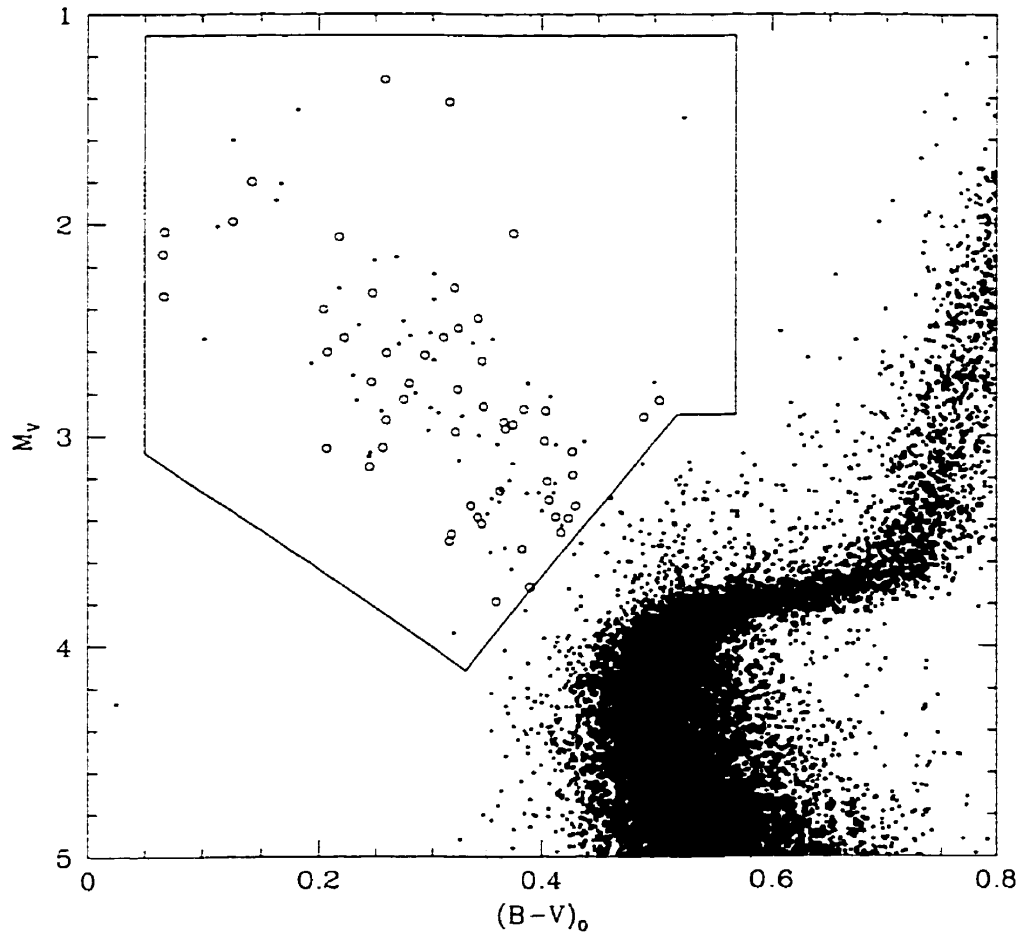
Figure 5.3: CMD of fake blue stragglers (open circles): the population consists of 50% turnoff collisional mergers and 50% equal-mass collisional mergers. Also shown are the data for 47 Tuc (small open squares; Rich et al., 1997). Note that the fake blue stragglers are not meant to be a good match to the blue stragglers in 47 Tuc.
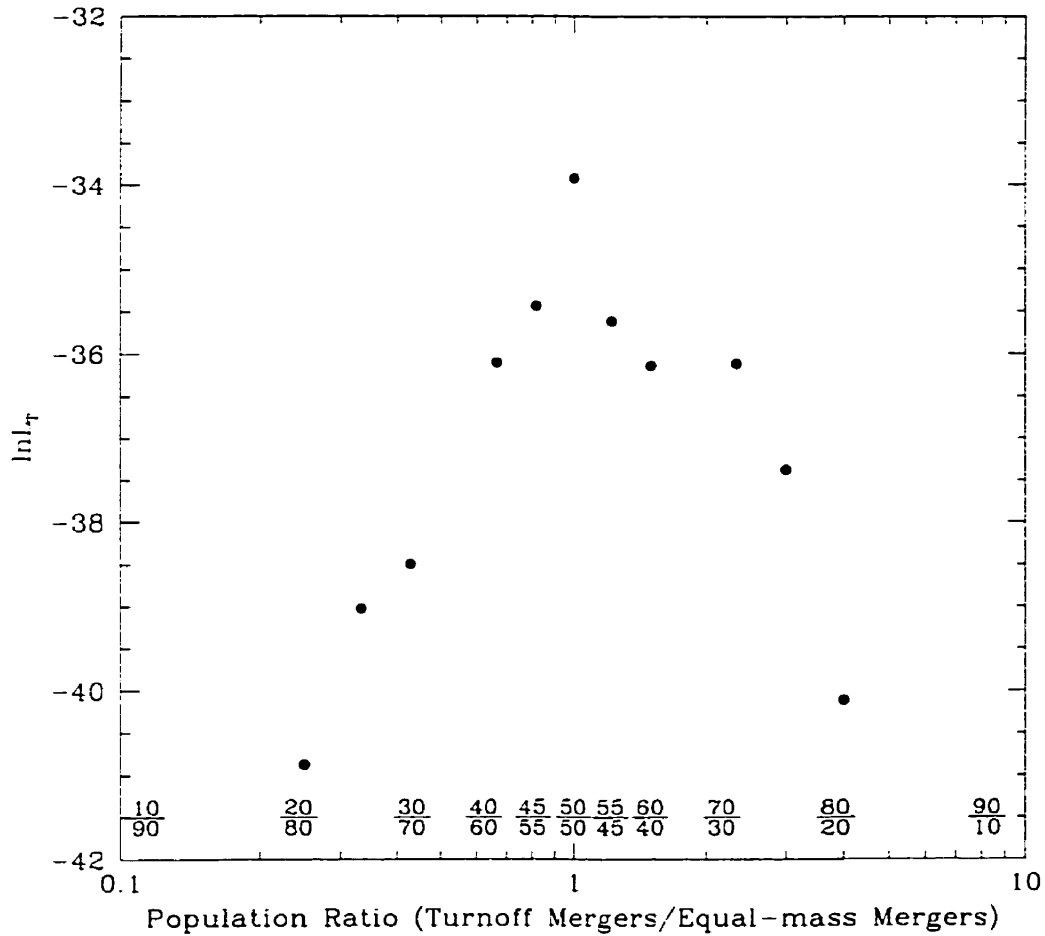
Figure 5.4: Likelihoods for varying turnoff merger/equal-mass merger population ratios matching the fake blue stragglers shown in Figure 5.3. The likelihoods for singular populations matching the input population are -52.83 for turnoff collisional mergers and -45.74 for equal-mass collisional mergers.

The first set of fake blue stragglers analysed consisted of 50% turnoff collisional mergers and 50% equal-mass collisional mergers and are shown in Figure 5.3 (the magnitudes of the fake blue stragglers have had the appropriate amount of photometric scatter added). Using the same methods as used with the real observations, these blue stragglers were compared with the predictions of the collisional mergers models assuming various population ratios. The input population ratio is recovered easily, as shown in Figure 5.4. In addition to the input population of 50% turnoff collisional mergers and 50% equal-mass collisional mergers having the maximum likelihood of matching the input population, the probability that this population ratio can provide a good match to the 'observed' Δ_Z distribution is $\sim$ 97%.

The second set of fake blue stragglers analysed in this way consisted of 90% turnoff collisional mergers and 10% equal-mass collisional mergers (Figure 5.5). The input population ratio is again recovered (Figure 5.6) with a probability of matching the 'observed' Δ_Z distribution of $\sim$ 89%.
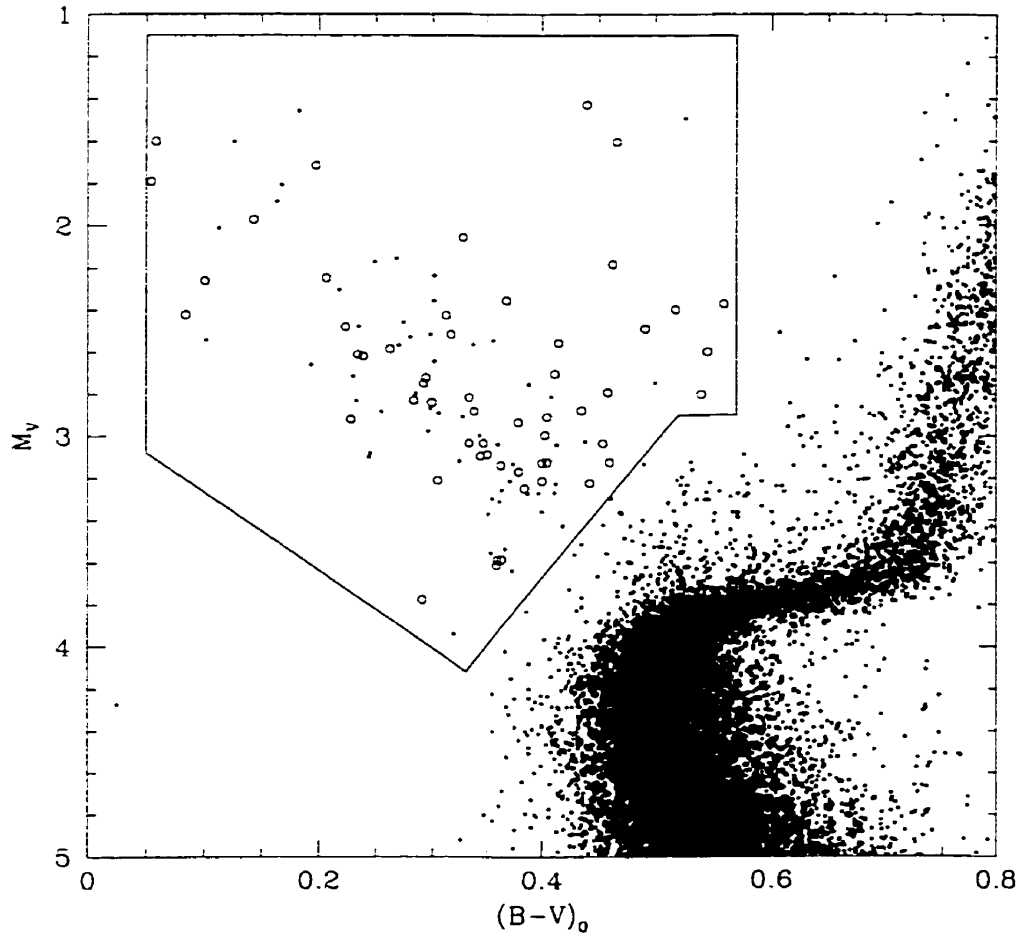
Figure 5.5: CMD of fake blue stragglers (open circles): the population consists of 90% turnoff collisional mergers and 10% equal-mass collisional mergers. Also shown are the data for 47 Tuc (small open squares; Rich et al., 1997). Note that the fake blue stragglers are not meant to be a good match to the blue stragglers in 47 Tuc.
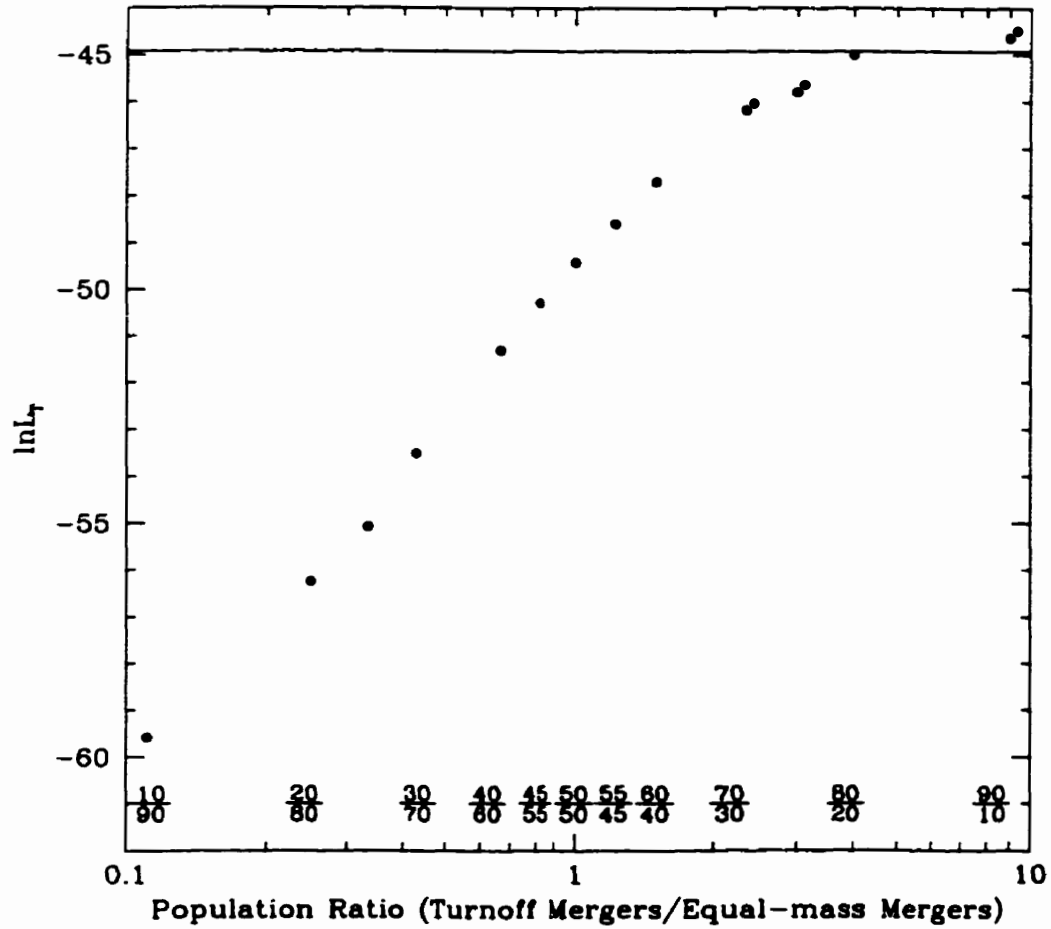
Figure 5.6: Likelihoods for varying turnoff merger/equal-mass merger population ratios matching the fake blue stragglers shown in Figure 5.5. The thick solid line shows the likelihood for a population consisting solely of turnoff mergers; the likelihood for a population consisting solely of equal-mass mergers is -63.49.

Appendix B

As mentioned in Chapter 3, it is possible to derive the entropy of an ideal monatomic gas using the first law of thermodynamics and a few identities. This Appendix contains a short derivation of the equation:

$$S = \frac{N_0 k}{\mu \gamma} \ln A + const \tag{5.1}$$

where S is the specific entropy of the gas, N_0 and k are Avogadro's number and the Boltzmann constant, respectively, μ is the mean molecular weight of the gas, γ is the ratio of the specific heats of the gas at constant pressure and volume ($\gamma = \frac{c_P}{c_V} = \frac{5}{3}$), and $A = P/\rho^{5/3}$.

First, a few handy identities:

- The definitions of the specific heats at constant volume and pressure:

$$dU = c_V dT \tag{5.2}$$

$$c_P = \left(\frac{\partial Q}{\partial T}\right)_P \tag{5.3}$$

- The relationship between the above specific heats for an ideal, monatomic

gas:

$$dQ = dU + PdV$$

$$\left(\frac{\partial Q}{\partial T}\right)_P = \left(\frac{\partial U}{\partial T}\right)_P + P\left(\frac{\partial V}{\partial T}\right)_P$$

$$c_P = c_V + P\left(\frac{Nk}{P}\right)$$

$$c_P = c_V + Nk \tag{5.4}$$

- The work done on the gas:

$$P = \frac{Nk}{V}T$$

$$PdV = NkT\frac{dV}{V}$$

$$PdV = (c_P - c_V)T\frac{dV}{V} \tag{5.5}$$

- Starting with the first law of thermodynamics and the definition of the entropy:

$$TdS = dU + PdV$$

$$= c_V dT + PdV$$

$$= c_V dT + (c_P - c_V)T\frac{dV}{V}$$

$$dS = c_V\frac{dT}{T} + (c_P - c_V)\frac{dV}{V}$$

- Integrating this last expression,

$$S = c_V \ln T + (c_P - c_V)\ln V + K$$

where K is a constant.

$$
\begin{aligned}
S &= (c_P - c_V)\left[\frac{c_V}{c_P - c_V}\ln T + \ln V\right] + K \\
&= Nk\left[\frac{1}{\gamma - 1}\ln T + \ln V\right] + K \\
S &= Nk\ln\left(VT^{\frac{1}{\gamma-1}}\right) + K
\end{aligned}
\tag{5.6}
$$

- Now, using two of the polytropic equations of state,

$$
T = K\rho^{\gamma-1} \tag{5.7}
$$

$$
P = K\rho^{\gamma} \tag{5.8}
$$

where the K's in the above expressions are not the same. This leads to

$$
T = KP^{\frac{\gamma-1}{\gamma}} \tag{5.9}
$$

where K is again constant, and is not necessarily the same as in the above two expressions. Using this in Eq. 5.6 and absorbing the constants into one constant,

$$
\begin{aligned}
S &= Nk\ln\left(VP^{\frac{1}{\gamma}}\right) + K \\
S &= \frac{Nk}{\gamma}\ln(P/\rho^{\gamma}) + K
\end{aligned}
\tag{5.10}
$$

where $V = 1/\rho$ is the specific volume.

- Now, using

$$
N = \frac{\rho N_0}{\mu} \tag{5.11}
$$

the specific entropy, $s = S/\rho$ is

$$
s = \frac{N_0 k}{\mu\gamma}\ln A + const \tag{5.12}
$$

VITA

Surname: Ouellette   Given Names: John Anders

Place of Birth: Gimli, Manitoba, Canada

Educational Institutes Attended:

University of Victoria   1985 - 1999

Degrees Awarded:

B.Sc. University of Victoria   1991

Honours and Awards:

Graduate Teaching Fellowship   1993 – 1999
R. M. Petrie Memorial Fellowship   1996, 1994

Publications:
Refereed Journals:

Ouellette, J. A. and Pritchet, C. J., 1998, *Astronomical Journal*, **115**, 2539, 'The Evolution of Blue Stragglers Formed Via Stellar Collisions.'

Conference Proceedings:

Ouellette, J. A. and Pritchet, C. J., 1996, 'On the Nature and Evolution of Blue Stragglers.' In E. F. Milone and J.-C. Mermilliod (eds.), The Origins, Evolution, and Destinies of Binary Stars in Clusters, Vol. 90 of ASP Conference Series, p. 356

Morris, S. L., Ouellette, J. A., Villemaire, A., Grandmont, F., and Moreau, L., 1999, 'A Canadian Imaging Fourier Transform Spectrometer for the Next Generation Space Telescope'. In E. Smith and M. Greenhouse (eds.), Proceedings from the Ad Hoc Science Working Group, Hyannis 1999.

Other Contributions:

Robb, R. M., Greimel, R., and Ouellette, J. A., 1997, *International Bulletin of Variable Stars*, **4504**, 'Observations of the GSC 3506_677 Field.'

Robb, R. M., Ouellette, J. A., and Larson, A., 1995, *Journal of the Royal Astronomical Society of Canada*, **89**, 161, 'Archival HST Observations of IC4182.'